GROUND STATE PHASE TRANSITIONS IN A ONE AND TWO-DIMENSIONAL HOLSTEIN-HUBBARD MODEL

Thesis submitted for the degree

of

DOCTOR OF PHILOSOPHY

in

PHYSICS

by

I.V. SANKAR

Supervisor: Prof. Ashok Chatterjee

School of Physics
University of Hyderabad
Hyderabad 500 046
India

February 2016

Dedicated to my parents

SURYA KUMARI - CHALAPATHI RAO

GURUS

DECLARATION

I, **I.V. Sankar**, hereby declare that the work presented in this thesis entitled **Ground state phase transitions in a one and two-dimensional Holstein-Hubbard model** has been carried out by me in the School of Physics, University of Hyderabad, India, under the supervision of **Prof. Ashok Chatterjee** as per the Ph.D. ordinances of the University. I declare, to the best of my knowledge, that no part of this thesis has been submitted for the award of a research degree of any other University. I hereby agree that my thesis can be deposited in Shodhganga/INFLIBNET.

A report on plagiarism statistics from the University librarian is enclosed.

Place: Hyderabad
Date :

I.V. Sankar
(Indhana Veera Sankar)
Reg. No. 08PHPH04

SCHOOL OF PHYSICS
UNIVERSITY OF HYDERABAD

CERTIFICATE

This is to certify that the thesis entitled **Ground state phase transitions in a one and two-dimensional Holstein-Hubbard model** being submitted to the University of Hyderabad by **I.V. Sankar** for the award of the degree of Doctor of Philosophy in Physics, is a record of bonafide work carried out by him under my supervision and is free of plagiarism.

This matter embodied in this report has not been submitted to any other University or Institution for the award of any degree or diploma.

Place: Hyderabad
Date :

Prof. Ashok Chatterjee
Thesis Supervisor

Dean
School of Physics
University of Hyderabad

ACKNOWLEDGEMENTS

It is a real delight to acknowledge those who have supported and encouraged me a lot to finish my Ph.D.

Firstly, I would like to express my deepest and sincere gratitude to my supervisor and well-wisher, Prof. Ashok Chatterjee, for his teaching and directing me to the exciting field of condensed matter theory. I would like to thank him for his guidance and motivation. It is an honor and privilege for me to work under his supervision. I am very much delighted with our countless discussions and particularly grateful for all the advice I received from him.

I would like to specially thank Dr. Soma Mukhopadhyay and Dr. Shreekantha Sil for several discussions and their help in the numerical computation.

I would like to thank my doctoral committee members, Dr. S. Srinath and Dr. S.V.S. Nageswara Rao for their valuable suggestions and comments on my research.

A special thanks goes to my colleagues: B. Aalu Naik, Monisha P.J., D. Sanjeev Kumar, Ch. Narasimha Raju, Ch. Uma Lavanya, Luhluh Jahan, M. Yadaiah for several discussions, my contemporaries: Siva N. Chari, M. Suman Kalyan and T. Hongrey for helping me basic computation in the beginning of my research career and my close friends: S. Siva N. Chari, Y. Shankarao and N. Manikantha Babu for their caring and support.

I thank former Deans of School of Physics, Prof. Vipin Srivatsava, Prof. C. Bansal and Prof. S.P. Tewari and a special thanks to Prof. S. Chaturvedi. And

finally, I thank the present Dean, Prof. R. Singh for providing needful facilities.

I thank Mr. T. Abraham and all other non-teaching staff of School of Physics for their help and support. The financial support provided by University of Hyderabad, BSR fellowship of UGC and CSIR-DSRF of UGC is greatly acknowledged.

I would like to thank my college and undergraduate teachers, Mr. K.V. Subba Rao and Mr. D. Rajesh and who inspired me through their teachings and constant encouragement.

The time in the Hyderabad has been great. I will always remember it as a rewarding life experience. Thanks to all who made my stay here so enjoyable and memorable.

Finally, I wish to thank my beloved parents for their caring, love and encouragement, without whom I would never have completed my Ph.D. I am fortunate to have parents like that who always try to give their best to help whatever way they can and extremely helpful not only for me but also for people surrounding them. A mere thanks may not be enough to show my gratitude but except saying that "I will be always grateful to them".

I.V. Sankar

CONTENTS

PREFACE

The electron-electron (*e-e*) interaction and electron-phonon (*e-p*) coupling are the most important fundamental interactions in almost all condensed matter materials and more so in *strongly correlated polaron systems*. We modeled such systems with the Holstein-Hubbard Hamiltonian which is a useful model for the study of the effect of *e-e* and *e-p* interactions and their competition with the hopping process. So far, it has not been possible to obtain the exact solution of the HH model in any dimensions and the difficulty lies essentially with the *e-p* interaction term. So, to study this problem one has to resort to some approximation technique. We treat the Holstein-Hubbard problem variationally using canonical transformations to convert the Holstein-Hubbard model into an effective Hubbard model that can be solved exactly at least in one dimension.

The ground state of the Holstein-Hubbard model has so far been considered to be fully insulating over the entire range of the *e-e* and *e-p* coupling parameters. For positive effective *e-e* interaction (resultant of *e-e* and *e-p* interactions) the ground state is believed to be a Mott insulating state and for negative effective *e-e* interaction the ground state is expected to be a Peierls insulating state. In 2003, the work by Takada and Chatterjee has revealed that an *intervening metallic phase* can emerge at the crossover region of the Mott insulating and Peierls insulating states for the half-filled band case. In the first half of this thesis, we re-examine the presence of this intervening metallic phase in the ground state of the Holstein-Hubbard quantum ring within the framework of Hartree-Fock approximation in the process of calculating the persistent current and also using the nested Bethe ansatz technique together with quantum entanglement concept for thermodynamic system in one dimension. In the latter half of this thesis we examine the effect of *e-p* interaction on the weakly and strongly correlated electron systems in two dimensions using the Hartree-Fock approximation. In

these analyses, we additionally include the correlations between successively emitted virtual phonons, which were neglected in the first half of the thesis. Our main aim here is to examine the nature of the so called *self-trapping transition* i.e., the transition from a mobile polaron (large polaron) to a localized polaron (small polaron) as a function of the *e-p* interaction coupling and study the corresponding phase separations in the adiabatic and anti-adiabatic regimes.

CHAPTER 1

INTRODUCTION

In condensed matter physics, the electron-electron (*e*-*e*) and electron-phonon (*e*-*p*) interactions are the two most fundamental and important interactions. Even the lone presence of either of the interactions makes it difficult to solve the associated quantum mechanical problem exactly to understand quantitatively the properties of materials such as Mott insulators, heavy fermions, polarons, Peierls insulators, conventional and unconventional superconductors like $C_{60}K_3$, TiN, Nb-25Ti, $La_{2-x}Sr_xCuO_4$, H_2S and so on.

Materials such as MnO, NiO, V_2O_3 and La_2CuO_4 are expected to be metals according to the band theory since these materials have partially filled $d-$ type bands. Mott and Peierls [1] were the first to suggest that the band theory fails in these materials because of neglecting the role of correlations of electrons in the $d-$ orbitals. Mott [2] and Hubbard [3] showed that the presence of *e*-*e* interaction splits a band into two: a lower subband consisting of spin-up electrons and an upper subband consisting of down-spin electrons or vice versa and these two sub ands are separated exactly by an energy U which is the strength of the onsite *e*-*e* interaction. When the *e*-*e* interaction strength is larger than the bare electron bandwidth, the Fermi level will be located in between the lower and the

upper Hubbard subbands making the system insulating. These insulators are called the Mott insulators (MI's) and can be understood theoretically by using the celebrated Hubbard model [3]. On the other hand, the *e-p* interactions, besides being responsible for scattering in materials and hence resistivity, are also known to play important roles in several other phenomena like superconductivity in conventional superconductors and Peierls instability in some one-dimensional (1D) systems. The *e-p* interaction is also known to form polarons in some materials. In ionic crystals and polar semiconductors, an electron in the conduction band distorts the lattice in its neighbourhood and the distortion in turn produces a polarization potential with which the electron interacts subsequently. The picture looks as if an electron carries a lattice distortion together with it as it wades through the lattice. The electron together with the self-induced lattice distortion can be considered to constitute a quasiparticle which is commonly referred to as a *polaron* [4-6]. Since the distortion of a lattice essentially means excitation of phonons, a polaron can be understood, in the language of field theory, as a complex consisting of an electron surrounded by a cloud of virtual phonons. If the lattice distortion is spread over many lattice sites, the resulting polaron is called a *large* polaron, whereas if the distortion is restricted within a single lattice spacing, the corresponding polaron is called a *small* polaron. Normally two electrons repel each other because of the Coulomb interactions. However, the *e-p* interaction can give rise to an attractive interaction between two electrons in second order. If this attractive interaction is strong enough to overcome the repulsive Coulomb interaction, then the two electrons can form a bound state which is known as a *bipolaron* [7,8]. Thus physically a bipolaron is a system of two electrons coupled with associated lattice distortions. In a 1D tight-binding lattice, if the onsite *e-p* interaction happens to be fairly large as compared

to the onsite *e-e* Coulomb repulsion, then the formation of onsite pairing of electrons can take place leading to the doubling of unit cells in the crystal. This distortion of the lattice which is known as the Peierls instability opens up a gap at the Fermi level for an exactly half-filled band case (one electron per site) making the system an insulator. This phenomenon was first predicted by Peierls in 1930 and the corresponding systems are called the Peierls insulators (PI's) [9]. This kind of systems can be studied with the help of the so called Holstein model [10].

A great deal of attention has been drawn in recent years to the study of exotic materials such as cuprates that show high temperature superconductivity [11-13], manganites that show colossal magneto-resistance [14,15] and so on. Available experimental results on these materials suggest that both *e-e* and *e-p* interactions are present in them. As we have discussed above, strong electron correlations lead to a Mott insulating state, whereas a strong *e-p* coupling gives rise to a Peierls insulating phase. Of course, the presence of the hopping term makes the dynamics of the problem even richer and more interesting. The hopping process obviously tries to delocalize the electrons. The study of a system in the presence of all these competing terms is possible with the help of the Holstein-Hubbard (HH) Hamiltonian which we describe in the following section. The HH model can explain a variety of phenomena for a *correlated polaron* system. In this thesis, we shall focus mainly on the nature of the ground state (GS) of such a system. In general, the GS can be of several types. One is the spin-density wave (SDW) state which is the Mott insulating state and the other is the charge-density wave (CDW) state which is the Peierls insulating state. It is understandable that as the *e-p* interaction is increased for a fixed value of the *e-e* interaction strength, the system's GS may undergo a transition from the SDW state to the CDW state. It is of considerable interest to study the nature of this transition.

The HH model also allows us to study the transition of the GS from a large polaron state to the small polaron state.

1.1 THE HOLSTEIN-HUBBARD MODEL

We now introduce the HH model which is given by the Hamiltonian

$$\mathcal{H} = -t\sum_{\langle ij\rangle\sigma} c_{i\sigma}^{\dagger}c_{j\sigma} + U\sum_{i} n_{i\uparrow}n_{i\downarrow} + \omega_0\sum_{i} b_i^{\dagger}b_i + \mathrm{g}\sum_{i\sigma} n_{i\sigma}\left(b_i^{\dagger} + b_i\right) \quad \langle 1.1\rangle$$

The first term in the above Hamiltonian refers to the kinetic energy, where $c_{i\sigma}^{\dagger}(c_{i\sigma})$ is the creation (annihilation) operator for an electron at the $i^{\mathrm{th}}-$site with spin σ (with $\sigma = \uparrow, \downarrow$), t is the hopping parameter and $\langle ij\rangle$ indicates that the summation is over nearest-neighbour (NN) sites i and j. The electron operators satisfy the anti-commutation relations: $\{c_{i\sigma}^{\dagger}, c_{j\sigma'}\} = \delta_{ij}\delta_{\sigma\sigma'}$ and $\{c_{i\sigma}, c_{j\sigma'}\} = 0 = \{c_{i\sigma}^{\dagger}, c_{j\sigma'}^{\dagger}\}$. The second term is the onsite *e-e* repulsive Coulomb interaction, where U is the corresponding correlation strength and $n_{i\sigma} = c_{i\sigma}^{\dagger}c_{i\sigma}$ is the number operator for the electron at site i with spin σ. The third term is the free phonon Hamiltonian, where $b_i^{\dagger}(b_i)$ is the creation (annihilation) operator for a local phonon at the $i^{\mathrm{th}}-$site satisfying the commutation relations: $[b_i^{\dagger}, b_j] = \delta_{ij}$ and $[b_i, b_j] = 0 = [b_i^{\dagger}, b_j^{\dagger}]$, and ω_0 is the dispersionless phonon frequency. The last term represents the onsite *e-p* interaction with the corresponding strength g. Here we have chosen $\hbar = 1$.

This model best describes a scenario where the wave functions of the electrons on neighbouring lattice sites overlap weakly. It also takes care of the fact that the Coulomb repulsion leads to an increase in the energy, if a lattice site is doubly occupied. The tight-binding kinetic energy term

tries to delocalize the electrons, whereas the onsite *e-e* interaction term induces electron localization leading to the formation of local moments and the onsite *e-p* interaction creates lattice distortions and hence a polarization potential which also tries to localize one (two) electron(s) at a lattice site for a large (small) onsite *e-e* and small (large) *e-p* interactions. The schematic representation of the above scenario in a square lattice modeled with the HH Hamiltonian is shown in Fig. 1.1.

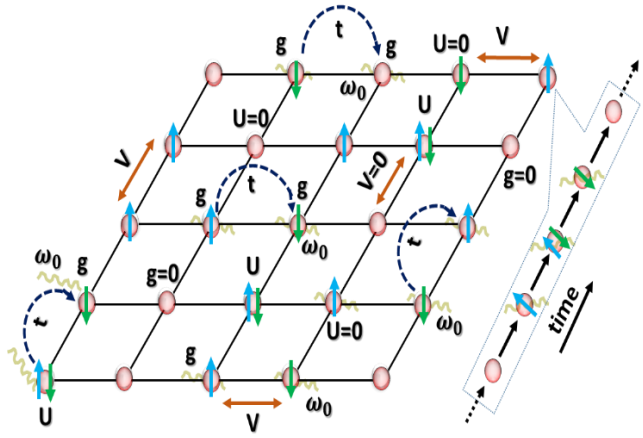

Fig. 1.1 Schematic representation of a 2D extended Holstein-Hubbard model: The onsite *e-e* interaction, *e-p* coupling and NN *e-e* interaction in a square lattice as described by the extended HH model. Electrons hop from one site to another with the probability amplitude t. When an electron hops from one site to another, it gives up a phonon of frequency ω_0 to a lattice site where it goes and another phonon of the frequency ω_0 may be emitted by the same electron when it leaves that lattice site. The quantum fluctuations in the occupation of electrons on a lattice site are indicated by the time sequence. A lattice site can either be unoccupied, or singly occupied ($\uparrow$ / $\downarrow$) or doubly occupied ($\uparrow\downarrow$). The pairing an electron with another electron costs an amount of energy $U > 0$.

We consider a lattice of atoms, each of which has a single atomic energy level that can be occupied by at most two electrons with opposite spins. That is, we are restricting ourselves to the study of the non-degenerate single-band HH model. A half-filled band case here thus means that each atom contributes exactly one electron to the band, i.e., there are just as many electrons as the total number of lattice sites

($n = N_e/N = 1$). Each site can have four possibilities for the occupation of electrons: empty $|0\rangle$, singly occupied either with spin-up $|\uparrow\rangle$ or spin-down $|\downarrow\rangle$ and doubly occupied $|\uparrow\downarrow\rangle$. In the case of a band that is less than half-filled, the system tries to avoid configurations with doubly occupied sites because it costs an additional energy $U > 0$. Similarly, for a system with a band that is more than half-filled, one expects to encounter configurations that would avoid empty sites.

As is well known, the hopping term (alone) has an exact solution in both the Bloch and the Wannier bases, the Hubbard part (i.e., the hopping term plus the onsite correlation term) has an exact solution in one dimension and the free phonon term together with the *e-p* interaction term can also be exactly diagonalized using the coherent state transformation, but unfortunately the total Hamiltonian cannot be solved exactly. In fact, the presence of *e-p* interaction makes it impossible to solve the Hamiltonian ⟨1.1⟩ exactly in the thermodynamic limit in any dimensions. To make progress, one normally considers the total wave function according to the Born-Oppenheimer approximation which allows one to write the total wave function as a product of the wave functions of the electronic and the phononic subsystems as follows:

$$\Psi = \psi(\{\boldsymbol{r}_i\}) \times \phi_{\boldsymbol{r}}(\{\boldsymbol{R}_i\}) = |\psi\rangle \times e^{-\mathcal{S}}|0\rangle$$

where $\{\boldsymbol{r}_i\}$ and $\{\boldsymbol{R}_i\}$ are the set of electron and phonon coordinates respectively, the operator $\mathcal{S}$ is a suitable anti-Hermitian operator which involves electron as well as phonon coordinates and $|0\rangle = \prod_i |0\rangle_i$ with $i = 1,2,3,4,5, \dots, N$, is the phonon vacuum or the zero-phonon state satisfying the condition $b_i|0\rangle_i = 0 \ \forall\, i$. The expectation value of the Hamiltonian ⟨1.1⟩ with respect to the total wave function Ψ is given by

$$E = \langle\Psi|\mathcal{H}|\Psi\rangle = \langle\psi|\,\langle 0|e^{\mathcal{S}}\mathcal{H}e^{-\mathcal{S}}|0\rangle\,|\psi\rangle = \langle\psi|\langle 0|\widetilde{\mathcal{H}}|0\rangle|\psi\rangle = \langle\psi|\,\mathcal{H}_e\,|\psi\rangle \quad \langle 1.2\rangle$$

where $\widetilde{\mathcal{H}} = e^{\mathcal{S}}\,\mathcal{H}\,e^{-\mathcal{S}}$ is the transformed Hamiltonian and $\mathcal{H}_e$ is the effective electron Hamiltonian obtained by taking the zero-phonon average of $\widetilde{\mathcal{H}}$. At lowest order, one may retain only the effective Hubbard part in $\mathcal{H}_e$ with renormalized hopping and correlation parameters t_e and U_e respectively. The problem then can be solved in 1D exactly using the nested Bethe ansatz technique following Lieb and Wu (LW) [16] and Shiba [17] and in 2D using several methods [18-29].

Now we shall qualitatively discuss about the possible GS's of the HH model for a half-filled band case. Since the onsite *e-p* interaction contributes a phonon-mediated attractive onsite *e-e* interaction, the repulsive *e-e* interaction and the *e-p* interaction together will give rise to an effective *e-e* interaction $U_e \equiv U_e(U, \mathrm{g})$ which can be either attractive or repulsive depending on the relative strengths of the interactions. If the *e-e* interaction is much stronger than the *e-p* interaction, the effective *e-e* interaction U_e will be still repulsive and favour localization of electrons. The GS will then be an antiferromagnetic Mott insulator or a polaronic spin-density wave insulator. On the other hand, if the *e-p* interaction is sufficiently large as compared to the *e-e* interaction, the effective *e-e* interaction U_e may become attractive favouring the formation of bound pairs of electrons at alternate sites. The GS will then be a Peierls insulator or a bipolaronic charge-density wave insulator. Therefore, it was generally believed, until 2003, that the GS of a HH system can be either an antiferromagnetic polaronic spin-density wave Mott insulator or a bipolaronic charge-density wave Peierls insulator [30,31] depending on the relative strengths of the onsite Coulomb correlation and the *e-p* interaction. The presence of the hopping term can of course make things more complicated.

Fazekas [32,33] has pointed out that a metal-insulator transition can occur at $U_e \sim W_e = 2zt_e$, where z is the coordination number. In 2003,

Takada and Chatterjee (TC) [34] have shown that there exists an *intervening metallic phase* at the cross-over region of the SDW phase and the CDW phase for a 1D HH model at half-filling [34,35]. One of the aims of the present thesis is to re-examine the results of TC [34] using the concept of quantum entanglement which can also be used to predict the nature of the GS's of a quantum many-particle system. We are also interested to study the existence of persistent current and the intervening metallic state in the GS of an extended HH quantum ring in the presence of Aharonov-Bohm flux at arbitrary band-fillings.

So far, we have discussed about a 1D HH model and the role played by the *e-e* and *e-p* interactions together with the hopping process and the nature of the phase transition at the cross-over region of the SDW and CDW phases. Now, we turn our attention to the effect of onsite and NN *e-p* interactions and their effects on the polaronic band width in the extended HH model in two dimension.

As discussed earlier, an electron moving in a polar lattice distorts the lattice in its vicinity creating a self-induced polarization potential with which it subsequently interacts giving rise to a quasi-particle called polaron. The nature of the GS of the system in this case depends on how strongly the lattice has been distorted by the electron. If the polarization potential created by the electron is very deep and the range of the potential is confined to a lattice distance, then the electron gets trapped in the self-created polarization potential forming as has been mentioned earlier a *small* or *localized polaron*. This happens in the case of strong *e-p* coupling. On the other hand, if the polarization potential happens to be shallow and is spread over several lattice points, the resulting quasi-particle is called the *large* or *mobile polaron*. As the *e-p* interaction is increased, a polaron can thus make a transition from a large polaron state to a small polaron

state. This is referred to as the *self-trapping* (ST) *transition.* Though there seems to be a good degree of unanimity as to the existence of such a transition, a general consensus over the nature of the transition is still lacking because of unavailability of its exact results even in one dimension.

There have been several investigations, both in 1D and 2D models [18,36-40] to examine whether the ST transition is continuous or abrupt. In the 2D HH model, Das and Sil (DS) [18] have studied the ST problem using a modified version of the celebrated Lang-Firsov (LF) transformation and an onsite squeezing transformation followed by a zero-phonon averaging of the transformed Hamiltonian and the Hartree-Fock approximation (HFA) for the effective electronic Hamiltonian. DS have shown that the ST transition is continuous in the anti-adiabatic ($t < \omega_0$) regime and discontinuous in the adiabatic ($t > \omega_0$) regime and they have attributed the discontinuity appearing in the adiabatic regime to the insufficient number of variational parameters used in their trial wave function for the phonon subsystem. The ST transition in a 1D extended HH model has been studied later by Krishna *et al.* [39]. They have employed the modified LF, onsite and NN squeezing transformations and then performed a zero-phonon averaging of the transformed Hamiltonian and finally used for the effective electronic Hamiltonian both the exact method of LW [16] and the HFA at half-filling. Their LW results suggest that the ST transition is continuous for both adiabatic and anti-adiabatic regimes, while the HFA solution provide, even after using the improved variational phonon state, qualitatively the same results as those of DS. Thus the contention of DS that the discontinuity in the ST transition is due to the insufficient number of parameters used in the variational wave function for the phonon subsystem is still a unresolved issue and requires a more critical investigation. In the present thesis, we

are interested in studying the ST transition problem in an extended HH model in 2D using a better variational phonon state than the one chosen by Krishna *et al.* [39].

1.2 ORGANIZATION OF THE THESIS

First of all we would like to mention that throughout this thesis, we use $\hbar\omega_0 = 1$, where ω_0 is the phonon frequency, i.e., we measure all energies in units of phonon energy.

In the chapter immediately following i.e., in **CHAPTER 2**, we consider a quantum ring in the presence of magnetic flux within the framework of the 1D extended HH model and obtain the persistent current and the GS phase diagram in the $g - U$ space. The phonon degrees of freedom are eliminated through the conventional LF transformation followed by a zero-phonon averaging. Finally the effective extended Hubbard model is solved by employing the HFA. The persistent current is found to be suppressed by the onsite *e-e*, *e-p* and NN *e-p* interactions. The phase diagram of the system shows the existence of an unexpected metallic phase in the GS, when *e-e* and *e-p* are comparable to each other. Also the width of the metallic phase is found to increase with the reduction in the electron density from the half-filling.

In **CHAPTER 3**, we consider a 1D HH model in the thermodynamic limit at $T = 0$ and eliminate the phonons by choosing a variational phonon state and solve the resultant effective Hubbard model exactly using the nested Bethe ansatz technique. With the help of the GS energy we calculate the double occupancy and single-site entanglement entropy

for all band fillings. The phase diagram shows the emergence of an intermediate metallic phase in the half-filled band case flanked by SDW and CDW insulating phases confirming the predictions of Takada and Chatterjee [34].

In **CHAPTER 4**, we consider a 2D HH model in the weak correlation regime $(U \ll t)$ and study the effect of *e-p* interaction on the GS. We find that the transition of a polaron from a large polaron state to a small polaron state is continuous in the anti-adiabatic regime whereas it is discontinuous in the adiabatic regime. Here, we consider an improved variational wave function for the phonon subsystem to examine the nature of the self-trapping transition. We confirm that the nature of the self-trapping transition does not change by just improving the variational phonon state.

CHAPTER 5 is devoted to the study of a 2D HH model in the strong correlation regime $(U \gg t)$. We find that even for strong *e-e* correlations in the quarter-filled band case, the electron undergoes the self-trapping transition for strong *e-p* interactions. Furthermore, the nature of the self-trapping transition turns out to be same as in Chapter 4. We obtain the self-trapping line and the surface which basically separate the small polaron and large polaron regions.

Finally, in **CHAPTER 6,** we present our conclusion in which we give a brief summary of our results and make a few comments on our findings.

REFERENCES

[1] N.F. Mott & R. Peierls, *Discussion of the paper by De Boer and Verwey*, Proc. Roy. Soc. London. Ser. A **49**, 72 (1937).

[2] N.F. Mott, *The basis of the theory of electron metals, with special reference to the metals*, Proc. Roy. Soc. London. Ser. A **62**, 416 (1949).

[3] J. Hubbard, *Electron correlations in narrow energy bands I, II & III*, Proc. R. Soc. London, A **276**, 238 (1963); *ibid*. **277**, 237 (1964); *ibid*. **281**, 401 (1964).

[4] T.K. Mitra, A. Chatterjee & S. Mukhopadhyay, *Polarons*, Phys. Rep. **153**, 91 (1987).

[5] J. Devreese, *Polarons*, arXiv:cond-mat/0004497 (2000).

[6] D. Emin, *Polarons*, Cambridge University Press (2013).

[7] A.S. Alexandrov & N.F. Mott, *Bipolarons*, Rep. Prog. Phys. B **57**, 1197 (1994).

[8] J.T. Devreese & A.S. Alexandrov, *Fröhlich polaron and bipolaron: recent developments*, Rep. Prog. Phys. **72**, 066501 (2009).

[9] R. Peierls, *More Surprises in Theoretical Physics*, Princeton University Press (1991).

[10] T. Holstein, *Studies of polaron motion I & II*, Ann. Phys. (N.Y.) **8**, 325 (1959) *ibid*. **8**, 343 (1959).

[11] J.P. Falck, A. Levy, M.A. Kastner & R.J. Birgeneau, *Optical excitation of polaronic impurities in* La_2CuO_{4+y}, Phys. Rev. B **48**, 4043 (1993).

[12] X.-X. Bi & P.C. Eklund, *Polaron contribution to the infrared optical response of* $La_{2-x}Sr_xCuO_{4+\delta}$ *and* $La_{2-x}Sr_xNiO_{4+\delta}$, Phys. Rev. Lett. **70**, 2625 (1993).

[13] G.-M. Zhao, M.B. Hunt, H. Keller & K.A. Müller, *Evidence for polaronic supercarriers in the copper oxide SC's* $La_{2-x}Sr_xCuO_4$, Nature **385**, 236 (1997).

[14] G.-M. Zhao, K. Conder, H. Keller & K.A. Müller, *Giant oxygen isotope shift in the magnetoresistive perovskite* $La_{1-x}Ca_xMnO_{3+y}$, Nature **381**, 676 (1996).

[15] H. Röder, J. Zang & A.R. Bishop, *Lattice effects in the colossal-magnetoresistance manganites*, Phys. Rev. Lett. **76**, 1356 (1996).

[16] E. Lieb & F. Wu, *Absence of Mott transition in an exact solution of the short-range, one-band model in one-dimension*, Phys. Rev. Lett. **20**, 1445 (1968).

[17] H. Shiba, *Magnetic susceptibility at zero temperature for the 1D Hubbard model*, Phys. Rev. B **6**, 930 (1972).

[18] A.N. Das & S. Sil, *A study of the polaronic band width and the small-large-polaron transition in a many-polaron system*, J. Phys.: Condens. Matter **5**, 8265 (1993).

[19] F. Mancini, S. Marra & H. Matsumoto, *Spin magnetic susceptibility in the two-dimensional Hubbard model*, Physics C **252**, 361 (1995).

[20] G. Kotliar & D. Vollhardt, *Strongly correlated materials: Insights from dynamical mean-field theory*, Phys. Today **57**, 53 (2004).

[21] A.N. Rubtsov, M.I. Katsnelson, A.I. Lichtenstein & A. Georges, *Dual fermion approach to the 2D Hubbard model: Antiferromagnetic fluctuations and Fermi arcs*, Phys. Rev. B **79**, 045133 (2009).

[22] M. Kohno, *Mott transition in the 2D Hubbard model*, Phys. Rev. Lett. **108**, 076401 (2012).

[23] Y. Yanagi & K. Ueda, *Continuous Mott transition in a 2D Hubbard model*, Phys. Rev. B **90**, 085113 (2014).

[24] E.G.C.P. van Loon *et al.*, *Beyond extended DMFT: Dual boson approach to the 2D extended Hubbard model*, Phys. Rev. B **90**, 235135 (2014).

[25] J.P.F. LeBlanc *et al.*, *Solutions of the 2D Hubbard model: Benchmarks and results from wide range of algorithms*, Phys. Rev. X **5**, 041041 (2015).

[26] X. Chen, J.P.F. LeBlanc & E. Gull, *Superconducting fluctuations in the normal state of the 2D Hubbard model*, Phys. Rev. Lett. **115**, 116402 (2015).

[27] B.-X. Zheng & G.K.-L.Chan, *GS phase diagram of the square lattice Hubbard model from density matrix embedding theory*, Phys. Rev. B **93**, 035126 (2016).

[28] P. Corboz, *Improved energy extrapolation with infinite projected entangled-pair states applied to the 2D Hubbard model*, Phys. Rev. B **93**, 045116 (2016).

[29] T. Schäfer, A. Toschi & K. Held, *Dynamical vertex approximation for the two-dimensional Hubbard model*, J. Magn. Magn. Mater. **400**, 107 (2016).

[30] J.E. Hirsch & E. Fradkin, *Phase diagram of 1D electron-phonon systems. II. The molecular-crystal model*, Phys. Rev. B **27**, 4302 (1983).

[31] J.E. Hirsch, *Phase diagram of the 1D molecular-crystal model with Coulomb interactions: Half-filled-band sector*, Phys. Rev. B **31**, 6022 (1985).

[32] P. Fazekus, *Lectures notes on electron correlation and magnetism*, World Scientific Publishing Co. Pte. Ltd. (1999).

[33] E. Fradkin, *Field theories in condensed matter physics*, Cambridge Univ. Press (2013).

[34] Y. Takada & A. Chatterjee, *Possibility of a metallic phase in the CDW-SDW crossover region in the 1D HH model at half-filling*, Phys. Rev. B **67**,081102 (R) (2003).

[35] P.M. Krishna & A. Chatterjee, *Existence of a metallic phase in 1D HH model at half-filling*, Physica C **457**, 55 (2007).

[36] Y. Toyozawa, *Self-trapping of an electron by the acoustical mode of lattice vibration I*, Prog. Theor. Phys. **26**, 29 (1961).

[37] H. Löwen, *Absence of phase transition in Holstein systems*, Phys. Rev. B **22**, 57 (1973).

[38] A. Chatterjee & S. Sil, *Phase transition in a many-electron gas in a 2D polar-semiconductor quantum well*, Phys. Rev. B **51**, 2223 (1995).

[39] R.P.M. Krishna, S. Mukhopadhyay & A. Chatterjee, *Nature of self-trapping transition in a 1D HH model*, Phys. Lett. A **327**, 67 (2004).

[40] E. Jeckelmann & S.R. White, *DMRG study of the polaron problem in the Holstein model*, Phys. Rev. B **57**, 6378 (1998).

CHAPTER 2

PERSISTENT CURRENT IN AN EXTENDED HOLSTEIN-HUBBARD QUANTUM RING

ABSTRACT

The aim of the present chapter is to calculate the *persistent current* and explore the possibility of *existence of an intervening metallic state* in the ground state of an *extended Holstein-Hubbard quantum ring* in the presence of *Aharonov-Bohm flux* at arbitrary band-fillings within the framework of *Hartree-Fock mean-field theory*.

2.1 INTRODUCTION

The magnetic flux Φ passing through an isolated quantum ring (QR) generates a nondissipative current $I(\Phi)$ in its ground state (GS) [1]. This, so called, persistent current (PC) has its genesis in a quantum mechanical phase coherence effect that shows up when the GS wave function has the coherence length of the order of the system size, a condition that is easily achievable in quantum dots and QR's. In other words, when a magnetic flux passes through an isolated QR, an equilibrium PC is produced so as to minimize the energy of the system. This PC has an interesting property of being periodic with a period Φ_0 equal to hc/e, where e the electron charge, c the velocity of light and h is the Planck's constant. Also, it is a piecewise linear function of Φ with finite discontinuities at $\Phi = \Phi_0/2$. Thus a QR with a magnetic flux passing through it can be thought of as an isolated artificial spin [2] and can be used as a qubit, for we have the flexibility of changing the orientation of the spin according to our wish. Several experiments [3-11] have already confirmed the existence of PC in QR's. Some studies have revealed that PC decreases with increasing number of atoms in a QR [12,13]. Though there have been several reports in the literature on PC in a Hubbard QR, no study has been made so far, to our knowledge, on the Holstein-Hubbard (HH) QR. The HH QR is more interesting because the electron-phonon (*e-p*) interaction can change the nature of the GS altogether. The aim of this chapter is to study the combined effect of electron-electron (*e-e*) and *e-p* interactions on PC in a HH QR and unravel the GS phase diagram which shows the existence of a metallic phase sandwiched between spin-density wave (SDW) and charge-density wave (CDW) insulating phases at $T = 0$ in the absence of any scattering centres and self-inductance of the QR. In our system, the magnetic flux passes

through the ring axially and the electrons move in a field-free region. The phase of the wave function of the electron changes by the Aharonov-Bohm (AB) effect. We shall treat the interacting electrons within the framework of the self-consistent Hartree-Fock (HF) mean-field approximation (MFA).

2.2 THE EXTENDED HOLSTEIN-HUBBARD MODEL

The extended HH model in the presence of AB flux is given by

$$\mathcal{H} = -\,t\,e^{i\phi}\sum_{\langle ij\rangle\sigma} c_{i\sigma}^{\dagger}c_{j\sigma} + U\sum_{i} n_{i\uparrow}n_{i\downarrow} + \omega_0\sum_{i} b_i^{\dagger}b_i + \mathrm{g}_0\sum_{i\sigma} n_{i\sigma}\left(b_i + b_i^{\dagger}\right) + \mathrm{g}_1\sum_{\langle ij\rangle\sigma} n_{i\sigma}\left(b_j + b_j^{\dagger}\right) \qquad \langle 2.1\rangle$$

where most of the notations have already been introduced in Chapter 1. The last term describes the nearest-neighbor (NN) *e-p* interaction with the interaction strength g_1. In the presence of the magnetic flux, the basis of the Hilbert space of each electron do acquire a phase which depends on the magnetic flux. The phase factor is $\phi = 2\pi(\Phi/\Phi_0)/N$, where N is the total number of sites. In general, the presence of *e-p* interactions makes it impossible to solve the Hamiltonian ⟨2.1⟩ exactly. As already pointed out in Chapter 1, we first perform a canonical transformation using a suitable generator. Since the *e-p* interactions in Hamiltonian ⟨2.1⟩ are linear in the phonon operators, the appropriate variational state for the phonon subsystem can be chosen in the form of a coherent state. This can be accomplished by performing a modified version of the conventional Lang-Firsov (LF) transformation [14] followed by an averaging of the transformed Hamiltonian $\widetilde{\mathcal{H}}$ with respect to the zero-phonon state

$|0\rangle = \prod_i |0\rangle_i$, where i runs over N sites. This gives an effective electronic Hamiltonian $\mathcal{H}_e$ which we finally solve using the mean-field HF approximation. Let us now carry out, in the next section, the LF transformation to obtain the transformed Hamiltonian $(\widetilde{\mathcal{H}})$.

2.3 THE LANG-FIRSOV TRANSFORMATION

We first consider a modified LF transformation [15-19] with a generator

$$\mathcal{S} = \frac{g_0'}{\omega_0} \sum_{i\sigma} n_{i\sigma} \left(b_i^\dagger - b_i\right) + \frac{g_1'}{\omega_0} \sum_{\langle ij\rangle\sigma} n_{i\sigma} \left(b_j^\dagger - b_j\right), \qquad \langle 2.2\rangle$$

where g_0' gives a measure of the depth of the lattice polarization potential created due to lattice distortion induced by the electron, while g_1' gives the spread of the lattice polarization potential. Both the variational parameters g_0' and g_1' will become dependent on the electron density or the filling factor through the minimization procedure. In the strong coupling regime, it turns out that $g_0' = g_0$ and $g_1' = g_1$, which would correspond to the conventional LF transformation for the extended HH model. The original LF transformation results if $g_0' = g_0$ and $g_1' = 0$. One may note that the LF transformation assumes that the phonon coherence coefficient depends linearly on the electron concentration n_i. The transformed Hamiltonian $\widetilde{\mathcal{H}}_1$ can be written as

$$\widetilde{\mathcal{H}}_1 = e^{\mathcal{S}}\, \mathcal{H}\, e^{-\mathcal{S}} = \mathcal{H} + [\mathcal{S}, \mathcal{H}] + \frac{1}{2!}\big[\mathcal{S}, [\mathcal{S}, \mathcal{H}]\big] + \frac{1}{3!}\Big[\mathcal{S}, \big[\mathcal{S}, [\mathcal{S}, \mathcal{H}]\big]\Big] + \cdots,$$

where we have used the Baker-Campbell-Hausdorff (BCH) formula. Let us first calculate the transformation of the hopping term using BCH formula.

$$\left[\mathcal{S}, \sum_{\langle ij\rangle\sigma} c_{i\sigma}^{\dagger} c_{j\sigma}\right]$$

$$= \left[\frac{g_0'}{\omega_0}\sum_{i'\sigma'} n_{i'\sigma'}\left(b_{i'}^{\dagger} - b_{i'}\right) + \frac{g_1'}{\omega_0}\sum_{\langle i'j'\rangle\sigma'} n_{i'\sigma'}\left(b_{j'}^{\dagger} - b_{j'}\right), \sum_{\langle ij\rangle\sigma} c_{i\sigma}^{\dagger} c_{j\sigma}\right]$$

$$= \frac{g_0'}{\omega_0}\sum_{i'\sigma'}\sum_{\langle ij\rangle\sigma}\left(b_{i'}^{\dagger} - b_{i'}\right)\left[n_{i'\sigma'}, c_{i\sigma}^{\dagger} c_{j\sigma}\right] + \frac{g_1'}{\omega_0}\sum_{\langle ij\rangle\sigma}\sum_{\langle i'j'\rangle\sigma'}\left(b_{j'}^{\dagger} - b_{j'}\right)\left[n_{i'\sigma'}, c_{i\sigma}^{\dagger} c_{j\sigma}\right]$$

Using the relation: $[AB, CD] = A\{B, C\}D - AC\{B, D\} + \{A, C\}DB - C\{A, D\}B$, we can simplify the above commutators to obtain

$$\left[\mathcal{S}, \sum_{\langle ij\rangle\sigma} c_{i\sigma}^{\dagger} c_{j\sigma}\right] = \sum_{\langle i'j'\rangle\sigma'} c_{i'\sigma'}^{\dagger}\, c_{j'\sigma'}\left(Y_{i'} - Y_{i'+\delta}\right),$$

where

$$Y_{i'} = \frac{g_0'}{\omega_0}\left(b_{i'}^{\dagger} - b_{i'}\right) + \frac{g_1'}{\omega_0}\sum_{\delta}\left(b_{i'+\delta}^{\dagger} - b_{i'+\delta}\right).$$

Next we have

$$\left[\mathcal{S}, \left[\mathcal{S}, \sum_{\langle ij\rangle\sigma} c_{i\sigma}^{\dagger} c_{j\sigma}\right]\right] = \left[\mathcal{S}, \sum_{\langle i'j'\rangle\sigma'} c_{i'\sigma'}^{\dagger}\, c_{j'\sigma'}\left(Y_{i'} - Y_{i'+\delta}\right)\right]$$

$$= \sum_{\langle i'j'\rangle\sigma'} c_{i'\sigma'}^{\dagger}\, c_{j'\sigma'}\left(Y_{i'} - Y_{i'+\delta}\right)^2,$$

and so on. Finally, we can write the transformed hopping term as

$$e^{\mathcal{S}}\left(-t\sum_{\langle ij\rangle\sigma}c_{i\sigma}^{\dagger}c_{j\sigma}\right)e^{-\mathcal{S}}=-t\sum_{\langle ij\rangle\sigma}c_{i\sigma}^{\dagger}c_{j\sigma}\,\boldsymbol{e}^{(Y_i-Y_{i+\delta})}. \qquad \langle 2.3\rangle$$

Similarly, we can transform the free phonon and the *e-p* interaction terms as shown below.

$$e^{\mathcal{S}}\left(\omega_0\sum_i b_i^{\dagger}b_i\right)e^{-\mathcal{S}}$$

$$=\omega_0\sum_i b_i^{\dagger}b_i-\mathrm{g}_0'\sum_{i\sigma}n_{i\sigma}\left(b_i^{\dagger}+b_i\right)+\mathrm{g}_1'\sum_{\langle ij\rangle\sigma}n_{i\sigma}\left(b_j^{\dagger}+b_j\right)$$

$$+\frac{\left(\mathrm{g}_0'^{\,2}+z\,\mathrm{g}_1'^{\,2}\right)}{\omega_0}\sum_{i\sigma\sigma'}n_{i\sigma}\,n_{i\sigma'}+\frac{2\mathrm{g}_0\,\mathrm{g}_1'}{\omega_0}\sum_{\langle ij\rangle\sigma\sigma'}n_{i\sigma}n_{j\sigma'}+\frac{\mathrm{g}_1'^{\,2}}{\omega_0}\sum_{i\delta'\sigma\sigma'}n_{i\sigma}n_{i+\delta',\sigma'}, \qquad \langle 2.4\rangle$$

and

$$e^{\mathcal{S}}\left(\mathrm{g}_0\sum_{i\sigma}n_{i\sigma}\left(b_i+b_i^{\dagger}\right)+\mathrm{g}_1\sum_{\langle ij\rangle\sigma}n_{i\sigma}\left(b_j+b_j^{\dagger}\right)\right)e^{-\mathcal{S}}$$

$$=\mathrm{g}_0\sum_{i\sigma}n_{i\sigma}\left(b_i+b_i^{\dagger}\right)+\mathrm{g}_1\sum_{\langle ij\rangle\sigma}n_{i\sigma}\left(b_j+b_j^{\dagger}\right)-\frac{2}{\omega_0}\left(\mathrm{g}_0\,\mathrm{g}_0'+z\,\mathrm{g}_1\,\mathrm{g}_1'\right)\sum_{i\sigma\sigma'}n_{i\sigma}\,n_{i\sigma'}$$

$$-\frac{2}{\omega_0}\left(\mathrm{g}_0\,\mathrm{g}_1'+z\,\mathrm{g}_1\,\mathrm{g}_0'\right)\sum_{\langle ij\rangle\sigma\sigma'}n_{i\sigma}\,n_{j\sigma'}-\frac{2}{\omega_0}\,\mathrm{g}_1\mathrm{g}_1'\sum_{i\delta'\sigma\sigma'}n_{i\sigma}\,n_{i+\delta',\sigma'}. \qquad \langle 2.5\rangle$$

From Eqs. ⟨2.4⟩ and ⟨2.5⟩, we can observe that the LF transformation induces various *e-e* interaction terms which include onsite, NN and next NN *e-e* interaction terms. Other electronic terms in the original Hamiltonian are invariant under the LF transformation. The total transformed Hamiltonian is finally obtained, after neglecting the NN and next NN *e-e* interaction terms, as

$$\widetilde{\mathcal{H}}_1 = \epsilon_0 \sum_{i\sigma} n_{i\sigma} - t\, e^{i\phi} \sum_{\langle ij\rangle\sigma} e^{(Y_i - Y_j)}\, c_{i\sigma}^{\dagger}\, c_{j\sigma} + \widetilde{U} \sum_{i} n_{i\uparrow}\, n_{i\downarrow} + \omega_0 \sum_{i} b_i^{\dagger}\, b_i$$
$$+ (\mathrm{g}_0 - \mathrm{g}_0') \sum_{i\sigma} n_{i\sigma} \left(b_i + b_i^{\dagger}\right) + (\mathrm{g}_1 - \mathrm{g}_1') \sum_{\langle ij\rangle\sigma} n_{i\sigma} \left(b_j + b_j^{\dagger}\right), \qquad \langle 2.6 \rangle$$

where

$$\epsilon_0 = \frac{1}{\hbar\omega_0}\left[\, 2\,(\mathrm{g}_0\, \mathrm{g}_0' + z\, \mathrm{g}_1\, \mathrm{g}_1') - \left(\mathrm{g}_0'^{\,2} + z\, \mathrm{g}_1'^{\,2}\right)\right], \qquad \langle 2.6a \rangle$$

$$\widetilde{U} = U - \frac{2}{\hbar\omega_0}\left[\, 2\,(\mathrm{g}_0\, \mathrm{g}_0' + z\, \mathrm{g}_1\, \mathrm{g}_1') - \left(\mathrm{g}_0'^{\,2} + z\, \mathrm{g}_1'^{\,2}\right)\right]. \qquad \langle 2.6b \rangle$$

To simplify matters, we consider: $\mathrm{g}_0' = \mathrm{g}_0$ and $\mathrm{g}_1' = \mathrm{g}_1$. This particular choice of parameters eliminates both onsite and NN *e-p* interaction terms as it is clearly apparent from Eq.⟨2.6⟩. The effective Hubbard Hamiltonian is obtained by taking the zero-phonon average of $\widetilde{\mathcal{H}}_1$ as

$$\mathcal{H}_e = \langle 0|\, \widetilde{\mathcal{H}}_1\, |0\rangle = -\epsilon_0 \sum_{i\sigma} n_{i\sigma} - t_e\, e^{i\phi} \sum_{\langle ij\rangle\sigma} c_{i\sigma}^{\dagger}\, c_{j\sigma} + U_e \sum_{i} n_{i\uparrow}\, n_{i\downarrow}, \qquad \langle 2.7 \rangle$$

where

$$\varepsilon_e = \frac{1}{\omega_0}\left(\, \mathrm{g}_0^2 + z\, \mathrm{g}_1^2\,\right), \qquad \langle 2.7a \rangle$$

$$U_e = U - \frac{2}{\omega_0}\left(\, \mathrm{g}_0^2 + z\, \mathrm{g}_1^2\,\right), \qquad \langle 2.7b \rangle$$

$$t_e = t\, \boldsymbol{e}^{-\left(\mathrm{g}_0 - \mathrm{g}_1\right)^2 + (z-1)\, \mathrm{g}_1^2\,]}. \qquad \langle 2.7c \rangle$$

For small *e-p* interaction strengths (compared to the bare *e-e* interaction strength), the effective hopping process can cause electrons to actuate from one site to the other, whereas the effective *e-e* interaction demands electrons to form localized spin magnetic moments at each site. The effective *e-e* interaction can be either positive or negative depending on

the relative strength of *e-e* and *e-p* interactions. For sufficiently large value of the bare *e-p* interaction, the effective *e-e* interaction becomes negative favouring the formation of localized bipolarons. The GS is then an insulating CDW state. On the other hand, if the effective *e-e* interaction becomes positive (which is possible when the *e-p* interaction is stronger than the *e-e* interaction), one has localized polarons. The GS state is then an insulating SDW state.

2.4 THE HARTREE-FOCK APPROXIMATION

In this section, we present the solution of the Hamiltonian ⟨2.7⟩ using Hartree-Fock approximation (HFA) [21] for a finite QR. This approximation looks very simple but provides a valuable insight into the physics of the model without changing its basic properties as far as the physics of metal-insulator transition (MIT) is concerned (though it may overestimate the critical value of U (U_c) , at which transition occurs). This approximation is reasonable for smaller electron densities and also if the band width dominates over the onsite *e-e* interaction. The role of HFA is basically to linearize the Coulomb correlation term by neglecting the fluctuation term as follows

$$n_{i\uparrow}n_{i\downarrow} = (n_{i\uparrow} - \langle n_{i\uparrow}\rangle + \langle n_{i\uparrow}\rangle)\,(n_{i\downarrow} - \langle n_{i\downarrow}\rangle + \langle n_{i\downarrow}\rangle)$$

$$= [\,\langle n_{i\downarrow}\rangle\,(n_{i\uparrow} - \langle n_{i\uparrow}\rangle) + \langle n_{i\downarrow}\rangle\,(n_{i\downarrow} - \langle n_{i\downarrow}\rangle)\,] + \underbrace{(n_{i\uparrow} - \langle n_{i\uparrow}\rangle)\,(n_{i\downarrow} - \langle n_{i\downarrow}\rangle)}_{\text{Fluctuations}}$$

$$\xrightarrow{\text{HFA}} n_{i\uparrow}\,\langle n_{i\downarrow}\rangle + n_{i\downarrow}\langle n_{i\uparrow}\rangle - \langle n_{i\uparrow}\rangle\,\langle n_{i\downarrow}\rangle\,.$$

The HFA, neglecting the fluctuations, allows us to treat the system as consisting of quasi-particles. These quasi-particles move freely in an

average potential created by all the other electrons and thus behave as uncorrelated electrons.

Without any loss of generality, we consider QR with an even number of sites and divide it into two sub-systems, namely, even-numbered sites ($\mathcal{A}$ sublattice) and odd-numbered sites ($\mathcal{B}$ sublattice). We then define the charge density ($n = N_e/N$), the CDW order parameter (c) and the SDW order parameter (s) for a given charge density (per site) as [20]:

$$2n = n_{\mathcal{A}\uparrow} + n_{\mathcal{A}\downarrow} + n_{\mathcal{B}\uparrow} + n_{\mathcal{B}\downarrow}, \qquad \langle 2.8a \rangle$$

$$2c = n_{\mathcal{A}\uparrow} + n_{\mathcal{A}\downarrow} - n_{\mathcal{B}\uparrow} - n_{\mathcal{B}\downarrow}, \qquad \langle 2.8b \rangle$$

$$2s = n_{\mathcal{A}\uparrow} - n_{\mathcal{A}\downarrow} - n_{\mathcal{B}\uparrow} + n_{\mathcal{B}\downarrow}, \qquad \langle 2.8c \rangle$$

where $n_{\mathcal{A}\sigma}$ and $n_{\mathcal{B}\sigma}$ are the average values of the operator $n_{i\sigma}$ for $i \in \mathcal{A}$ and $i \in \mathcal{B}$, respectively. Now we express the onsite *e-e* interaction term in terms of charge density and other order parameters as follows

$$\sum_i n_{i\uparrow} n_{i\downarrow} = \frac{U_e N_{\mathcal{AB},\sigma}}{2}(c - s) + \frac{U_e N_{\mathcal{AB},-\sigma}}{2}(c + s) + \frac{NU_e}{2}(n^2 - c^2 + s^2), \quad \langle 2.9 \rangle$$

where

$$N_{\mathcal{AB},\sigma} = (N_{\mathcal{A}\sigma} - N_{\mathcal{B}\sigma}) = \sum_{i\in\mathcal{A}} n_{i\sigma} - \sum_{i\in\mathcal{B}} n_{i\sigma}.$$

The linearized effective electronic Hamiltonian finally reduces to

$$\mathcal{H}_e = -\, t_e\, e^{i\phi} \sum_{\langle ij\rangle\sigma} c_{i\sigma}^{\dagger}\, c_{j\sigma} + \varepsilon_{A\sigma} \sum_{i\in\mathcal{A},\sigma} n_{i\sigma} + \varepsilon_{B\sigma} \sum_{i\in\mathcal{B},\sigma} n_{i\sigma} + K, \qquad \langle 2.10 \rangle$$

where

$$\varepsilon_{\mathcal{A}\uparrow} = -\varepsilon_0 + \frac{1}{2} U_e (n + c - s), \qquad \langle 2.10a \rangle$$

$$\varepsilon_{\mathcal{A}\downarrow} = -\varepsilon_0 + \frac{1}{2}U_e(n + c + s), \qquad \langle 2.10b \rangle$$

$$\varepsilon_{\mathcal{B}\uparrow} = -\varepsilon_0 + \frac{1}{2}U_e(n - c + s), \qquad \langle 2.10c \rangle$$

$$\varepsilon_{\mathcal{B}\downarrow} = -\varepsilon_0 + \frac{1}{2}U_e(n - c + s), \qquad \langle 2.10d \rangle$$

$$K = \frac{1}{4}N\,U_e(-n^2 - c^2 + s^2\,). \qquad \langle 2.10e \rangle$$

So far we could make only the spin-coupled Hamiltonian ⟨2.7⟩ into a spin separable Hamiltonian ⟨2.10⟩ and did not diagonalize the full Hamiltonian. The kinetic energy term is still in a non-diagonal form.

To diagonalize the hopping term we use the Fourier transformations

$$c_{j\sigma}^{\dagger} = \frac{1}{\sqrt{N}}\sum_k c_{k\sigma}^{\dagger}\, e^{ikja}, \qquad c_{j\sigma} = \frac{1}{\sqrt{N}}\sum_k c_{k\sigma}\, e^{-ikja}.$$

The hopping term then takes the diagonal form as

$$\sum_{\langle ij\rangle\sigma} c_{i\sigma}^{\dagger}c_{j\sigma} = 2\sum_{k\sigma} c_{k\sigma}^{\dagger}c_{k\sigma}\cos(ka), \qquad \langle 2.11 \rangle$$

Since we have divided the system (with a lattice constant a) into two subsystems (with lattice constants $2a$), each state k is coupled to the state $k + \frac{\pi}{a}$ as is clearly evident from the following two equations:

$$\sum_{i=1}^{N/2} c_i^{\dagger}c_i = \frac{1}{2}\sum_k c_k^{\dagger}c_k + \frac{1}{2}\sum_k c_k^{\dagger}c_{k+\left(\frac{\pi}{a}\right)}, \qquad \langle 2.12a \rangle$$

$$\sum_{i=1}^{N/2} c_i^{\dagger}c_i = \frac{1}{2}\sum_k c_k^{\dagger}c_k - \frac{1}{2}\sum_k c_k^{\dagger}c_{k+\left(\frac{\pi}{a}\right)}. \qquad \langle 2.12b \rangle$$

The effective Hamiltonian now reads in the first Brillouin zone (BZ) as

$$\mathcal{H}_e = \sum_{k\in \mathrm{BZ},\sigma} (\Delta_+^\sigma - \varepsilon_k) c_{k\sigma}^\dagger c_{k\sigma} + \sum_{k\in \mathrm{BZ},\sigma} (\Delta_+^\sigma + \varepsilon_k) c_{k+\left(\frac{\pi}{a}\right),\sigma}^\dagger c_{k+\left(\frac{\pi}{a}\right),\sigma}$$

$$+ \sum_{k\in \mathrm{BZ},\sigma} \Delta_-^\sigma \left(c_{k\sigma}^\dagger c_{k+\left(\frac{\pi}{a}\right),\sigma} + c_{k+\left(\frac{\pi}{a}\right),\sigma}^\dagger c_{k\sigma} \right) + K, \qquad \langle 2.13 \rangle$$

where

$$\varepsilon_k = 2\, t_e \cos(ka), \qquad \langle 2.13a \rangle$$

$$\Delta_\pm^\sigma = \frac{1}{2}(\varepsilon_{A\sigma} \pm \varepsilon_{B\sigma}). \qquad \langle 2.13b \rangle$$

To diagonalize Hamiltonian ⟨2.13⟩ we perform the Bogoliubov transformations

$$c_{k\sigma} = \cos(\theta_{k\sigma}) \alpha_{k\sigma} - \sin(\theta_{k\sigma})\, \beta_{k\sigma},$$

$$c_{k+\left(\frac{\pi}{a}\right),\sigma} = \sin(\theta_{k\sigma}) \alpha_{k\sigma} + \cos(\theta_{k\sigma})\, \beta_{k\sigma}.$$

with $\theta_{k\sigma} = \tan^{-1}[-(\Delta_-^\sigma/\varepsilon_k)]/2$. The Hamiltonian $\mathcal{H}_e$ is finally obtained in a fully diagonalized form in the reduced BZ (RBZ) ($-\frac{\pi}{2a} \leq k \leq \frac{\pi}{2a}$) as

$$\mathcal{H}_e = \sum_{k\in RBZ.\sigma} \left[E_{k\sigma}^\alpha\, \alpha_{k\sigma}^\dagger \alpha_{k\sigma} + E_{k\sigma}^\beta\, \beta_{k\sigma}^\dagger \beta_{k\sigma} \right] + K, \qquad \langle 2.14 \rangle$$

where

$$E_{k\sigma}^\alpha = \Delta_+^\sigma - x_k^\sigma, \qquad \langle 2.14a \rangle$$

$$E_{k\sigma}^\beta = \Delta_+^\sigma + x_k^\sigma, \qquad \langle 2.14b \rangle$$

$$x_k^\sigma = \varepsilon_k^2 + \Delta_-^\sigma\,. \qquad \langle 2.14c \rangle$$

Equations $\langle 2.14a\rangle$, $\langle 2.14b\rangle$ define the quasi-particle energies for each momentum k with spin σ. The order parameters c and s are given by

$$c = \frac{1}{N}\sum_{i,\sigma}\left[\langle n_{2i,\sigma} - n_{2i-1,\sigma}\rangle\right] = -\frac{1}{N}\sum_{k\in \mathrm{BZ},\sigma}\left(\frac{\Delta_-^{\sigma}}{x_k^{\sigma}}\right)\left[f_{\alpha,\sigma} - f_{\beta,\sigma}\right], \qquad \langle 2.15a\rangle$$

$$s = \frac{1}{N}\sum_{i}\left[\langle n_{2i,\uparrow} - n_{2i,\downarrow}\rangle + \langle n_{2i-1,\downarrow} - n_{2i-1,\uparrow}\rangle\right]$$

$$= -\left(\frac{1}{N}\right)\sum_{k\in \mathrm{BZ}}\left\{\left(\frac{\Delta_-^{\uparrow}}{x_k^{\uparrow}}\right)\left[f_{\alpha\uparrow} - f_{\beta\uparrow}\right] - \left(\frac{\Delta_-^{\downarrow}}{x_k^{\downarrow}}\right)\left[f_{\alpha\downarrow} - f_{\beta\downarrow}\right]\right\}, \qquad \langle 2.15b\rangle$$

where

$$f_{\alpha\sigma} = \langle \alpha_{k\sigma}^{\dagger}\alpha_{k\sigma}\rangle = \frac{1}{1 + e^{(E_{k\sigma}^{\alpha} - \mu)/k_BT}},$$

$$f_{\beta\sigma} = \langle \beta_{k\sigma}^{\dagger}\beta_{k\sigma}\rangle = \frac{1}{1 + e^{\left(E_{k\sigma}^{\beta} - \mu\right)/k_BT}},$$

In this work we are interested in the $T = 0$ case. Equations $\langle 2.15a\rangle$ and $\langle 2.15b\rangle$ can be used as self-consistent conditions to find the order parameters c and s. The GS energy of the HH model is finally obtained as

$$E(\Phi) = \sum_{k\in \mathrm{RBZ},\sigma}\left[E_{k\sigma}^{\alpha} f_{\alpha\sigma} + E_{k\sigma}^{\beta} f_{\beta\sigma}\right] + K. \qquad \langle 2.16\rangle$$

PC (I_{PC}) and the Drude weight (DW) (D) [23,24] are defined as

$$I_{PC}(\Phi) = -\frac{1}{2\pi}\frac{\mathrm{d}E(\Phi)}{\mathrm{d}\Phi}, \qquad \langle 2.17\rangle$$

$$D = \frac{N}{4\pi^2}\frac{\mathrm{d}^2E(\Phi)}{\mathrm{d}\Phi^2}\bigg|_{\Phi=\Phi_{\mathrm{m}}}, \qquad \langle 2.18\rangle$$

where Φ_m is the location of the minimum of $E(\Phi)$ which can be 0 or $1/2$ depending on the parity of the number of electrons in QR.

2.5 NUMERICAL RESULTS

We divide our numerical results into two parts. In the first part we show mainly the nature of PC and the effect of different interactions on it. In the second part, we construct several phase diagrams which show the existence of a metallic phase in between the two insulating phases (SDW and CDW) in half-filled and non-half-filled band cases.

(i) PERSISTENT CURRENT

The average electron density or the filling factor n can be defined as: $n = N_e/N$, where N_e is the total number of electrons and N, as defined earlier, is the total number of sites in a QR. Here, we consider $N = 200$, and perform calculations for several electron densities namely $n = 1$ (half-filled band case), $n = 0.99$ (nearly half-filled band case), $n = 0.5$ (quarter-filled band case), and $n = 0.49$ (nearly quarter-filled band case). In Fig. 2.1 we show results for a non-interacting tight-binding electron system for $n = 0.99$ with $t = 0.5,1$ and 1.5 and measure energies in terms of the phonon energy $(\hbar\omega_0)$. From Figs. 2.1(a) and 2.1(b), it is evident that the GS energy $E(\Phi)$ and PC $I_{PC}(\Phi)$ are periodic in Φ with period Φ_0. It is also clear that the GS energy decreases as the hopping parameter t increases, while the magnitude of PC, as expected, increases with increasing t. The observed periodicity of the GS energy and PC suggests that it is enough to plot figures for $|\Phi| \leq 1$. Fig. 2.1(c) shows the variation of DW as a function of the phase Φ for three values of t. One can easily

see that DW has the same periodicity as observed for the GS energy and PC. One may also note that qualitatively DW looks like a mirror image of the GS energy.

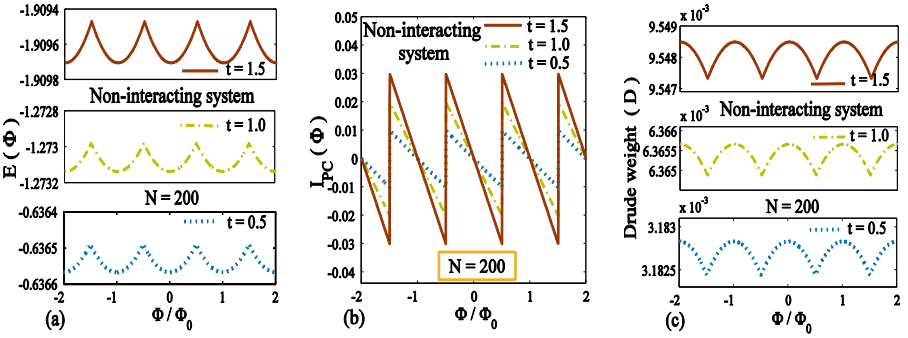

Fig. 2.1 Non-interacting ($\boldsymbol{U = 0}$, $\mathbf{g_0 = 0}$ **and** $\mathbf{g_1 = 0}$) QR with $\boldsymbol{N_e = 198}$ and $\boldsymbol{N = 200}$: (a) Ground state energy $E(\Phi)$ vs. Φ/Φ_0; (b) Persistent current $I_{PC}(\Phi)$ vs. Φ/Φ_0; (c) Drude weight D (after removing the points at discontinuities) vs. Φ/Φ_0 for different values of the hopping parameter (t).

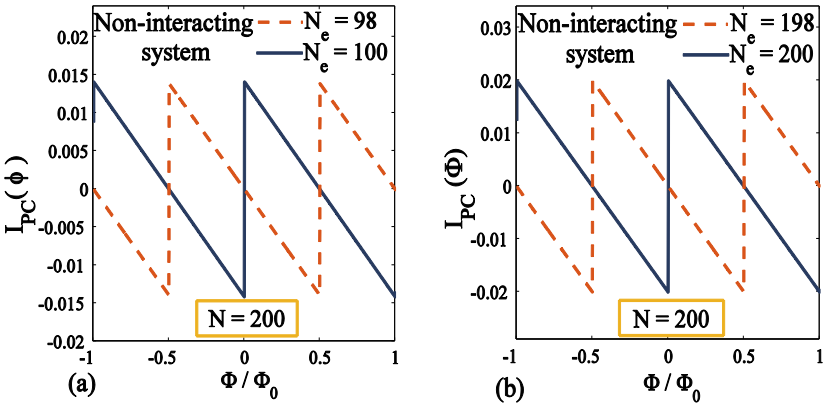

Fig. 2.2 Parity effects for a non-interacting QR ($\boldsymbol{U = 0}$, $\mathbf{g_0 = g_1 = 0}$) for $\boldsymbol{t = 1}$ with $\boldsymbol{N = 200}$: (a) Quarter ($N_e = 100$) and nearly quarter-filled ($N_e = 98$) and cases; (b) Half-filled ($N_e = 200$) nd nearly half-filled ($N_e = 198$) band cases.

In Fig. 2.2(a), we have plotted PC vs. Φ for a non-interacting QR for $t = 1$ with two different values of N_e, namely $N_e = 100$ and $N_e = 98$. PC in the two cases have exactly the opposite phases due to the parity effect [23,24]. Because of the removal of one electron each from the sub-

systems $\mathcal{A}$ and $\mathcal{B}$, both the sublattices contain 49 electrons each. Removing an electron causes the downward shift in the Fermi energy in QR. Similar explanation also holds good for Fig. 2.2(b).

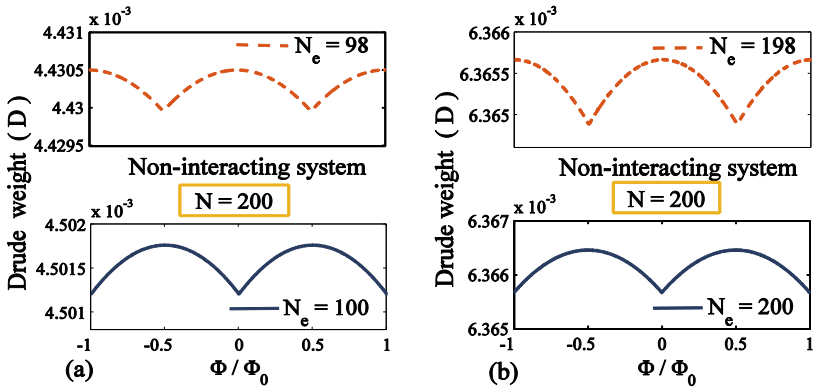

Fig. 2.3 Drude weights for a non-interacting QR ($\boldsymbol{U = 0, g_0 = g_1 = 0}$) for $\boldsymbol{t = 1}$ with $\boldsymbol{N = 200}$ as a function of $\boldsymbol{\Phi/\Phi_0}$: (a) Quarter ($N_e = 100$) and nearly quarter-filled ($N_e = 98$) band case; (b) Half-filled ($N_e = 200$) and nearly half-filled ($N_e = 198$) band case.

In Fig. 2.3(a) we show the behavior of DW for a non-interacting QR as a function of Φ for a quarter-filled and a nearly quarter-filled band case and in Fig. 2.3(b) for a half-filled and a nearly half-filled band case. The δ –function discontinuities at $\Phi_0/2$ have been removed to capture the over-all finite scale behavior of the DW. The parity effects are clearly visible. That the DW is finite and positive implies that QR is *metallic* and *diamagnetic* in nature.

In Fig. 2.4(a) we plot PC vs. Φ for several values of the *e-e* interaction strength in the absence of onsite *e-p* coupling. There have been several investigations for this case [25-27].

Our mean-field solution predicts that there is no sizable effect of U on the Φ– dependence of PC below a certain critical value of U (U_c) which depends on the value of t. In fact, the PC curves below U_c are essentially

degenerate with $U = 0$ curve. Above U_c, the magnitude of the PC decreases with increasing *e-e* interaction strength. Since MFA underestimates the *e-e* interaction, the hopping term below $U \cong U_c$ may dominate over the *e-e* interaction which then ceases to play any significant role. For example, at $U = 4.4$, the SDW order parameter s is found to have the value 0.791 for $t = 1$. As U is increased further, s approaches 1.0 confirming that the GS is an antiferromagnetic (AF) SDW insulator. To see explicitly the effect of U on PC and SDW order parameter, we plot the maximum value of $|I_{PC}|$ and s as a function of U

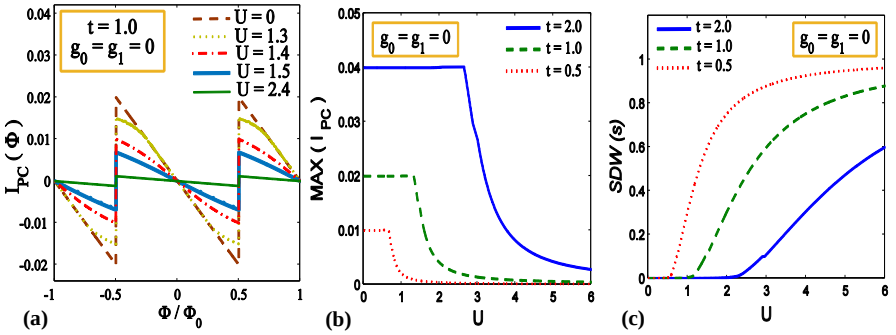

Fig. 2.4 Effect of *e-e* interaction on PC and the SDW order parameter in QR for $N_e = 198$ and $N = 200$ in the absence of e-p interaction: (a) $I_{PC}(\Phi)$ vs. Φ/Φ_0 for different values U; (b) $(I_{PC})_{max}$ vs. U for different values of t; (c) SDW order parameter (s) vs. U for different values of t.

in Fig. 2.4(b) and 2.4(c). The figures clearly show that there does exist a critical $U(U_c)$ for a given t such that $s = 0$ for $U < U_c$. For $t = 1$, we find that $U_c \sim 1.3$, which agrees with the result we have obtained from the I_{PC} vs. U graph (Fig. 2.4a). The result that U_c is proportional to t is easily understandable from the fact that a larger value of t leads to a larger mobility. The figures furthermore show that as t decreases, s approaches 1.0 at a smaller value of U. In other words, as U is increased, the system goes into a SDW state at a relatively smaller value of t. We conclude that the system undergoes a quantum phase transition

(QPT) at this point from a diamagnetic metallic state $(D > 0)$ to the AF Mott insulating state.

In Fig. 2.5(a) we plot PC vs. Φ for a QR system for several values of the *e-p* coupling constant and in Fig. 2.5(b) we plot PC as a function of the onsite *e-p* coupling constant g_0 for a HH QR in the absence of *e-e* and NN *e-p* interactions. The figure shows that unlike *e-e* interaction, the onsite *e-p* interaction has in general a stronger effect on PC. Thus, even at values much smaller than t, the onsite *e-p* interaction has an observable effect

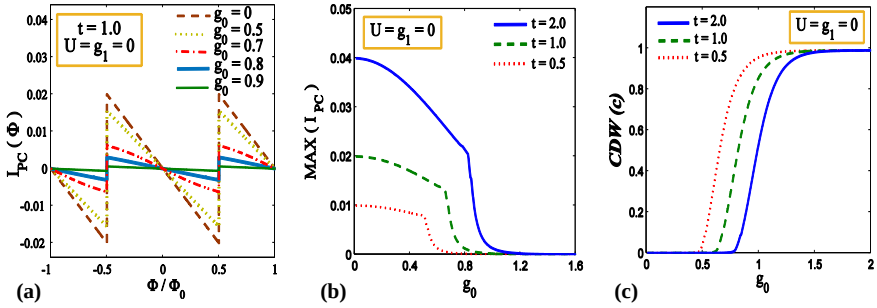

Fig. 2.5 Effect of $\mathbf{g_0}$ on PC and the CDW parameter in QR for $N_e = 198$ and $N = 200$ in the absence of *e-e* interaction: (a) $I_{PC}(\Phi)$ vs. Φ/Φ_0 for different values g_0; (b) $(I_{PC})_{max}$ vs. g_0 for different values of t; (c) CDW order parameter (c) vs. g_0 for different values of t.

on PC. Consequently, a considerable suppression in PC occurs at much smaller values of g_0 as compared to that of U. The behaviour of the CDW order parameter (c) as a function of g_0 is shown in Fig. 2.5(c). The figure clearly indicates that up to a critical g_0, c is essentially zero. As g_0 increases, c increases rather rapidly and reaches 1.0 at a value of g_0 which is more or less independent of t. The $c = 1$ state corresponds to a pure CDW (Peierls) insulating state. Thus here QR system undergoes a QPT from a diamagnetic metallic state to the Peierls CDW insulating state in a continuous and smooth way.

We have also studied the effect of g_1 on PC and the CDW order parameter in Fig. 2.6. The qualitative effect of the NN *e-p* interaction is found to be the same as that of the onsite *e-p* interaction, but the transition

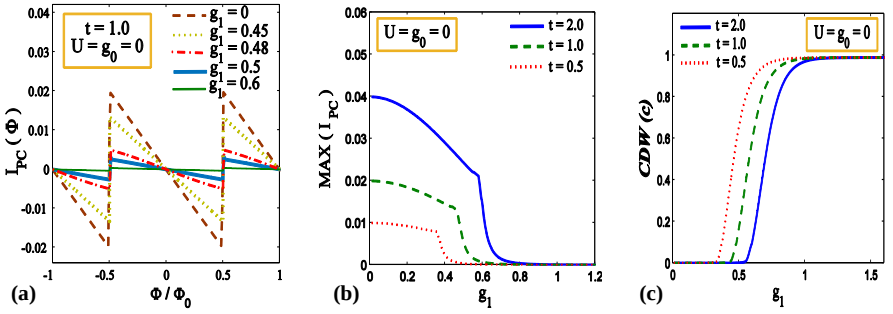

Fig. 2.6 Effect of g_1 on PC and the SDW parameter in QR for $N_e = 198$ and $N = 200$ in the absence of onsite *e-p* and *e-e* interactions: (a) $I_{PC}(\Phi)$ vs. Φ/Φ_0 for different values g_1; (b) $(I_{PC})_{max}$ vs. g_1 for different values of t; (c) CDW order parameter (c) vs. g_1 for different values of t.

from $c = 0$ to $c = 1$ occurs at lower values of g_1. Our results also indicate that the effect of NN *e-p* interaction is stronger than the onsite *e-p* interaction as is clearly evident from Eq. ⟨2.7*c*⟩.

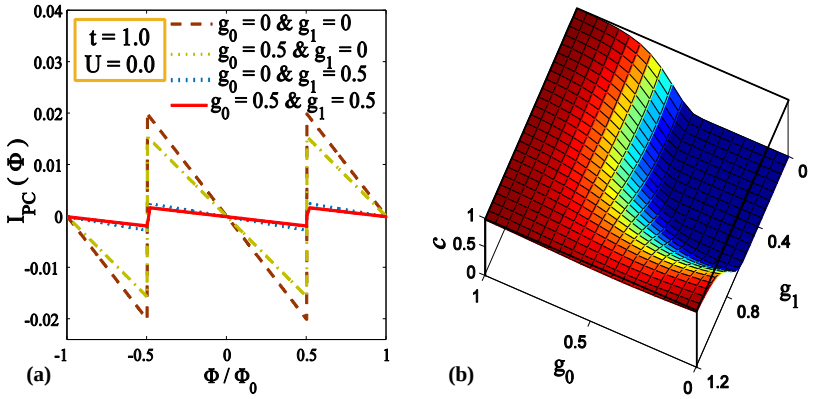

Fig. 2.7 Effect of both the onsite and the NN *e-p* interaction on PC in QR for $N_e = 198$ and $N = 200$ in the absence of the onsite *e-e* interaction: (a) $I_{PC}(\Phi)$ vs. Φ/Φ_0 for different combinations of g_0 and g_1; (b) c as a function of g_0 and g_1.

In Fig. 2.7 we study the combined effect of the onsite and the NN *e-p* interactions on PC and c. Interestingly, our results reveal that the NN *e-p* interaction has a more dominant effect than the on-site *e-p* interaction.

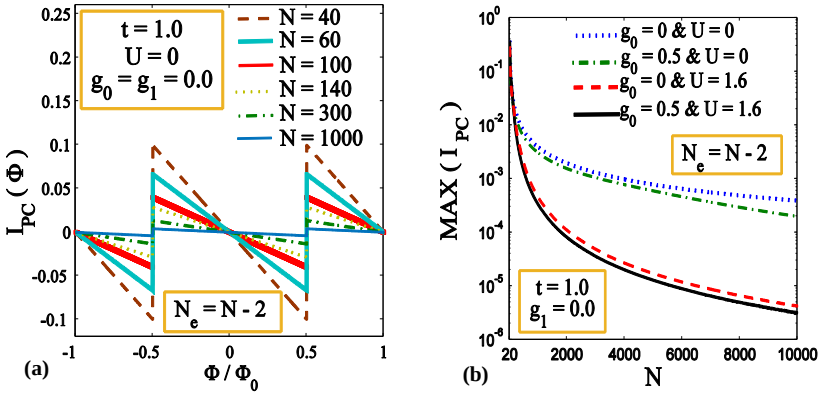

Fig. 2.8 PC in a QR with $N_e = (N-2)$: (a) PC vs. Φ/Φ_0 for different values of N for nonintercting QR; (b) $(I_{PC})_{max}$ vs. N for different combinations of U and g_0 at $g_1 = 0$.

In Fig. 2.8(a), we study the behavior of PC as a function Φ for several values of N in the absence of *e-e* and *e-p* interactions. The magnitude of PC in this case is found to decrease with increasing number of sites. In Fig. 2.8(b), we plot PC vs. N for different combinations of g_0 and U. PC clearly decreases with increasing N. The reason is understandable. For a small system, the electron wave function is coherent over the entire ring and this causes a larger current in the QR. We have chosen for our calculation: $N_e = (N-2)$. There is no specific reason for this choice and our results are in fact valid for all values of the band fillings.

(ii) EXISTENCE OF AN INTERVENING METALLIC PHASE

The presence of both the onsite *e-e* and the *e-p* interactions makes the situation a bit more complicated. Before we deal with this situation we shall make a few comments on the effective onsite *e-e* interaction

potential U_e. The value of U_e can be used to define the nature of the phase of a system. If U_e is less than $zero$, the interaction between the electrons will be attractive and the system is more likely to be found in the CDW phase for large negative U_e, while if $U_e > 0$, the *e-e* interaction will be repulsive and for large positive U_e, the GS of the system is expected to be a SDW state. In both cases, the hopping parameter would be smaller than U_e. Thus there exists a possibility of occurrence of an intermediate state for the system for which one would expect $U_e \sim 0$. In this case, the system could be found in a metallic state [15-17].

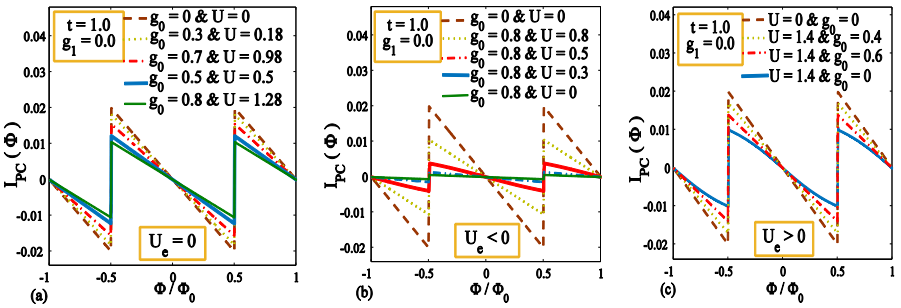

Fig. 2.9 Effect of both onsite *e-e* and *e-p* interactions on PC in QR with $N_e = 198$ and $N = 200$: (a) $U_e = 0$; (b) $U_e < 0$ and (c) $U_e > 0$.

As promised above, we now consider a few cases in which both *e-e* and *e-p* interactions exist together. Let us take $g_1 = 0$ for simplicity. We first consider $U_e = 0$ i.e., we choose U and g_0 in such a way that U_e is always $zero$. From Eq. ⟨2.7⟩ one can see that the effective Hamiltonian now describes just a tight-binding model with the effective hopping parameter t_e and the site energy ε_e. Thus analytically one can conclude that in this case the GS of the system should be metallic and the order parameters c and s would be $zero$. In Fig. 2.9(a) we plot the corresponding numerical results which clearly confirm the analytically predicted metallic behavior. Next we consider the case for which $U_e < 0$. Corresponding results are shown in Fig. 2.9(b). For large negative U_e, the

system's GS is a CDW state which is possible for small U and large g_0 values. Physically, a large g_0 value is expected to favour the formation of local electron pairs because a large *e-p* interaction would produce at a particular site a phonon-mediated strong attractive interaction between electrons that may dominate over the repulsive Coulomb interaction at the same site making the effective onsite interaction between electrons attractive. We also find that for a large value of g_0, the magnitude of the PC increases with increasing U. This may be due to the fact that with increasing U, U_e approaches $zero$ which corresponds to a metallic state. Finally, we consider the $U_e > 0$ case and the corresponding results are shown in Fig. 2.9(c). For small g_0 and large U values, U_e remains positive and the corresponding GS is an insulating SDW state.

To see the explicit nature of PC due to the simultaneous presence of both onsite *e-e* and *e-p* interactions, we display in Fig. 2.10, the behavior of $|(I_{PC})_{max}|$ as a function of g_0 and U, which is obviously a surface.

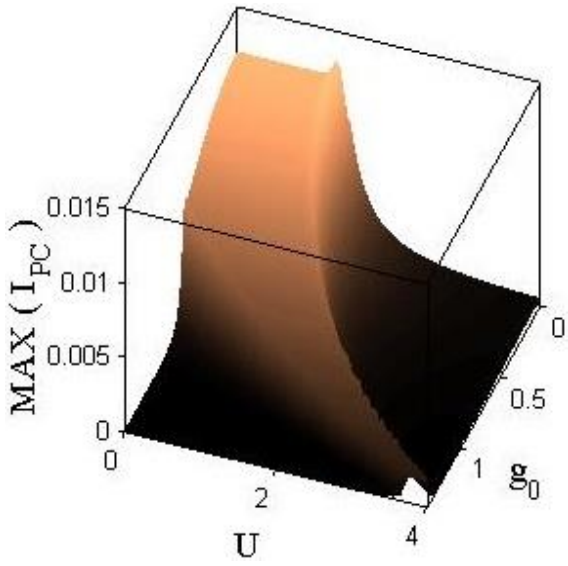

Fig. 2.10 PC as a function of g_0 and U for $t = 1$ and $g_1 = 0$.

The surface lying above the $g_0 - U$ plane corresponds to the metallic state whereas the one lying on the same plane corresponds to the insulating state.

To uncover the explicit nature of the phase transition we plot the 2D phase diagrams in the $g_0 - U$ plane. We draw the phase diagrams by calculating DW which is *positive* for a diamagnetic metallic phase and

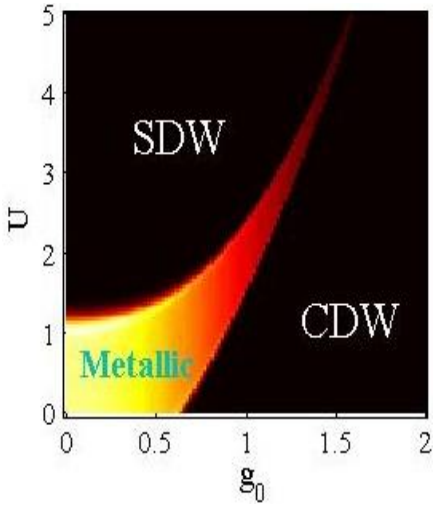

Fig. 2.11 Phase diagram of HH QR: Half-filling band case for $t = 1$ and $g_1 = 0$.

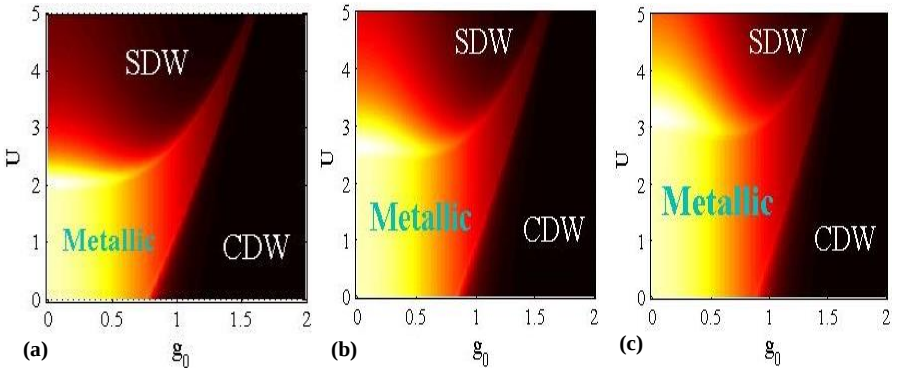

Fig. 2.12 Phase diagrams of HH QR for non-half-filled band cases at $\boldsymbol{t = 1}$ and $\boldsymbol{g_1 = 0}$: (a) $N_e = 190$; (b) $N_e = 180$; (c) $N_e = 170$.

zero for an insulating phase. The insulating phase can be either a CDW phase ($c\sim1$) or SDW phase ($s\sim1$) depending on the relative interaction strengths. Fig. 2.11 shows the phase diagram for a half-filled band. The figure clearly shows the existence of an intermediate metallic phase in between the two insulating phases. It is evident that the metallic phase is favoured at small values of g_0 and U. Fig. 2.12 shows the phase diagrams for a band which is less than half-filled. It is clearly visible that the metallic phase is now wider as compared to the half-filled band case. This implies that the correlation is stronger at half-filling. One can also observe that for cases with lesser band-filling the metallic phase becomes even wider. Thus we conclude that the intermediate metallic phase becomes wider as the band-filling decreases from 1.0. The reason is easily understandable because when the band is less than half-filled, more sites are available for the electrons to avoid double occupancy and lower the energy. One can also observe that the metallic phase widens more towards the SDW phase as the band-filling decreases from the half-filled case. The reason for this is not very clear.

2.6 SUMMARY

We have studied the *e-e* and *e-p* interaction effects on PC in a 1D HH QR pierced by a magnetic flux. First the phonon degrees of freedom have been eliminated by using the conventional LF transformation followed by a zero-phonon averaging to obtain an effective Hubbard model which is subsequently studied by using HFA. The resulting linearized Hamiltonian is then written in terms of CDW and SDW order parameters which are calculated by a self-consistent approach. Our calculation shows the existence of PC in QR which is periodic in Φ with a period $\Phi_0 = hc/e$.

Our results further show that DW is positive definite which implies that PC is diamagnetic in nature. The parity effects in QR's have also been revealed by our investigation. We have shown that all the three interactions namely, the onsite *e-e*, onsite *e-p* and NN *e-p* interactions cause suppression in PC in a QR. It turns out that the *e-p* interaction plays a more dominant role as compared to the Coulomb interaction. We have furthermore shown that PC increases with decreasing number of sites. This is due to the increasing coherence of the electron wave function as the number of sites decreases. The enhancement in PC with decreasing system size appears to be continuous precluding any possibility of an abrupt transition from the bulk to the nano-phase. Finally we have obtained the phase diagram in the $g_0 - U$ plane which predicts the existence of an intervening metallic phase in a HH QR in between the CDW-SDW phases.

REFERENCES

[1] M. Büttiker, Y. Imry & R. Landauer, *Josephson behavior in small normal one-dimensional rings*, Phys. Lett. A **96**, 365 (1983).

[2] O.V. Kibis, O. Kyriienko & I.A. Shelykh, *Persistent current induced by vacuum fluctuations in a quantum ring*, Phys. Rev. B **87**, 245437 (2013).

[3] L.P. Levy, G. Dolan, J. Dunsmuir & H. Bouchiat, *Magnetization of mesoscopic copper rings: Evidence for persistent currents*, Phys. Rev. Lett. **64**, 2074 (1990).

[4] V. Chadrasekhar *et al.*, *Magnetic response of a single, isolated gold loop*, Phys. Rev. Lett **67**, 3578 (1991).

[5] D. Mailly, C. Chapelier & A. Benoit, *Experimental observation of persistent currents in a GaAs-AlGaAs single loop*, Phys. Rev. Lett. **70**, 2020 (1993).

[6] E.M.Q. Jariwala, P. Mohanty, M.B. Ketchen & R.A. Webb, *Diamagnetic PC in diffusive normal-metal rings*, Phys. Rev. Lett. **86**, 1594 (2001).

[7] R. Deblock *et al.*, *Diamagnetic orbital response of mesoscopic Silver rings*, Phys. Rev. Lett. **89**, 206803 (2002).

[8] H. Bluhm, *Persistent currents in normal metal rings*, Phys. Rev. Lett. **102**, 136802 (2009).

[9] A.C. Bleszynski-Jayich *et al.*, *Persistent currents in normal metal rings*, Science **326,** 272 (2009).

[10] G.M. Souche *et al.*, *Searching for thermal signatures of persistent currents in normal-metal rings*, Phys. Rev. B **87**, 115120 (2013).

[11] M.A. Castellanos-Beltran *et al.*, *Measurement of the full distribution of PC in normal-metal rings*, Phys. Rev. Lett. **110**, 156801 (2013).

[12] B.-B. Wei, S.-J. Gu & H.-Q. Lin, *Persistent current in the 1D mesoscopic Hubbard ring*, J. Phys.: Condens. Matter **20**, 395209 (2008).

[13] A. Moskova, M. Mosko & J. Tobik, *Theoretical study of persistent current in a nonoring made of a band insulator*, Phys. Status Solidi B **250**, 147 (2013).

[14] I. Lang & Y.A. Firsov, *Kinetic theory of semiconductors with low mobility*, Sov. Phys. JETP **16**, 1301 (1963).

[15] Y. Takada & A. Chatterjee, *Possibility of a metallic phase in the CDW-SDW crossover region in the one-dimensional Hubbard-Holstein model at half filling*, Phys. Rev. B **67**, 081102 (R) (2003).

[16] A. Chatterjee & Y. Takada, *The Hubbard-Holstein model with anharmonic phonons in one-dimension*, J. Phys. Soc. Jpn. **73**, 964 (2004).

[17] P.M. Krishna & A. Chatterjee, *Existence of a metallic phase in a 1D Holstein-Hubbard model at half filling*, Physica C **457**, 55 (2007).

[18] I.V. Sankar, S. Mukhopadhyay & A. Chatterjee, *Localization-delocalization transition in a 2D Holstein-Hubbard model*, J. Phys. C **480**, 55 (2012).

[19] I.V. Sankar & A. Chatterjee, *Self-trapping phase diagram for the strongly correlated EHH model in two-dimensions*, Eur. Phys. J. B **87**, 154 (2014).

[20] D. Cabib & E. Callen, *Charge order and AF order in the Hubbard model with NN Coulomb interaction: Weak coupling*, Phys. Rev. B **12**, 5249 (1975).

[21] W. Kohn, *Theory of the insulating state*, Phys. Rev. A **133**, 171 (1964).

[22] B.S. Shastry & B. Sutherlland, *Twisted boundary conditions and effective mass in Heisenberg-Ising and Hubbard rings*, Phys. Rev. Lett. **65**, 243 (1990).

[23] H.-F. Cheung, Y. Gefen, E.K. Riedel & W.-H. Shih, *Persistent currents in small one-dimensional metal rings*, Phys. Rev. B **37**, 6050 (1988).

[24] D. Sticlet, B. Dora & J. Cayssol, *Persistent currents in Dirac fermion rings*, Phys. Rev. B **88**, 205401 (2013).

[25] P. Koskinen & M. Manninen, *Persistent currents in small, imperfect Hubbard rings*, Phys. Rev. B **68**, 195304 (2003).

[26] S.K. Maiti, J. Chowdhury & S.N. Karmakar, *Strange behavior of persistent currents in small Hubbard rings*, Phys. Lett. A **332**, 497 (2004).

[27] S.K. Maiti, *Magnetic response in mesoscopic Hubbard rings: A mean-field study*, Solid State Commun. **150**, 2212 (2010).

CHAPTER 3

QUANTUM PHASE TRANSITIONS IN A 1D HOLSTEIN-HUBBARD MODEL

ABSTRACT

The aim of the present chapter is to apply the concept of *quantum entanglement entropy* to a 1D *Holstein-Hubbard model* and obtain the phase diagrams to show the *existence of an intervening metallic phase* in between the polaronic SDW Mott antiferromagnetic insulating phase and the bipolaronic CDW Peierls-insulating phase using a variational state for the phonon subsystem and the exact *Bethe ansatz technique* for the effective electronic model.

3.1 INTRODUCTION

The phase transition that takes place at *zero* temperature due to the variation of non-thermal physical parameters (*e.g.* magnetic field, doping, electron-electron and electron-phonon interaction strengths, *etc.*) can be called quantum phase transitions (QPT's) [1-3]. In QPT's, the non-thermal external parameters or the Hamiltonian parameters induce quantum fluctuations, due to the Heisenberg uncertainty principle, which are the lone changers of the ground state (GS) order. Before we explore the possible QPT's in the Holstein-Hubbard (HH) model, let us rewrite the HH model as

$$\mathcal{H} = \mathcal{H}_t + \mathcal{H}_U + \mathcal{H}_p + \mathcal{H}_{\mathrm{g}}$$

$$= -t \sum_{\langle ij \rangle \sigma} c_{i\sigma}^{\dagger} c_{j\sigma} + U \sum_i n_{i\uparrow} n_{i\downarrow} + \omega_0 \sum_i b_i^{\dagger} b_i + \mathrm{g}_0 \sum_{\mathrm{i}} n_{i\sigma} \left(b_i + b_i^{\dagger} \right), \langle 3.1 \rangle$$

where the notations have the same meaning as described in Chapter 1. Here, we define $\mathrm{g}_0 = \omega_0 \sqrt{\alpha}$, where α is the dimensionless electron-phonon (*e-p*) coupling constant. We have dropped the nearest-neighbor (NN) *e-p* interaction term just for the sake of simplicity.

Now we try to understand qualitatively how QPT's can take place in the above HH model. This model consists mainly of three competing terms namely, the hopping term ($\mathcal{H}_t$), the onsite electron-electron (*e-e*) interaction ($\mathcal{H}_U$) and the onsite *e-p* interaction ($\mathcal{H}_{\mathrm{g}}$). Since these three competing terms do not commute, they have different quantum states. Suppose, in the anti-adiabatic case ($t < \omega_0$), if $U \gg \mathrm{g}$, then the GS is an eigenstate of $\mathcal{H}_U$ which is an insulating SDW state and on the other hand, if $U \ll \mathrm{g}$ then GS is dominated by the states of $\mathcal{H}_{\mathrm{g}}$ which is an insulating CDW state. It was first predicted by Takada and Chatterjee (TC) [4] in

2003 that the QPT that the GS undergoes from the spin-density wave (SDW) state to the charge-density wave (CDW) state is not a direct transition, but it goes through an *intervening metallic phase*. Subsequently, a number of investigators have confirmed this assertion [4-11]. The reason for the possible existence of such an intervening metallic phase may be the following. When the *e-e* and the *e-p* interactions are comparable or one of them is slightly weaker than the other, the *effective e-e interaction* may not be able to compete with the *effective hopping process* and this may lead to the emergence of a new phase namely the metallic phase at the phase boundary of the SDW and CDW phases. These QPT's in many-body physics have an interesting connection with quantum entanglement (QE) and this was first pointed out in 2002 [12,13]. Later, it was also realized that QE-measure can act as an indicator of QPT's [14-21]. We will discuss how QE can be used to demonstrate QPT's in the HH model in the section 3.4.

In Chapter 2, we have obtained the phase diagram of a finite HH ring in the half and non-half-filled band cases using Hartree-Fock decoupling method. It has been shown that in between the SDW and CDW phases there exists an intermediate metallic phase and the width of which increases rather rapidly towards the SDW region with the reduction in the electron density. In the present chapter, we shall take up the one dimensional (1D) HH model in the thermodynamic limit and obtain the phase diagrams for the half-filled band case using the nested Bethe ansatz technique. As usual, we first eliminate the phonon degrees of freedom by choosing a variational wave function for the phonon subsystem. However, here we choose a more improved phonon state as compared to one considered in Chapter 2 to obtain an effective Hubbard model which we solve using the method of Bethe ansatz.

3.2 VARIATIONAL PHONON STATE

In Chapter 2, we have considered the conventional Lang-Firsov (LF) transformation which works pretty well in the strong coupling regime. To obtain the GS energy in the weak and intermediate coupling regions we use a modified LF transformation with a generator $\mathcal{S}_1$ (say), followed by the Takada-Chatterjee (TC) transformation [4] with a generator $\mathcal{S}_2$ (say). The TC transformation takes into account the phonon coherence effect that is independent of the electron concentration. The phonon state is written as

$$\left|\Phi_{ph}\right\rangle = e^{-\mathcal{S}_2}\, e^{-\mathcal{S}_1}|0\rangle \qquad \langle 3.2\rangle$$

where

$$\mathcal{S}_1 = \frac{\mathrm{g}_0'}{\omega_0}\sum_{i\sigma} n_{i\sigma}\left(b_i^{\dagger} - b_i\right), \qquad \langle 3.2a\rangle$$

$$\mathcal{S}_2 = h\sum_{i}\left(b_i^{\dagger} - b_i\right), \qquad \langle 3.2b\rangle$$

where $\mathrm{g}_0' = \omega_0\sqrt{\alpha}\,\eta$, $|0\rangle = \prod_i |0\rangle_i$ is the zero-phonon state with $i = 1,2,3,4,5,\ldots,N$ and η and h are the variational parameters. The modified LF transformation has already been performed in Chapter 2 to obtain $\widetilde{\mathcal{H}}_1$ (Eq. ⟨2.6⟩). So we can straightaway use the same result here for the transformed Hamiltonian $\widetilde{\mathcal{H}}_1$ with $\mathrm{g}_1' = \mathrm{g}_1 = 0$ and $\phi = 0$ and apply the TC transformation on $\widetilde{\mathcal{H}}_1$ to obtain the next transformed Hamiltonian $\widetilde{\mathcal{H}}_2$. The transformations of the phonon coordinates by the TC transformation can be accomplished by using the Baker-Campbell-Hausdorff formula as shown below.

$$\tilde{b}_i = e^{\mathcal{S}_2}\, b_i\, e^{-\mathcal{S}_2} = b_i + [\mathcal{S}_2, b_i] + \frac{1}{2!}\left[\mathcal{S}_2, [\mathcal{S}_2, b_i]\right] + \cdots = b_i - h,$$

$$\widetilde{b_i^\dagger} = e^{\mathcal{S}_2}\, b_i^\dagger\, e^{-\mathcal{S}_2} = b_i^\dagger - h,$$

$$\widetilde{b_i^\dagger b_i} = e^{\mathcal{S}_2}\, b_i^\dagger b_i\, e^{-\mathcal{S}_2} = \tilde{b}_i^\dagger \tilde{b}_i = b_i^\dagger b_i - h\big(b_i^\dagger + b_i\big) + h^2,$$

$$\tilde{q}_i \equiv \widetilde{b_i^\dagger + b_i} = b_i^\dagger + b_i - 2h\,,$$

$$\tilde{p}_i \equiv \widetilde{b_i^\dagger - b_i} = b_i^\dagger - b_i,$$

$$\tilde{Y}_i = Y_i.$$

The new transformed Hamiltonian, after using the above equations, reduces to

$$\tilde{\mathcal{H}}_2 = \tilde{\epsilon}_0 \sum_{i\sigma} n_{i\sigma} - t \sum_{\langle ij\rangle\sigma} e^{(Y_i - Y_j)}\, c_{i\sigma}^\dagger c_{j\sigma} + \tilde{U}_1 \sum_i n_{i\uparrow}\, n_{i\downarrow} + \omega_0 \sum_i \big[b_i^\dagger b_i - h q_i + h^2\big]$$
$$+ (\mathrm{g}_0 - \mathrm{g}_0') \sum_{i\sigma} n_{i\sigma}(q_i - 2h) + (\mathrm{g}_1 - \mathrm{g}_1') \sum_{\langle ij\rangle\sigma} n_{i\sigma}\big(q_j - 2h\big), \qquad \langle 3.3\rangle$$

Note that the electronic terms in the Hamiltonian are invariant under the TC transformation since its generator does not include any electronic coordinates. Now, we calculate the expectation value of the new transformed Hamiltonian $\tilde{\mathcal{H}}_2$ with respect to the zero-phonon state $|0\rangle$ to obtain an effective electronic (Hubbard) Hamiltonian as

$$\mathcal{H}_e = \epsilon_e \sum_{i\sigma} n_{i\sigma} - t_e \sum_{\langle ij\rangle\sigma} c_{i\sigma}^\dagger\, c_{j\sigma} + U_e \sum_i n_{i\uparrow}\, n_{i\downarrow} + \omega_0 h^2, \qquad \langle 3.4\rangle$$

where

$$t_e = t\, e^{-\alpha\,\eta^2}, \qquad \langle 3.4a\rangle$$

$$U_e = U - 2\,\omega_0\,\sqrt{\alpha}\,\eta\,(1-\eta), \qquad \langle 3.4b\rangle$$

$$\epsilon_e = \omega_0\left[h^2 - \alpha\eta(2-\eta) - 2\sqrt{\alpha}\eta\,(1-\eta)\right]. \qquad \langle 3.4c\rangle$$

where ϵ_e is the effective electronic onsite energy, t_e is the effective (renormalized) hopping parameter and U_e is the effective (renormalized) onsite *e-e* interaction strength. We, now, proceed to apply the Bethe ansatz technique to the effective Hubbard Hamiltonian ⟨3.4⟩ in order to obtain the electronic GS energy of the 1D thermodynamic system.

3.3 BETHE ANSATZ: APPLIED TO EFFECTIVE HUBBARD MODEL

The Bethe ansatz was used to solve 1D electronic systems with delta-function interaction by Yang [22] and Gaudin [23] in 1967. In the same year, Lieb and Wu (LW) [24] generalized Yang's solution to a lattice model and obtained the exact GS energy of the Hubbard model for the half-filled band case ($n = 1$). In this section, we apply the Bethe ansatz method to the effective Hubbard model following LW [24-27] to get the GS energy.

The general eigenstate of any Hamiltonian is given as

$$|\Psi\rangle_{M,N} = \sum_{\{1\le x_1\le N_a\}} f(x_1,\dots,x_M,x_{M+1},\dots,x_N)\prod_{j=1}^{M} c^{\dagger}_{x_j\downarrow}\prod_{j=1}^{N} c^{\dagger}_{x_j\uparrow}|\mathbf{0}\rangle, \qquad \langle 3.5\rangle$$

where $x_1, x_2, x_3, \dots, x_M$ are the positions of the M down spins, N is the total number of electrons, f is the probability amplitude function and $|\mathbf{0}\rangle$ is the electronic vacuum state. We define a sector $\mathcal{D}_{\mathbb{Q}}$, called the fundamental sector, in the N particle space such that

$$\mathcal{D}_{\mathbb{Q}} := \left\{ \boldsymbol{x} : 1 \leq x_1^{(\mathbb{Q})} \leq x_2^{(\mathbb{Q})} \leq \cdots \leq x_N^{(\mathbb{Q})} \leq N_a \right\}, \qquad \langle 3.6 \rangle$$

where $\mathbb{Q}$ denotes a permutation of N numbers $\{1,2,3,4,5 \ldots, N\}$. The NN sector $\mathcal{D}_{\mathbb{Q}\langle ij \rangle}$ of $\mathcal{D}_{\mathbb{Q}}$ can be obtained from the fundamental sector $\mathcal{D}_{\mathbb{Q}}$ by interchanging $x_i^{(\mathbb{Q})}$ and $x_j^{(\mathbb{Q})}$. Let $f_{\mathbb{Q}}$ be the amplitude function in the sector $\mathcal{D}_{\mathbb{Q}}$. The celebrated Bethe ansatz for the amplitude functions that diagonalizes the Hamiltonian is given by

$$f_{\mathbb{Q}}(x_1, \ldots, x_M, x_{M+1}, \ldots, x_N) = \sum_{\mathbb{P}} [\mathbb{Q}, \mathbb{P}] \exp\left(\boldsymbol{i} \sum_{j=1}^{N} k_j^{(\mathbb{P})} x_j^{(\mathbb{Q})} \right), \qquad \langle 3.7 \rangle$$

where the permutation $\mathbb{P}$ of $\{1,2,3,4,5 \ldots, N\}$ is associated with the quasi-momenta $\{k_i\}$ and $\mathbb{Q}$ with the site locations $\{x_i\}$ of all the electrons. Let $[\mathbb{Q}, \mathbb{P}]$ be a set of $N! \times N!$ coefficients which can be determined from the boundary conditions imposed on the amplitude $f_{\mathbb{Q}}$. The Schrödinger equation for the Hamiltonian $\mathcal{H}_e$ is

$$\mathcal{H}_e \, |\Psi\rangle_{M,N} = E(M,N) \, |\Psi\rangle_{M,N}, \qquad \langle 3.8 \rangle$$

Now, substituting Eq. ⟨3.5⟩ in the above Schrödinger equation, we get

$$-t \sum_{i=1}^{N} \sum_{s=\pm 1} f(x_1, x_2, \ldots, x_i + s, x_{i+1}, \ldots, x_{N-1}, x_N) + U \sum_{i<k} \delta_{ik} \, f(x_1, x_2, x_3, \ldots, x_N)$$
$$= E \, f(x_1, x_2, x_3, \ldots, x_N), \qquad \langle 3.9 \rangle$$

where δ_{ik} is a Kronecker delta function. The periodic boundary condition is obtained as [29-31]:

$$e^{\boldsymbol{i} k_j N} = \prod_{\beta=1}^{M} \frac{\sin k_j - \Lambda_\beta + i \frac{U_e}{4}}{\sin k_j - \Lambda_\beta - i \frac{U_e}{4}}, \qquad \langle 3.10a \rangle$$

$$\prod_{j=1}^{N} \frac{\Lambda_\alpha - \sin k_j + i\frac{U_e}{4}}{\Lambda_\alpha - \sin k_j - i\frac{U_e}{4}} = -\prod_{\beta=1}^{M} \frac{\Lambda_\alpha - \Lambda_\beta + i\frac{U_e}{2}}{\Lambda_\alpha - \Lambda_\beta - i\frac{U_e}{2}}, \qquad \langle 3.10b \rangle$$

Taking the logarithm of the above two equations we have

$$N_a k_i = 2\pi I_j - 2\sum_{\beta=1}^{M} \tan^{-1}\left(\frac{\sin k_j - \Lambda_\beta}{U_e'}\right), \qquad \langle 3.11a \rangle$$

$$2\sum_{j=1}^{N} \tan^{-1}\left(\frac{\Lambda_\alpha - \sin k_j}{U_e'}\right) = 2\pi J_\alpha + \sum_{\beta=1}^{M} \tan^{-1}\left(\frac{\Lambda_\alpha - \Lambda_\beta}{2U_e'}\right), \qquad \langle 3.11b \rangle$$

Here the $I_j's$ are integers (half-odd integers) for even (odd) M and the $J_\alpha's$ are integers (half-odd integers) for odd (even) $(N-M)$. The eigenvalue and the total momentum is given by

$$E(n,t,U,\alpha,\eta,h) = \omega_0 h^2 + \epsilon_e\, n + \frac{(U_e - |U_e|)n}{4} - 2\, t_e \sum_{i=1}^{N} \cos k_i, \qquad \langle 3.12a \rangle$$

$$K = \frac{2\pi}{N_a}\left[\sum_j I_j + \sum_\alpha J\_\alpha\right]. \qquad \langle 3.12b \rangle$$

The third term in the above equation (Eq. $\langle 3.12a \rangle$) takes cares of both positive and negative U_e cases. In the thermodynamic limit, Eqs. $\langle 3.12a \rangle$ and $\langle 3.12b \rangle$ become

$$2\pi\rho(k) = 1 + \left(\frac{8|U_e|\cos k}{t_e}\right) \int_{-B}^{B} \frac{\sigma(\Lambda)\,\mathrm{d}\Lambda}{\left(\frac{|U_e|}{t_e}\right)^2 + 16(\sin k - \Lambda)^2}, \qquad \langle 3.13a \rangle$$

$$\frac{8|U_e|}{t_e} \int_{-Q}^{Q} \frac{\rho(k)\,\mathrm{d}k}{\left(\frac{|U_e|}{t_e}\right)^2 + 16(\Lambda - \sin k)^2} = 2\pi\sigma(\Lambda) + \frac{4|U_e|}{t_e} \int_{-B}^{B} \frac{\sigma(\Lambda')\,\mathrm{d}\Lambda'}{\left(\frac{|U_e|}{t_e}\right)^2 + 4(\Lambda - \Lambda')^2}, \langle 3.13b \rangle$$

The integral limits Q and B are defined through

$$n = \int_{-Q}^{Q} \mathrm{d}k\, \rho(k), \qquad \langle 3.14a \rangle$$

$$m = \int_{-B}^{B} \sigma(\Lambda)\, \mathrm{d}\Lambda, \qquad \langle 3.14b \rangle$$

where $\rho(k)$ and $\sigma(\Lambda)$ are two distribution functions, $n = N/N_a$ is the band filling and $m = M/N$ is the down spin electron density.

$$E(n, t, U, \alpha, \eta, h) = \omega_0 h^2 + \epsilon_e\, n + \frac{(U_e - |U_e|)n}{4} - 2\, t_e \int_{-Q}^{Q} \mathrm{d}k\, \cos k\, \rho(k)\,, \langle 3.15 \rangle$$

The coupled integral equations $\langle 3.13a \rangle$ and $\langle 3.13b \rangle$ can be solved analytically at $Q = \pi,\ B = \infty$. Substituting these limiting solutions into Eq. $\langle 3.13a \rangle$ gives

$$\sigma(\Lambda) = \frac{1}{2\pi} \int_{-\pi}^{\pi} \frac{J_o(\omega) \cos(\omega\Lambda)}{\cosh(\omega\Lambda/4)}\, \mathrm{d}\omega, \qquad \langle 3.16 \rangle$$

where $J_o(\omega) = \frac{1}{\pi}\int_0^{\pi} \cos(\omega \sin\theta)\, \mathrm{d}\theta$, is the zeroth order Bessel function. On substituting $\langle 3.13a \rangle$ into $\langle 3.13b \rangle$, we get

$$\rho(k) = \frac{1}{2\pi} + \frac{\cos k}{\pi} \int_{0}^{\infty} \frac{J_o(\omega) \cos(\omega \sin k)}{1 + \exp(\omega |U_e|/2t_e)}\, \mathrm{d}\omega, \qquad \langle 3.17 \rangle$$

Finally, the GS energy of the HH model (or effective Hubbard model) for the half-filled band case can be obtained by substituting the above equation in $\langle 3.15 \rangle$ as

$$E(n,t,U,\alpha,\eta,h)=\omega_0 h^2+\epsilon_e n+\frac{(U_e-|U_e|)n}{4}-4t_e\int_{-Q}^{Q}\frac{J_o(\omega)\,J_1(\omega)\,\mathrm{d}\omega}{\omega\left(1+\exp\left(\frac{\omega|U_e|}{2t_e}\right)\right)}, \langle 3.18\rangle$$

where $J_1(\omega)=\frac{1}{\pi}\int_0^{\pi}\sin(\omega\sin\theta)\sin\theta\,\mathrm{d}\theta$, is the first order Bessel function.

For arbitrary band fillings, however, no such analytical solution is possible. According to the Lieb-Mattis theorem, the GS of the system is always a singlet for any band filling [28]. This corresponds to $m=M/N_e=1/2$ which is possible for $B=\infty$. In this case, the coupled integral equations $\langle 3.13a\rangle$ and $\langle 3.13b\rangle$ reduce to a single equation which is given by [29]:

$$2\pi\rho(k)=1+\left(\frac{2t_e\cos k}{|U_e|}\right)\int_{-Q}^{Q}\mathrm{d}k_1\rho(k_1)\int_{-\infty}^{\infty}\frac{\mathrm{sech}\left(\frac{\pi k_2}{2}\right)\mathrm{d}k_2}{1+\left[\frac{4t_e(\sin k-\sin k_1)}{|U_e|}+k_2^2\right]^2}, \quad \langle 3.19\rangle$$

Minimization of $\mathcal{H}_e$ with respect to h gives: $h=n\sqrt{\alpha}\,(1-\eta)$. Finally the GS energy is obtained numerically. For a given n, Eq. $\langle 3.15\rangle$ is solved self-consistently together with Eqs. $\langle 3.14a\rangle$ and $\langle 3.19\rangle$. The self-consistency procedure also involves the process of optimization in order to get the variational GS energy of the system for a given electron density. Once we obtain the GS energy the entanglement entropy (EE) of the HH model can be determined.

3.4 QUANTUM ENTANGLEMENT VS QPT

Quantum entanglement [30-33], an inherent feature of quantum mechanical systems, allows nonlocal quantum correlation (QC) which enables possibilities such as quantum teleportation, quantum information

and quantum computing. The, so called, entangled particles (EP's) seem to share a common code among them, which executes even if we measure any one of them and tells us the state of the other EP's regardless of their spatial separation. QC's arising as a result of interactions among the particles are of a different nature altogether and can be studied through entanglement measure to predict the nature of the GS's [14-21]. We would like to point out that here when we say a many-particle system is maximally entangled or correlated, we will mean that it is a non-interacting system in the quantum information sense (though according to the physics of condensed matter the connotation is completely different). This has already been addressed in recent times [18]. Indeed, a number of researchers [16-21], have studied the physics of the strongly correlated systems (SCS's) in the recent past from the QE prospective to understand the well-known QPT's. There have been some investigations to study QPT's within the framework of the extended Hubbard model to obtain the different possible phases of this model [16-21]. Our aim is to calculate the EE for the HH model and use it as an indicator of QPT's to obtain the GS phases of the HH model in the thermodynamic limit and verify the present results vis-à-vis the results of TC [4].

The entanglement properties of the HH model can be inferred by dividing the system into two subsystems $\mathcal{A}$ and $\mathcal{B}$. The subsystem $\mathcal{A}$ contains any one site with four possible states: $|0\rangle, |\uparrow\rangle, |\downarrow\rangle$ and $|\uparrow\downarrow\rangle$ and $\mathcal{B}$ contains the rest of the system ($\mathrm{N}-1$ number of sites) with Hilbert space of dimension $4^{\mathrm{N}-1}$. Then the single-site EE is defined as

$$E_v = -\mathrm{Tr}\,(D_R \log_2 D_R), \qquad \langle 3.20 \rangle$$

where the reduced density matrix D_R (containing only the subsystem $\mathcal{B}$) is obtained from the full density matrix $D = |\Psi\rangle\langle\Psi|$, $|\Psi\rangle$ being the pure

state of the total system, through the relation: $D_R = \mathrm{Tr}_{\mathrm{N}-1}(D)$. D_R can be written as

$$D_R = \omega_e\,|0\rangle\langle 0| + \omega_\uparrow\,|\uparrow\rangle\langle\uparrow| + \omega_\downarrow\,|\downarrow\rangle\langle\downarrow| + \omega\,|\uparrow\downarrow\rangle\langle\uparrow\downarrow|, \qquad \langle 3.21\rangle$$

where the occupation numbers are defined as

$$\omega = \langle\, n_{i\uparrow}\, n_{i\downarrow}\rangle, \qquad \langle 3.21a\rangle$$

$$\omega_\uparrow = \omega_\downarrow = \frac{n}{2} - \omega, \qquad \langle 3.21b\rangle$$

$$\omega_e = 1 - \omega_\uparrow - \omega_\downarrow - \omega. \qquad \langle 3.21c\rangle$$

Using the Hellman-Feynman theorem, we get $\partial E/\partial U = \langle\, n_{i\uparrow}\, n_{i\downarrow}\rangle$ and consequently, all the relevant occupation numbers are calculated and E_ν is determined.

3.5 NUMERICAL RESULTS

(i) GROUND STATE ENERGY & ENTANGLEMENT ENTROPY

In Fig. 3.1 we show the GS energy E as a function of n at $t = 1$ for a few combinations of U and α. The present results are better than those provided by the conventional LF scheme (not shown here). In the case of $\alpha = 0$, E does not seem to change much with U until $n \lesssim 0.3$ (see also [29]), while when $\alpha \neq 0$, E changes considerably with U. For $\alpha = 0$, our GS energy results perfectly agree with those of Shiba [29] as expected. Fig. 3.1 also shows that in the case of $\alpha = 0$, E has a minimum that shifts towards $n = 0.5$ as U increases. However, when the *e-p* interaction is switched on, the minimum shifts towards $n = 1$ with increasing α. The *e-p* interaction reduces the repulsive *e-e* interaction which leads to the

shifting of the minimum towards $n = 1$. Another observation one can make from Fig. 3.1 is that the energy variation with respect to U is much more pronounced at the half-filled case than at a non-half-filled case,

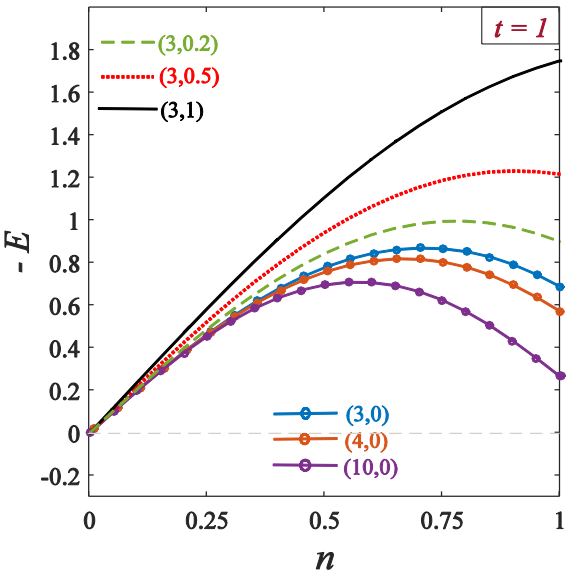

Fig. 3.1 GS energy (E) as a function of electron density (n) for different combinations of the interaction strengths (U, α).

which means that correlation effects are stronger at half-filling. The lesser correlation in the case of non-half-filling may be attributed to the greater availability of vacancies in this case.

Fig. 3.2 shows that the $E_v -$ results for the SDW and CDW cases separate into two distinct sets of curves, the upper one corresponding to SDW states and the lower one to the CDW states. In the non-interacting case i.e., when $U = 0 = \alpha$ and also when $U_e = 0$, each particle behaves in the same way and the system has the maximum symmetry. This makes the system maximally entangled [16-21]. If either U or α is large (as compared to t), then the system may be found in an insulating state which is a symmetry-breaking state corresponding to a lower value of E_v.

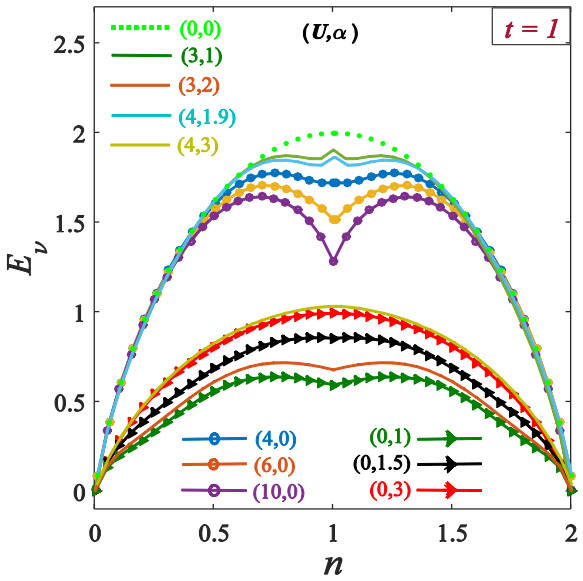

Fig. 3.2 Single-site EE (E_v) as a function of n at $t = 1$ for (U, α).

Thus for a given n, the maximum value of E_v corresponds to a metallic state. The point where E_v is maximum is commonly referred to as the quantum critical point (QCP).

(ii) EXISTENCE OF AN INTERVENING METALLIC PHASE IN THE HALF-FILLED BAND CASE

In Fig. 3.3, we study the variation of effective hopping parameter t_e, the effective onsite Coulomb interaction coefficient U_e, the double-occupancy parameter ω and single-site EE E_v with respect to U for a few values of α. Fig. 3.3(a) shows that for small and intermediate values of α, as U is increased, the effective hopping parameter t_e increases continuously to the Hubbard value t. In contrast, in the strong coupling limit, t_e goes to the Hubbard t through a discontinuous jump at a critical U. If α is sufficiently large as compared to U, the effective e-e interaction can become negative giving to an overall attractive e-e

interaction which can induce the formation of bipolaronic pair (Fig. 3.3(b)). The bipolaron formation can be quantitatively estimated by a parameter ω which gives a measure of double occupancy. Fig. 3.3(c) shows that as U increases, ω decreases, while as α increases, ω increases.

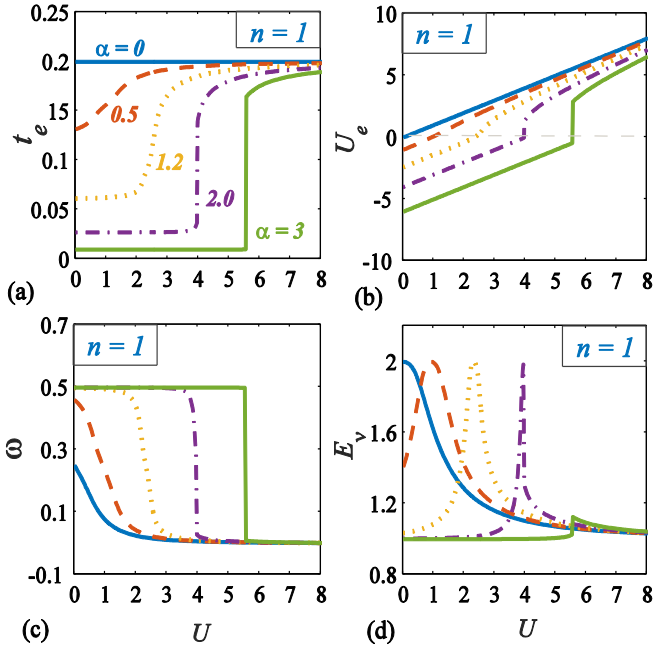

Fig. 3.3 (a) t_e vs. U, (b) U_e vs. U, (c) ω vs. U and (d) E_v vs. U for $t = 0.2$ at half-filling $(n = 1)$.

The condition $U_e < 0$ corresponds to a CDW state, whereas $U_e > 0$ favours a SDW state. Also, the minimum value of ω refers to a SDW state while the maximum value of ω indicates a CDW state. It is to be noted here that, for arbitrarily small $U_e > 0$ the GS is not a Mott insulating, rather it is a weakly correlated unstable antiferromagnetic state which is a consequence of the nesting property of the band structure. The true Mott insulating GS sets in at $U_e \sim W_e$, where the band width $W_e = 2zt_e$ (Here, z is the number of NN's) [34,35]. It is also evident from the results of double occupancy that for arbitrary small U_e, $\omega < 0.5$ which corresponds

to the weakly correlated SDW state. Pure SDW Mott insulating GS will appear for $U_e \geq W_e$ for which $\omega = 0$. The same explanation is also true for attractive *e-e* interaction ($U_e < 0$) strengths where GS's are Peierls insulating bipolaronic CDW type. Fig. 3.3(d) shows the variation of E_v as a function of U for a few values of α. In general, E_v shows a peak structure, the maximum of which corresponds to QCP. As α increases, the width of E_v shrinks and QCP shifts towards higher values of U. For a given α, as U increases, the system goes from a CDW phase to a SDW phase through a metallic state.

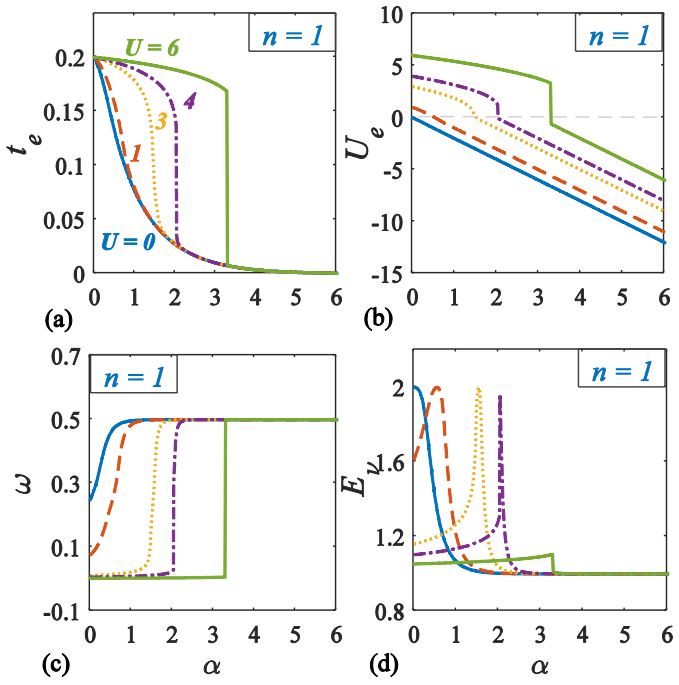

Fig. 3.4 t_e, U_e, ω and E_v as a function of the *e-p* interaction $(g = \omega_0\sqrt{\alpha})$ for $t = 0.2$ at half-filling $(n = 1)$.

In Fig. 3.4 we study t_e, U_e, ω and E_v directly as a function of α. At small α, $t_e = t$, $U_e > 0$ and the system is in a SDW state. At a sufficiently large α, $t_e \simeq 0$, $U_e \ll 0$ and ω is maximum and the system is in a CDW

state. For an intermediate value of α, depending on U, E_v would have a maximum implying the existence of a metallic state. Thus we see that as α increases from small and intermediate values to a large value, U_e changes sign and ω crosses the mean value 0.25 and consequently, E_v goes through a maximum. This indicates a QPT from an antiferro-magnetic Mott type polaronic SDW insulating phase to an insulating Peierls type bipolaronic CDW phase through a metallic phase.

To see the effect of both *e-e* and *e-p* interactions together we plot in Fig. 3.5, the surfaces of double occupancy, EE and projection of the EE on to the (U, α) plane which clearly show the QPT from a SDW to a CDW state through an intermediate metallic phase. That for $U_e = 0$, EE exhibits a unique peak around which the Mott-Hubbard (MH) criterion ($|U_e| \leq 2zt_e$) is satisfied also suggests that EE can be used as an indicator of the metallic state. It may be mentioned that the single-site EE can indeed characterize a long-range order because it is obtained from the average GS energy per site and thus contains the information of the bulk system in an average way.

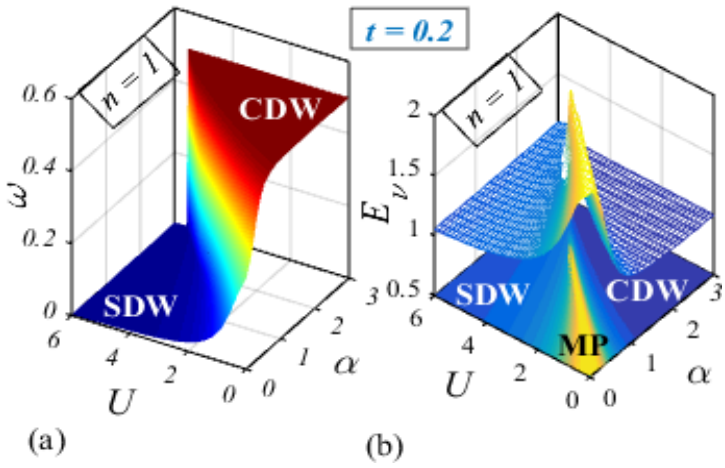

Fig. 3.5 ω and E_v surfaces for $t = 0.2$ at half-filling ($n = 1$).

To confirm the nature of the intermediate phase we also use the MH criterion which is a reasonable condition for a metallic state. For this, we plot the bandwidth W_e and $|U_e|$ surfaces in Fig. 3.6 from which one can see that the region satisfying the MH condition clearly matches with the metallic phase predicted in Fig. 3.5.

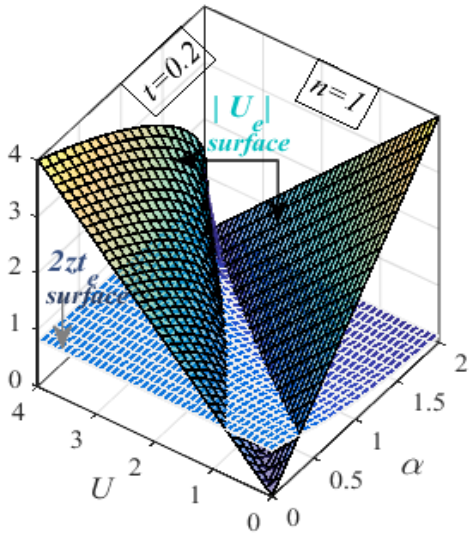

Fig. 3.6 $|U_e|$ and $W = 2zt_e$ surfaces for $n = 1$ at $t = 0.2$.

The average KE can be calculated directly from the GS energy of the system. In Fig. 5.7 we draw a multi-dimensional plot to show the variation of the KE, $E_v, |U_e|$ and $2zt_e$ as a function of U and α for $n = 1$ and $t = 0.6$. It can be seen from the figure that the average KE of the system is maximum where the MH criterion holds good. One can also identify that the maximum KE lies at the same region where EE peaks. The maximum KE and the peak of EE both correspond to the metallic state. The boundaries of the metallic phase is obtained by using the MH criterion.

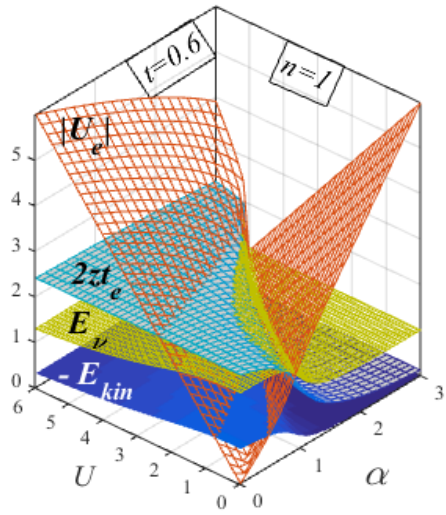

Fig. 3.7 Kinetic energy (E_{kin}), E_v, $|U_e|$ and $2zt_e$ surfaces for $n = 1$ at $t = 0.6$.

In Fig. 5.8 we plot the SDW-CDW phase diagrams in the $U - \alpha$ plane for two values of t. The contour lines are obtained by calculating EE. As expected, an increase in t leads to a broadening of the metallic phase. The boundaries of the metallic phase are obtained by MH criterion. We would like to emphasize that the results obtained by the method of QE agree completely with those obtained by TC.

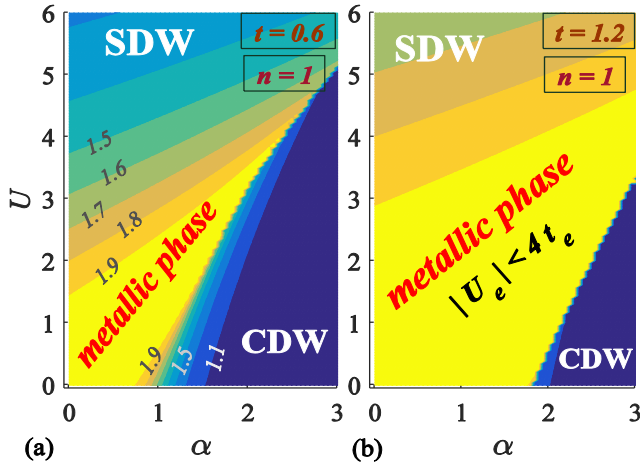

Fig. 3.8 Phase diagrams at (a) $t = 0.6$ and at (b) $t = 1.2$ at $n = 1$. The numbers on the contour lines correspond to the values of EE.

3.6 SUMMARY

To conclude, we have considered the 1D HH model at $T = 0$ in the thermodynamic limit. Using a variational phonon state, we have obtained an effective Hubbard model which we have solved exactly for an arbitrary band filling using the nested Bethe ansatz technique. We have calculated the GS energy and the EE which together with the double occupancy parameter have been used to predict the different phases of the system. We have shown that for the half-filled band case the HH model system undergoes QPT's and there exists an intermediate metallic phase flanked by SDW and CDW phases which supports the assertion TC. It may however be mentioned that since the phonon subsystem has been treated in our work in a variational way, more rigorous treatments are called for to confirm the actual nature the phase diagram of the HH model.

REFERENCES

[1] S. Sachdev, *Quantum Phase Transitions*, Canbridge University Press (2011).

[2] M. Vojta, *Quantum phase transitions*, Rep. Prog, Phy. **66**, 2069 (2003).

[3] L.D. Carr, *Understanding Quantum Phase Transitions*, Taylor & Francis group, LLC (2010).

[4] Y. Takada & A. Chatterjee, *Possibility of a metallic phase in the CDW-SDW crossover region in the one-dimensional Hubbard-Holstein model at half-filling*, Phys. Rev. B **67**,081102 (R) (2003).

[5] W. Koller, D. Meyer, Y. Ono & A.C. Hewson, *First- and second-order phase transition in the Holstein-Hubbard model*, Europhys. Lett. **66**, 559 (2004).

[6] T.T. Clay & R.P. Hardikar, *Intermediate phase of the one-dimensional half-filled Hubbard-Holstein model*, Phys. Rev. Lett **95**, 096401 (2005).

[7] P.M. Krishna & A. Chatterjee, *Existence of a metallic phase in 1D Holstein-Hubbard model at half-filling*, Physica C **457**, 55 (2007).

[8] R.P. Hardikar & R.T. Clay, *Phase diagram of the one-dimensional Hubbard-Holstein model at half and quarter filling*, Phys. Rev. B **75**, 245103 (2007).

[9] M. Tezuka, R. Arita & H. Aoki, *Phase diagram for the one-dimensional Hubbard-Holstein model: A density-matrix renormalization group study*, Phys. Rev. B **76**, 155114 (2007).

[10] A. Chatterjee, *Existence of an intermediate metallic phase at the SDW-CDW crossover region in the 1D Holstein-Hubbard model at half-filling*, Adv. Condens. Matt. Phys. **2010**, 350787 (2010).

[11] S. Ejima & H. Fehske, *DMRG analysis of the SDW-CDW crossover region in the 1D half-filled Hubbard-Holstein model*, J. Phys.: Conf. Ser. **200**, 012031 (2010).

[12] A. Osterloh, l. Amico, G. Falci & R. Fazio, *Scalling of entanglement close to a quantum phase transition*, Nature **416**, 608 (2002).

[13] T.J. Osborne & M.A. Nielsen, *Entanglement in a simple quantum phase transition*, Phys. Rev. A **66**, 032110 (2002).

[14] P. Zarandi, *Quantum entanglement in fermionic lattices*, Phys. Rev. A **65**, 042101 (2002).

[15] J. Wang & S. Kais, *Scaling of entanglement at a quantum phase transition for a two-dimensional array of quantum dots*, Phys. Rev. A **70**, 022301 (2004).

[16] S.-J. Gu, S.-S. Deng, Y.-Q. Li & H.-Q. Lin, *Entanglement and quantum phase transition in the extended Hubbard model*, Phys. Rev. Lett. **93**, 086402 (2004).

[17] D. Larsson & H. Johannesson, *Entanglement scaling in the one-dimensional Hubbard model at criticality*, Phys. Rev, Lett. **95**, 196406 (2005); *ibid*. **96**, 169906 (2006).

[18] V.V. Franca & K. Capelle, *Entanglement of strongly interacting low-dimensional fermions in metallic, superfluid and AF insulating systems*, Phys. Rev. A **74**, 042325 (2006).

[19] A. Anfossi, P. Giorda & A. Montorsi, *Entanglement in extended Hubbard models and quantum phase transitions*, Phys. Rev. B **75**, 165106 (2007)

[20] H. Johannesson & D. Larsson, *Entanglement in fermionic systems at a quantum phase transition*, Low Temp. Phys. **33**, 935 (2007).

[21] T. Mendes-Santos, T. Paiva & R.R. dos Santos, *Entanglement, magnetism and metal-insulator transition in fermionic superlattices*, Phys. Rev. B **87**, 214407 (2013).

[22] C.N. Yang, *Some exact results for the many-body problem in one dimension with repulsive delta-function interaction*, Phys. Rev. Lett. **19**, 1312 (1967).

[23] M. Gaudin, *Un systeme a une dimension de fermions en interaction*, Phys. Lett. A **24**, 55 (1967).

[24] E. Lieb & F. Wu, *Absence of Mott transition in an exact solution of the short-range, one-band model in one-dimension*, Phys. Rev. Lett. **20**, 1445 (1968).

[25] E.H. Lieb and F.Y. Wu, *The 1D Hubbard model: a reminiscence*, Physica A **321**, 1 (2003).

[26] Z.N.C. Ha, *Quantum many-body systems in one-dimension*, Wold Scientific, Singapore (1996).

[27] M. Takahashi, *Thermodynamic of 1D solvable models*, Cambridge University Press (2005).

[28] E. Lieb & D. Mattis, *Theory of ferromagnetism and the ordering of electronic energy levels*, Phys. Rev. **125**, 164 (1962).

[29] H. Shiba, *Magnetic susceptibility at zero temperature for the one-dimensional Hubbard model*, Phys. Rev. B **6**, 930 (1972).

[30] E. Schrodinger, *Discussion of probability relations between separated systems*, Mathematical Proceedings of the Cambridge Philosophical Society **31**, 555 (1935).

[31] C.H. Bennett, D.P. DiVincenzo, J.A. Smolin & W.K. Woorrers, *Mixed-state entanglement and quantum error correction*, Phys. Rev. A **54**, 3824 (1996).

[32] L. Amico, R. Fazio, A. Osterloh & V. Vedral, *Entanglement in many-body systems*, Rev. Mod. Phys. **80**, 517 (2008).

[33] R. Horodecki, P. Horodecki, M. Horodecki & K. Horodecki, *Quantum entanglement*, Rev. Mod. Phys. **81**,865 (2009).

[34] P. Fazekus, *Lectures notes on electron correlation and magnetism*, World Scientific Publishing Co. Pte. Ltd. (1999).

[35] E. Fradkin, *Field theories of condensed matter physics*, Cambridge Univ. Press (2013).

CHAPTER 4

SELF-TRAPPING TRANSITION IN A 2D EXTENDED HOLSTEIN-HUBBARD MODEL IN WEAK-CORRELATION REGIME

ABSTRACT

The aim of the present chapter is to study the nature of the *self-trapping transition* in a 2D *extended Holstein-Hubbard model* in the *weak correlation regime* within the framework of the *Hartree-Fock mean-field theory*.

4.1 INTRODUCTION

In this chapter, we consider a two-dimensional (2D) extended Holstein-Hubbard (HH) model in the weak correlation (WC) regime. Correlations can be considered as weak when the electron-electron (*e-e*) interaction (U) is small in comparison with the hopping probability amplitude (t) of the system (i.e., $U \ll t$) and also if the electron density or the filling fraction (n) is smaller than that of the half-filled band case (i.e., $n < 1$). In this regime, the ground state (GS) energy of the system lies in the low-energy sector of the energy spectrum and the corresponding GS is a ferromagnetic metallic state [1,2]. On the contrary, the high-energy sector corresponds to strong *e-e* correlations which lead the GS to an antiferromagnetic insulating state in the half-filled band case ($n = 1$) [1,3]. In the present chapter, our aim is to study the effect of electron-phonon (*e-p*) interaction on the GS of a weakly correlated system (WES) within the framework of the 2D extended HH model.

We have already introduced the concept of large and small polarons in Chapter 1. In the weak *e-p* coupling regime, the electron-induced lattice distortion spreads over many lattice points and the corresponding polarization potential experienced by the electron is shallow. Thus the resulting polaron, in this case, becomes essentially delocalized and one is then said to have a *mobile* large polaron. On the contrary, if the coupling between the electron and the lattice vibrations is strong, the lattice distortion would be essentially restricted within one lattice spacing and then the lattice polarization potential would be deep enough to trap the electron and the corresponding polaron is referred to as a *localized* small polaron. It has been theoretically established that as the *e-p* coupling is increased, at some critical value of the coupling constant (say, $g = g_c$) a

large polaron transforms into a small polaron which is often referred as the *self-trapping* (ST) transition.

Though there is no dispute over the existence of ST transition, a general consensus on the nature of the ST transition for a many-polaron system [4-7] is still lacking. In fact, the phase transition problem in a small polaron system was studied long ago by Toyozawa [4]. Toyozawa and collaborators [5,6] have studied the small polaron problem in the adiabatic approximation and have obtained a *discontinuous* phase transition [4-6]. Several other authors [8-10] have obtained similar *abrupt* changes in the polaron properties, whereas quite a few investigations [11-13] have also shown *continuous* transition. Löwen [13] has investigated the exact nature of the phase transition of the small polaron problem within the framework of Holstein model [14,15] and has shown that for finite phonon frequencies the GS of an *e-p* system does not exhibit any non-analytical phase transition as the phonon coupling increases. It thus appears that the discontinuities in the polaron properties obtained by various authors might rather be consequences of the approximations used. Krishna *et al.* [16] have studied the nature of the ST transition in a 1D HH model where it has been shown almost conclusively that this transition is *continuous*. However the nature of the ST transition is more important in higher dimensions. Das and Sil (DS) [17] have studied the ST transition for a many-polaron system in the 2D HH model and they have shown that the crossover from large polaron to small polaron regime is continuous in the anti-adiabatic case ($t < \omega_0$), whereas in the adiabatic case ($t > \omega_0$) discontinuous jumps appear in the polaron properties. They have attributed the discontinuity observed in the crossover region to the selection of variational phonon wave function. In view of the importance of ST transition in manganites, high T_c–superconductors, semiconductor nanostructures and other materials, we believe that a more careful

investigation of ST transition in the 2D HH model is certainly called for. Recently, we have carried out a rigorous investigation [18] on the nature of the ST transition in the extended HH model using a much better variational wave function than that used by DS. In the present chapter, we discuss this work and the relevant results.

4.2 THE EXTENDED HOLSTEIN-HUBBARD MODEL

The extended Holstein-Hubbard (EHH) model may be written as

$$\begin{aligned}\mathcal{H} = & -t\sum_{\langle ij\rangle\sigma} c_{i\sigma}^{\dagger}\, c_{j\sigma} + U\sum_{i} n_{i\uparrow}\, n_{i\downarrow} \\ & + \omega_0 \sum_{i} b_i^{\dagger}\, b_i + \mathrm{g}_0 \sum_{i\sigma} n_{i\sigma}\left(b_i + b_i^{\dagger}\right) + \mathrm{g}_1 \sum_{\langle ij\rangle\sigma} n_{i\sigma}\left(b_j + b_j^{\dagger}\right) \\ & + V_1 \sum_{\langle ij\rangle\sigma\sigma'} n_{i\sigma} n_{j\sigma'} + V_2 \sum_{i\delta'\sigma\sigma'} n_{i\sigma} n_{i+\delta',\sigma'} + V_3 \sum_{i\delta''\sigma\sigma'} n_{i\sigma} n_{i+\delta'',\sigma'}, \qquad \langle 4.1\rangle\end{aligned}$$

where many of the notations have already been defined earlier. The last three terms, which are new, represent NN, next NN (NNN) and next NNN *e-e* interactions with V_1, V_2 and V_3 giving the corresponding interaction strengths and δ, δ' and δ'' referring to NN, next NN and next NNN sites respectively. The above Hamiltonian does not admit an exact solution. To solve it even approximately, we have to first eliminate the phonon degrees of freedom. To do that, we choose a variational phonon state and calculate the expectation value of the Hamiltonian [18] with respect to this state. This gives us an effective electronic Hamiltonian.

4.3 IMPROVED PHONON STATE AND EFFECTIVE ELECTRONIC HAMILTONIAN

To obtain a variational solution of ⟨4.1⟩, we perform a series of canonical transformations, the first two being the modified LF and the Takada and Chatterjee (TC) [19] transformations respectively with the generators:

$$\mathcal{S}_1 = \frac{g_0'}{\omega_0}\sum_{i\sigma} n_{i\sigma}\left(b_i^\dagger - b_i\right) + \frac{g_1'}{\omega_0}\sum_{\langle ij\rangle\sigma} n_{i\sigma}\left(b_j^\dagger - b_j\right), \qquad \langle 4.2\rangle$$

$$\mathcal{S}_2 = h\sum_i \left(b_i^\dagger - b_i\right), \qquad \langle 4.3\rangle$$

Using the procedure delineated in Chapter 2, we can transform the Hamiltonian $\mathcal{H}$ by $e^{\mathcal{S}_1}$ to get $\widetilde{\mathcal{H}}_1$ and then by $e^{\mathcal{S}_2}$ to get the transformed Hamiltonian $\widetilde{\mathcal{H}}_2$. This procedure however neglects the correlations between two successively emitted virtual phonons caused by the electron recoil effect. These correlations can be incorporated by a squeezing transformation with the generator [20]:

$$\mathcal{S}_3 = \alpha\sum_i \left(b_i b_i - b_i^\dagger b_i^\dagger\right), \qquad \langle 4.4\rangle$$

where α is the squeezing parameter to be obtained variationally. It may also be noted that phonon anharmonicity has been ignored in the Hamiltonian ⟨4.1⟩. But in reality, the phonon life time is finite due to phonon-phonon interactions, which is precisely the phonon anharmonicity effect. This phonon dynamics effect gets indirectly, albeit, partially included in the problem by the squeezing transformation. Let us see how the phonon operators change under the above transformation using the Baker-Campbell-Hausdorff (BCH) formula.

$$e^{\mathcal{S}_3}\, b_i\, e^{-\mathcal{S}_3} = b_i + [\mathcal{S}_3, b_i] + \frac{1}{2!}\big[\mathcal{S}_3, [\mathcal{S}_3, b_i]\big] + \frac{1}{3!}\Big[\mathcal{S}_3, \big[\mathcal{S}_3, [\mathcal{S}_3, b_i]\big]\Big] + \cdots$$

$$e^{\mathcal{S}_3} b_i e^{-\mathcal{S}_3} = b_i + (2\alpha) b_i^\dagger + \frac{(2\alpha)^2}{2!} b_i + \frac{(2\alpha)^3}{3!} + \cdots$$

$$= b_i^\dagger \cosh(2\alpha) + b_i \sinh(2\alpha),$$

$$e^{\mathcal{S}_3}\, b_i^\dagger\, e^{-\mathcal{S}_3} = b_i^\dagger + (2\alpha) b_i + \frac{(2\alpha)^2}{2!} b_i^\dagger + \frac{(2\alpha)^3}{3!} b_i + \cdots$$

$$= b_i \cosh(2\alpha) + b_i^\dagger \sinh(2\alpha),$$

$$e^{\mathcal{S}_3}\, b_i^\dagger b_i\, e^{-\mathcal{S}_3} \quad = \frac{e^{4\alpha}}{4}\big(b_i^\dagger + b_i\big)^2 - \frac{e^{4\alpha}}{4}\big(b_i^\dagger - b_i\big)^2 - \frac{1}{2},$$

$$e^{\mathcal{S}_3}\, q_i\, e^{-\mathcal{S}_3} \equiv e^{\mathcal{S}_3}\big(b_i^\dagger + b_i\big) e^{-\mathcal{S}_3} = \big(b_i^\dagger + b_i\big) e^{2\alpha},$$

$$e^{\mathcal{S}_3}\, p_i\, e^{-\mathcal{S}_3} \equiv e^{\mathcal{S}_3}\big(b_i^\dagger - b_i\big)\, e^{-\mathcal{S}_3} = \big(b_i^\dagger - b_i\big) e^{2\alpha},$$

$$e^{\mathcal{S}_3}\, Y_i\, e^{-\mathcal{S}_3} = e^{-2\alpha}\, Y_i.$$

The new transformed Hamiltonian $\widetilde{\mathcal{H}}_3 = e^{\mathcal{S}_3}\, \widetilde{\mathcal{H}}_2\, e^{-\mathcal{S}_3}$ can be obtained, after substituting the above transformed operators in the transformed Hamiltonian $\widetilde{\mathcal{H}}_2$ (Chapter 2) as

$$\begin{aligned}
\widetilde{\mathcal{H}}_3 = {} & \tilde{\tilde{\epsilon}}_0 \sum_{i\sigma} n_{i\sigma} - t \sum_{\langle ij\rangle\sigma} \exp\big[\big(Y_i - Y_j\big)\, e^{-2\alpha}\big]\; c_{i\sigma}^\dagger\, c_{j\sigma} + \widetilde{U}_1 \sum_i n_{i\uparrow}\, n_{i\downarrow} \\
& + (\mathrm{g}_0 - \mathrm{g}_0')e^{2\alpha} \sum_{i\sigma} n_{i\sigma}\, q_i + \; (\mathrm{g}_1 - \mathrm{g}_1')e^{2\alpha} \sum_{\langle ij\rangle\sigma} n_{i\sigma}\, q_j \\
& + V_1 \sum_{\langle ij\rangle\sigma\sigma'} n_{i\sigma}\, n_{j\sigma'} + V_2 \sum_{i\delta'\sigma\sigma'} n_{i\sigma}\, n_{i+\delta',\sigma'} + \; V_3 \sum_{i\delta''\sigma\sigma'} n_{i\sigma}\, n_{i+\delta'',\sigma'} \\
& + \omega_0 \sum_i \left[\frac{e^{4\alpha}}{4}\, q_i^2 - \frac{e^{-4\alpha}}{4}\, p_i^2 - h e^{2\alpha} q_i + h^2\right],
\end{aligned} \qquad \langle 4.5 \rangle$$

where

$$\tilde{\tilde{\epsilon}}_0 = \tilde{\epsilon}_0 - 2h\,[(\mathrm{g}_0 - \mathrm{g}_0') + z(\mathrm{g}_1 - \mathrm{g}_1')]\,.$$

This transformation takes care of the phonon correlation at a particular site. However, it neglects intersite phonon correlations. Lo and Sollie [21] have suggested a correlated squeezing state that includes the NN phonon correlations and leads to a further lowering of the GS energy. Following Lo and Sollie, we now perform an additional unitary transformation with a generator

$$\mathcal{S}_4 = \frac{1}{2}\sum_{i\neq j}\beta_{ij}\left(b_i b_j - b_i^{\dagger} b_j^{\dagger}\right), \qquad \langle 4.6\rangle$$

where we choose $\beta_{ij} = \beta$, when i and j are NN's and $\beta_{ij} = 0$ otherwise. To find how the phonon operators transform under this transformation, we calculate the following commutators:

$$[\mathcal{S}_4, b_i] = \left[\frac{1}{2}\sum_{k\neq k_1}\beta_{kk'}\left(b_k b_{k_1} - b_k^{\dagger} b_{k_1}^{\dagger}\right), b_i\right] = -\frac{1}{2}\sum_{k\neq k_1}\beta_{kk_1}\left[b_k^{\dagger} b_{k'}^{\dagger}, b_i\right]$$

$$= -\frac{1}{2}\sum_{k\neq k_1}\beta_{kk_1}\left(-b_{k_1}^{\dagger}\,\delta_{ki} - \delta_{k_1 i}\,b_k^{\dagger}\right) = \sum_{k\neq i}\beta_{ki}\,b_k^{\dagger},$$

$$\left[\mathcal{S}_4, [\mathcal{S}_4, b_i]\right] = \left[\mathcal{S}_4, \frac{1}{2}\sum_{k\neq i}\beta_{ki}\,b_k^{\dagger}\right] = \frac{1}{2}\sum_{k\neq i}\beta_{ki}\left[\mathcal{S}_4, b_k^{\dagger}\right]$$

$$= \sum_{k\neq i}\beta_{ki}\sum_{k_1\neq k}\beta_{k_1 k}\,b_{k'} = \sum_{k k_1}\beta_{ik}\,\beta_{kk_1}\,b_{k_1},$$

$$\left[\mathcal{S}_4, \left[\mathcal{S}_4, [\mathcal{S}_4, b_i]\right]\right] = \sum_{k k_1 k_2}\beta_{ik}\,\beta_{kk_1}\,\beta_{k_1 k_2}\,b_{k_2}^{\dagger}\,,$$

and so on. We have dropped the restriction on the summation indices, since all the diagonal terms are zero ($\beta_{ii} = 0$). Now, we can write the transformed phonon operators as:

$$e^{\mathcal{S}_4}\, b_i\, e^{-\mathcal{S}_4} = \sum_j \left(\mu_{ij}\, b_j + \nu_{ij}\, b_j^\dagger\right),$$

$$e^{\mathcal{S}_4}\, b_i^\dagger\, e^{-\mathcal{S}_4} = \sum_j \left(\mu_{ij}\, b_j^\dagger + \nu_{ij}\, b_j\right),$$

$$e^{\mathcal{S}_4}\, q_i\, e^{-\mathcal{S}_4} \equiv\ e^{\mathcal{S}_4}\, (b_i^\dagger + b_i)\, e^{-\mathcal{S}_4} = \sum_j \left(\mu_{ij} + \nu_{ij}\right)\left(b_j + b_j^\dagger\right),$$

$$e^{\mathcal{S}_4}\, p_i\, e^{-\mathcal{S}_4} \equiv\ e^{\mathcal{S}_4}(b_i^\dagger - b_i)\, e^{-\mathcal{S}_4} = \sum_j \left(\mu_{ij} - \nu_{ij}\right)\left(b_j - b_j^\dagger\right),$$

$$e^{\mathcal{S}_4}\, e^{(Y_i - Y_j)e^{-2\alpha}} e^{-\mathcal{S}_4} = \exp\left[e^{\mathcal{S}_4}\left(Y_i - Y_j\right)e^{-2\alpha}\, e^{-\mathcal{S}_4}\right] = \exp\left[\sum_k \mathcal{B}_k^{ij}\left(b_i^\dagger - b_i\right)\right],$$

where

$$\mathcal{B}_m^{ij} = \frac{\mathrm{g}_0'}{\omega_0}\left[\left(\mu_{im} + \nu_{im}\right) - \left(\mu_{jm} + \nu_{jm}\right)\right]$$

$$+ \frac{\mathrm{g}_0'}{\omega_0}\sum_\delta \left[\left(\mu_{jm} + \nu_{jm}\right) - \left(\mu_{j+\delta,m} + \nu_{j+\delta,m}\right)\right], \text{here}, j = i + \delta$$

$$\mu_{ij} = \delta_{ij} + \frac{1}{2!}\sum_k \beta_{ik}\, \beta_{kj} + \frac{1}{4!}\sum_{klm} \beta_{ik}\, \beta_{kl}\, \beta_{lm}\, \beta_{mj} + \cdots,$$

$$\nu_{ij} = \beta_{ij} + \frac{1}{3!}\sum_{kl} \beta_{ik}\, \beta_{kl}\, \beta_{lj} + \frac{1}{5!}\sum_{klmn} \beta_{ik}\, \beta_{kl}\, \beta_{lm}\, \beta_{mn}\, \beta_{nj} + \cdots,$$

If we add or subtract above two equations, we get

$$\mu_{ij} \pm \nu_{ij} = \delta_{ij} \pm \beta_{ij} + \frac{1}{2!}\sum_{k} \beta_{ik}\,\beta_{kj} \pm \frac{1}{3!}\sum_{kl} \beta_{ik}\,\beta_{kl}\,\beta_{lj} + \frac{1}{4!}\sum_{klm} \beta_{ik}\,\beta_{kl}\,\beta_{lm}\,\beta_{mj} \pm \cdots$$

$$= (\mathbb{I})_{ij} \pm (\boldsymbol{\beta})_{ij} + \frac{1}{2!}(\boldsymbol{\beta}^2)_{ij} \pm \frac{1}{3!}(\boldsymbol{\beta}^3)_{ij} + \frac{1}{4!}(\boldsymbol{\beta}^4)_{ij} \pm \cdots = \left(e^{\boldsymbol{\beta}}\right)_{ij},$$

where $\boldsymbol{\beta}$ is a matrix of order $N \times N$. Using above equations, we obtain the new transformed Hamiltonian, $\widetilde{\mathcal{H}}_4 = e^{\mathcal{S}_4}\widetilde{\mathcal{H}}_3\, e^{-\mathcal{S}_4}$ as

$$\widetilde{\mathcal{H}}_4 = \tilde{\tilde{\epsilon}}_0 \sum_{i\sigma} n_{i\sigma} - t \sum_{\langle ij\rangle\sigma} \exp\left[e^{-2\alpha}\sum_{m} \mathcal{B}_m^{ij}\, p_m\right] c_{i\sigma}^{\dagger}\, c_{j\sigma}$$

$$+ \omega_0 \sum_{i}\left[\frac{e^{4\alpha}}{4}\left\{\sum_{m}(e^{\boldsymbol{\beta}})_{im} q_m\right\}^2 - \frac{e^{-4\alpha}}{4}\left\{\sum_{m}(e^{-\boldsymbol{\beta}})_{im} p_m\right\}^2 - h\, e^{2\alpha}\left\{\sum_{m}(e^{\boldsymbol{\beta}})_{im} q_m\right\} + h^2\right]$$

$$+ (\mathrm{g}_0 - \mathrm{g}_0')e^{2\alpha}\sum_{i\sigma} n_{i\sigma}\left[\sum_{m}\left(e^{\boldsymbol{\beta}}\right)_{im} q_m\right] + (\mathrm{g}_1 - \mathrm{g}_1')e^{2\alpha}\sum_{\langle ij\rangle\sigma} n_{i\sigma}\left[\sum_{m}\left(e^{\boldsymbol{\beta}}\right)_{jm} q_m\right]$$

$$+ V_1 \sum_{\langle ij\rangle\sigma\sigma'} n_{i\sigma}\, n_{j\sigma'} + V_2 \sum_{i\delta'\sigma\sigma'} n_{i\sigma}\, n_{i+\delta',\sigma'} + V_3 \sum_{i\delta''\sigma\sigma'} n_{i\sigma}\, n_{i+\delta'',\sigma'}, \qquad \langle 4.7\rangle$$

Obviously, the last two transformations spoil the coherence of phonons at the expense of including correlations. In order to restore coherence, we therefore perform another coherent state transformation with the generator

$$\mathcal{S}_5 = h' \sum_{i}\left(b_i^{\dagger} - b_i\right), \qquad \langle 4.8\rangle$$

where h' is another variational parameter. The transformed Hamiltonian $\widetilde{\mathcal{H}}_5 = e^{\mathcal{S}_5}\,\widetilde{\mathcal{H}}_4\, e^{-\mathcal{S}_5}$ is given by

$$\widetilde{\mathcal{H}}_5 = \tilde{\tilde{\epsilon}}_0 \sum_{i\sigma} n_{i\sigma} - t \sum_{\langle ij\rangle\sigma} \exp\left[e^{-2\alpha} \sum_m \mathcal{B}_m^{ij}\, p_m\right] c_{i\sigma}^{\dagger}\, c_{j\sigma}$$

$$+\omega_0 \sum_i \left[\frac{e^{4\alpha}}{4}\left\{\sum_m \left(e^{\boldsymbol{\beta}}\right)_{im}(q_m - 2h')\right\}^2 - \frac{e^{-4\alpha}}{4}\left\{\sum_m \left(e^{-\boldsymbol{\beta}}\right)_{im} p_m\right\}^2\right]$$

$$-\omega_0 \sum_i \left[h\, e^{2\alpha}\left\{\sum_m \left(e^{\boldsymbol{\beta}}\right)_{im}(q_m - 2h')\right\} - h^2\right]$$

$$+ (\mathrm{g}_0 - \mathrm{g}_0')e^{2\alpha} \sum_{i\sigma} n_{i\sigma}\left[\sum_m \left(e^{\boldsymbol{\beta}}\right)_{im}(q_m - 2h')\right]$$

$$+ (\mathrm{g}_1 - \mathrm{g}_1')e^{2\alpha} \sum_{\langle ij\rangle\sigma} n_{i\sigma}\left[\sum_m \left(e^{\boldsymbol{\beta}}\right)_{im}(q_m - 2h')\right]$$

$$+ V_1 \sum_{\langle ij\rangle\sigma\sigma'} n_{i\sigma} n_{j\sigma'} + V_2 \sum_{i\delta'\sigma\sigma'} n_{i\sigma} n_{i+\delta',\sigma'} + V_3 \sum_{i\delta''\sigma\sigma'} n_{i\sigma} n_{i+\delta'',\sigma'}. \quad \langle 4.9\rangle$$

Averaging the transformed Hamiltonian $\widetilde{\mathcal{H}}_5$ with respect to the zero-phonon state, we then obtain the following effective extended Hubbard Hamiltonian as

$$\mathcal{H}_e = \langle 0|\, \widetilde{\mathcal{H}}_5\, |0\rangle$$

$$= \epsilon_e \sum_{i\sigma} n_{i\sigma} - t_e \sum_{\langle ij\rangle\sigma} c_{i\sigma}^{\dagger}\, c_{j\sigma} + U_e \sum_i n_{i\uparrow}\, n_{i\downarrow}$$

$$+ V_1^e \sum_{\langle ij\rangle\sigma\sigma'} n_{i\sigma}\, n_{j\sigma'} + V_2^e \sum_{i\delta'\sigma\sigma'} n_{i\sigma}\, n_{i+\delta',\sigma'} + V_3^e \sum_{i\delta''\sigma\sigma'} n_{i\sigma}\, n_{i+\delta'',\sigma'}$$

$$+ N\omega_0\left[\frac{e^{4\alpha}}{4}\left(e^{2\boldsymbol{\beta}}\right)_{00} + \frac{e^{-4\alpha}}{4}\left(e^{-2\boldsymbol{\beta}}\right)_{00} - \frac{1}{2}\right]$$

$$+ N\omega_0\,[h^2 + h'\, e^{2\alpha}(2hM_1 + h'\, e^{2\alpha} M_2)], \quad \langle 4.10\rangle$$

where

$$\epsilon_e = -\frac{1}{\omega_0}\left[\,2(\,\mathrm{g}_0\,\mathrm{g}_0' + z\,\mathrm{g}_1\,\mathrm{g}_1'\,) - (\,\mathrm{g}_0'^{\,2} + z\,\mathrm{g}_1'^{\,2}\,)\,\right]$$

$$-2\,(\,h + h'\,e^{2\alpha}\,M_1\,)[\,(\,\mathrm{g}_0\,+\,z\,\mathrm{g}_1\,) - (\,\mathrm{g}_0' + z\,\mathrm{g}_1'\,)\,], \qquad \langle 4.10a\rangle$$

$$t_e = t\,e^{-\frac{1}{2}e^{-4\alpha}\mathcal{B}_{ij}}, \qquad \langle 4.10b\rangle$$

$$\mathcal{B}_{ij} = \frac{2\mathrm{g}_0'^{\,2}}{\omega_0^{\,2}}\left[\left(e^{-2\boldsymbol{\beta}}\right)_{00} - \left(e^{-2\boldsymbol{\beta}}\right)_{01}\right] + \frac{4\,\mathrm{g}_0'\mathrm{g}_1'}{\omega_0^{\,2}}\sum_{\delta'}\left[\left(e^{-2\boldsymbol{\beta}}\right)_{0\delta'} - \left(e^{-2\boldsymbol{\beta}}\right)_{i+\delta,i+\delta'}\right]$$

$$+\frac{2\mathrm{g}_1'^{\,2}}{\omega_0^{\,2}}\sum_{\delta'\delta''}\left[\left(e^{-2\boldsymbol{\beta}}\right)_{i+\delta',i+\delta''} - \left(e^{-2\boldsymbol{\beta}}\right)_{i+\delta',j+\delta''}\right], \qquad \langle 4.10c\rangle$$

$$\left(e^{\pm 2\boldsymbol{\beta}}\right)_{00} = \pm\sum_{m=0}^{\infty}\binom{2m}{m}\frac{(2\beta)^{2m}}{m!\,m!}, \qquad \langle 4.10d\rangle$$

$$\left(e^{\pm 2\boldsymbol{\beta}}\right)_{0n} = \pm\sum_{m=1}^{\infty}\binom{\left[2m+\left(\frac{n-1}{2}+1\right)\right]}{m}\frac{(2\beta)^{\left[2m+\left(\frac{n-1}{2}+1\right)\right]}}{m!\left[m+\left(\frac{n-1}{2}+1\right)\right]!}, \boldsymbol{n}\text{: odd} \qquad \langle 4.10e\rangle$$

$$\left(e^{\pm 2\boldsymbol{\beta}}\right)_{0n} = \pm\sum_{m=1}^{\infty}\binom{\left[2m+\left(\frac{n}{2}+1\right)\right]}{m+1}\frac{(2\beta)^{\left[2m+\left(\frac{n}{2}+1\right)\right]}}{m!\left[m+\left(\frac{n}{2}+1\right)\right]!}, \quad \boldsymbol{n}\text{: even} \qquad \langle 4.10f\rangle$$

$$U_e = U - \frac{2}{\omega_0}\left[\,2(\mathrm{g}_0\,\mathrm{g}_0' + z\,\mathrm{g}_1\,\mathrm{g}_1'\,) - (\,\mathrm{g}_0'^{\,2} + z\,\mathrm{g}_1'^{\,2}\,)\right], \qquad \langle 4.10g\rangle$$

$$V_1^e = V_1 - \frac{2}{\omega_0}[(\mathrm{g}_0\mathrm{g}_1' + \mathrm{g}_1\mathrm{g}_0') - \mathrm{g}_0'\mathrm{g}_1'], \qquad \langle 4.10h\rangle$$

$$V_2^e = V_2 - \frac{1}{\omega_0}[(2\mathrm{g}_1 - \mathrm{g}_1')\,\mathrm{g}_1'], \qquad \langle 4.10i\rangle$$

$$V_3^e = V_3 \quad \text{(Always positive)}, \qquad \langle 4.10j\rangle$$

$$M_n = \left(e^{n\boldsymbol{\beta}}\right)_{00} + 2\,n\sum_{m}\left(e^{n\boldsymbol{\beta}}\right)_{0m}, \qquad n = 1, 2. \qquad \langle 4.10k\rangle$$

In the above equations z, z' and z'' represent the number of NN, NNN and next NNN sites respectively.

4.4 GROUND STATE ENERGY: HFA

We consider the square density of states for the electrons and use the mean-field Hartree-Fock decoupling scheme (see Chapter 1) for the correlated terms. After decoupling the correlated terms, we finally obtain the GS energy as

$$E = \frac{E_g}{N} = \epsilon_e n + \frac{1}{4}U_e n^2 - \frac{1}{2}(2n - n^2)\, z\, t_e + V_1^e z\, n^2 + V_2^e z'\, n^2 + V_3^e z''\, n^2$$

$$+ \omega_0[\, h^2 + h' e^{2\alpha}\, (\, 2\, h\, M_1 \; + \; h'\, e^{2\alpha} M_2)]$$

$$+ \omega_0 \left[\frac{e^{4\,\alpha}}{4}(e^{2\,\beta})_{00} + \frac{e^{-4\,\alpha}}{4}(e^{-2\,\beta})_{00} - \frac{1}{2}\right], \qquad \langle 4.11 \rangle$$

where g_0', g_1', h, α, β and h' are six variational parameters with respect to which the energy expression $\langle 4.11 \rangle$ has to be minimized to obtain the GS energy.

4.5 NUMERICAL RESULTS

Equation $\langle 4.11 \rangle$ cannot be minimized analytically and therefore we have to resort to numerical computations. For the purpose of numerical calculation, we choose to work with two values of the hopping parameter, namely $t = 0.5$ and $t = 2$ and thus we consider both the anti-adiabatic ($t < \omega_0$) and the adiabatic ($t > \omega_0$) cases. The results for the

GS energy are shown in Fig. 4.1. Fig. 4.1(a) provides results for the anti-adiabatic region ($t = 0.5$), while Fig. 4.1(b) gives those for the adiabatic case ($t = 2.0$). The figures also show the comparison with the results of DS [17]. To make the comparison possible we have considered $V_1 = V_2 = V_3 = 0$ and $g_1 = 0$ in our calculation. It is clearly evident that energy results calculated from our variational wave function are much better

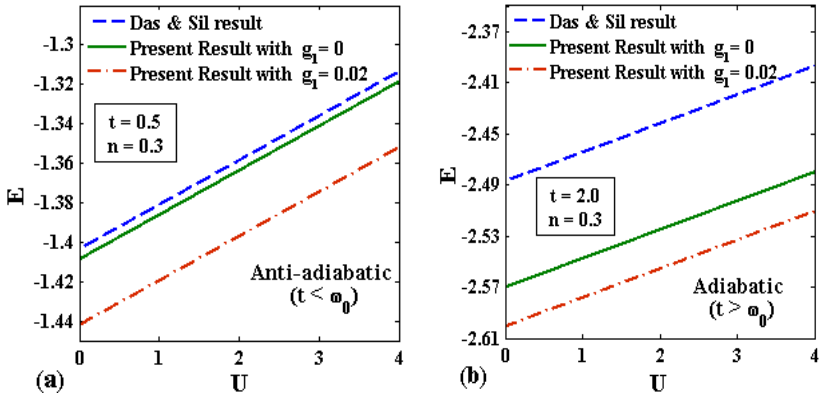

Fig. 4.1. **E** vs. $\boldsymbol{U}$ for $\boldsymbol{n = 0.3}$ and $\boldsymbol{g_0 = 2}$: (a) Anti-adiabatic case; (b) Adiabatic case.

than those obtained by using the wave function of DS [17], more so in the adiabatic case. We also obtain results for a non-zero value of g_1. Results for $g_1 = 0.02$ show that the NN *e-p* interaction further reduces the energy, the reduction being more pronounced in the anti-adiabatic region.

In Fig. 4.2, we show the variations of g_0'/g_0 (Fig. 4.2a) and g_1'/g_0' Fig. 4.2b) with onsite *e-p* strength g_0 for the electron concentration $n = 0.3$ and for different values of the NN *e-p* interaction strength ($g_1 = 0, 0.1, 0.25$) for the anti-adiabatic case ($t = 0.5$). One can find out from the figures that for small values of g_0, $g_0' < g_0$, but $g_1' > g_1$. This implies that in this region the phonon cloud associated with the polaron is thin but is spread over many lattice sites and thus one has a large polaron.

As g_0 increases, g_0' also increases and eventually becomes equal to g_0, but g_1' decreases substantially so much so that g_1' becomes smaller than g_1. Thus the phonon cloud around the electron becomes confined essentially to a single lattice site and one has a small polaron. Thus the formation of a small polaron and the concomitant localization occur at a critical value of $g_0 = g_{anti-ad}$. In Fig. 4.2, we have shown results for two non-zero values of g_1, namely $g_1 = 0.1$ and 0.25. We find that even at

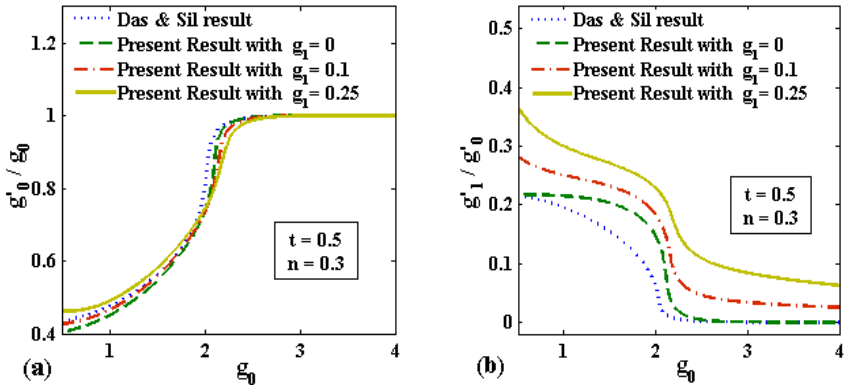

Fig. 4.2 (a) g_0'/g_0 vs. g_0 for $t = 0.5$; (b) g_1'/g_0 vs. g_0 for $t = 0.5$.

larger values of g_1, we have large polarons for small values of g_0, but their sizes are slightly smaller than the polaron in the $g_1 = 0$ case, while for large values of g_0, we have small polarons with slightly larger size than the polaron in the $g_1 = 0$ case. So the effect of the NN *e-p* interaction is to slightly reduce the size of the large polaron and increase the size of the small polaron but it does not change the behavior of the transition. Thus one can see that in the anti-adiabatic regime, the ST transition from a large polaron to a small polaron (which may be called a quantum phase transition) is continuous.

In Fig. 4.3, we show the transition of a polaron from an large polaron state to an small polaron state for $g_1 = 0, 0.1$ and 0.25 in an adiabatic

case ($t = 2$). Again for small values of g_0, we have a large polaron and for large values of g_0, we have a small polaron. But the transition is now discontinuous. For non-zero values of g_1, the size of a polaron becomes slightly different from that for $g_1 = 0$ as also happens in the anti-adiabatic case. Thus we conclude that in the adiabatic regime, irrespective of the value of g_1, a sharp discontinuous transition occurs from a large polaron to a small polaron as g_0 is increased. However, now the transition occurs at large values of g_0. It is seen that the abrupt changes in the values of g_0' and g_1', i.e., the amount of the discontinuities in g_0' and g_1' at transition decreases with the reduction in t and the transition becomes continuous below a certain value of t. This may be termed as the critical hopping parameter t_c.

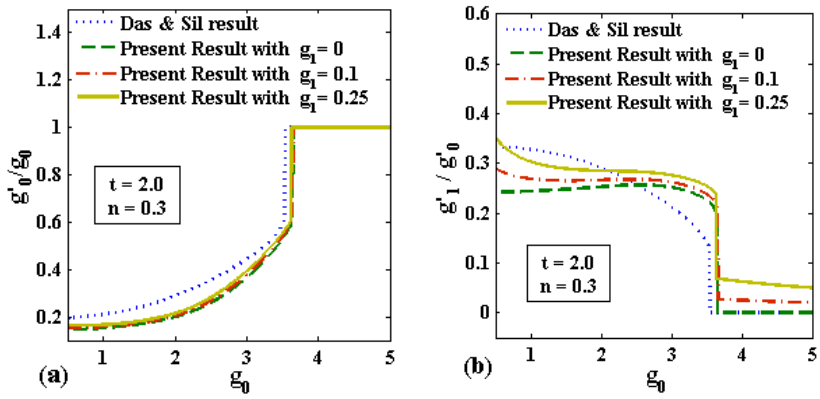

Fig. 4.3 (a) g_0'/g_0 vs. g_0 for $t = 2$; (b) g_1'/g_0' vs. g_0 for $t = 2$.

To confirm the above scenario we also study the behavior of the parameters α and β which give respectively the onsite and the NN phonon correlations. In Fig. 4.4, we plot α and β as a function of g_0. For g_0 larger than certain critical values, the squeezing parameters (α and β) become zero confirming the existence of localized (small) polarons in both the anti-adiabatic and adiabatic cases. One can observe that the values of α increase with increasing g_0, reach their maxima and

then start decreasing and finally go to zero continuously as g_0 approaches a critical value $g_{anti-ad}$ for $t = 0.5$, while for $t = 2$, α drops to zero discontinuously from its maximum as g_0 approaches the critical value g_{ad}. The behavior of β is however slightly more dramatic in the anti-adiabatic case. As g_0 increases, β also increases and reaches a maximum, but on further increase in g_0, β decreases to a negative value and as g_0 increases further, it goes to zero continuously at $g_0 = g_{anti-ad}$.

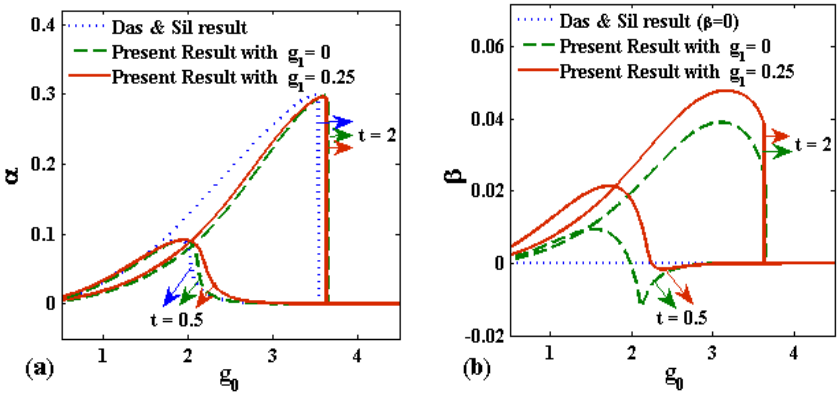

Figure 4.4 (a) α vs. g_0 for $n = 0.3$; (b) β vs. g_0 for $n = 0.3$.

The behavior of β in the adiabatic case is simple. As g_0 increases, β increases monotonically to a maximum and then decreases on further increase in g_0 and finally drops to zero discontinuously at $g_0 = g_{ad}$. As we have already pointed out, $g_{anti-ad} < g_{ad}$. It is clear from the above observation that the phonon correlation effects are most important in the intermediate-coupling region and are essentially unimportant in the strong-coupling limit.

To reconfirm the nature of the ST transition, we finally study the variation of the effective hopping integral t_e which is proportional to the polaron band width ($W = 2zt_e$) and thus gives a measure of the polaron

mass which is a physical quantity. Fig. 4.5 shows that t_e is a decreasing function of g_0 which is however understandable because of the band

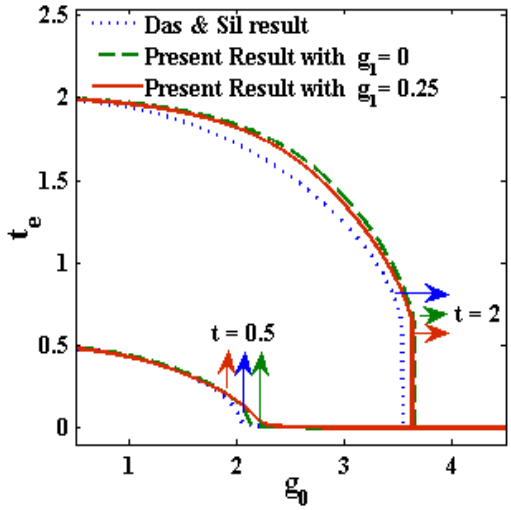

Fig. 4.5 Variation of t_e with g_0 for $n = 0.3$ for two values of t.

narrowing effect associated with the polaron formation. Our results suggest that t_e decreases as g_0 increases and finally becomes zero continuously for $t = 0.5$, but for $t = 2$ our results predict a continuous decrease in t_e only until g_0 attains a critical value of 3.7 at which however t_e undergoes a discontinuous drop indicating a sharp ST transition.

4.6 SUMMARY

In this chapter, we have studied the nature of ST transition in an extended HH model in two dimensions using a variational method. We have employed a series of canonical transformations followed by a zero-phonon averaging to obtain an effective extended HH model which we have solved by the mean-field HFA. Our results show that the ST

transition is continuous in the anti-adiabatic regime and discontinuous for the adiabatic case. It has been pointed out by Das and Sil that the discontinuity in the ST transition in the adiabatic case could be due to insufficient number of variational parameters used in their wave function. Since in our calculation we have considered quite an accurate wave function with a good number of parameters, we believe that the discontinuity at the ST transition, if at all an artifact, could be arising due to mean-field approximation. Therefore a better method to deal with the effective HH model is certainly called for.

REFERENCES

[1] W. Nolting, *Fundamentals of Many-body Physics*, Springer-Verlag Berlin Heidelberg (2009).

[2] Y. Nagaoka, *Ferromagnetism in a narrow, almost half-filled s band*, Phys. Rev. **147**, 392 (1966). *ibib.* Solid State Commun. **3**, 409 (1965).

[3] P. Fulde, *Electron Correlations in Molecules and Solids*, Springer-Verlag Berlin Heidelberg (1995).

[4] Y. Toyozawa, *Self-trapping of an electron by the acoustical mode of lattice vibration. I*, Prog. Theor. Phys. **26**, 29 (1961).

[5] K. Cho & Y. Toyozawa, *Exciton-phonon interaction and optical spectra- ST, zero-phonon line and phonon sidebands*, J. Phys. Soc. Jpn. **30**, 1555 (1971).

[6] Y. Shinozuka & Y. Toyozawa, *Self-trapping in mixed crystal-clustering, dimensionality, percolation*, J. Phys. Soc. Jpn. **46**, 505 (1979).

[7] A. Chatterjee & S. Sil, *Phase transition in a many-electron gas in a 2D polar-semiconductor quantum well*, Phys. Rev. B **51**, 2223 (1995).

[8] D. Emin, *On the existence of free & self-trapped carriers in insulators: An abrupt temp.-dependent conductivity transition*, Adv. Phys. **22**, 57 (1973).

[9] D. Yarkony & R. Silbey, J. Chem. Phys. **65**, 1042 (1976) *ibid.* J. Chem. Phys. **67**, 5818 (1977).

[10] H. De Raedt & A. Lagendijk, *Monte Carlo simulation of quantum statistical lattice models*, Phys. Rep. **127**, 233 (1985).

[11] P.O.J. Scherer, E.W. Knapp & S.F. Fischer, *Exciton-phonon self-trapping: A continuous transition*, Chem. Phys. Lett. **106**, 191 (1984).

[12] G. Venzl & S.F. Fisher, *Theory of exciton-phonon coupling in one-dimensional molecular crystals: A variational treatment with delocalized solitary states*, Phys. Rev. B **32**, 6437 (1985).

[13] H. Löwen, *Absence of phase transition in Holstein systems*, Phys. Rev. B **22**, 57 (1973).

[14] T. Holstein, *Studies of polaron motion: Part I. The molecular-crystal model*, Ann. Phys. (N.Y.) **8**, 325 (1959).

[15] T. Holstein, *Studies of polaron motion: Part I. The "small" polaron*, Ann. Phys. (N.Y.) **8**, 343 (1959).

[16] R.P.M. Krishna, S. Mukhopadhyay & A. Chatterjee, *Nature of self-trapping transition in a 1D Holstein-Hubbard model*, Phys. Lett. A **327**, 67 (2004).

[17] A.N. Das & S. Sil, *A study of the polaronic band width and the small-to-large-polaron transition in a many-polaron system*, J. Phys.: Condens. Matter **5**, 8265 (1993).

[18] I.V. Sankar, P J Monisha, S. Sil & A. Chatterjee, *Persistent current and the existence of a metallic phase flanked by two insulating phases in a quantum ring with both e-e and e-p interactions*, Physica E **73**, 175 (2015).

[19] Y. Takada & A. Chatterjee, *Possibility of a metallic phase in the CDW-SDW crossover region in the one-dimensional HH model at half-filling*, Phys. Rev. B **67**,081102 (R) (2003).

[20] Z. Hang, *Variational ground state for the periodic Anderson model with an indirect hybridization*, Phys. Rev. B **36**, 8736 (1987).

[21] C.F. Lo & R. Sollie, *Correlated squeezed polaron states in 1D*, Phys. Rev. B **48**, 10183 (1993).

CHAPTER 5

SELF-TRAPPING TRANSITION IN A 2D EXTENDED HOLSTEIN-HUBBARD MODEL IN STRONG-CORRELATION REGIME

ABSTRACT

The aim of the present chapter is to study the nature of the *self-trapping transition* in a 2D *extended Holstein-Hubbard model* in the *strong correlation regime* within the framework of the *Hartree-Fock mean-field theory*.

5.1 INTRODUCTION

The discovery of high T_c - superconductivity [1] in doped La_2CuO_4 and $YBa_2Cu_3O_6$ and the subsequent suggestion by Anderson [2] about the importance of electron correlation for the superconductivity in these materials led us to study the strong correlation (SC) regime ($U \gg t$) of the Hubbard model. Since small polarons are also likely to play an important role in high– T_c superconductors [3-5] it is also interesting to study the Holstein-Hubbard (HH) model in the SC regime in this context. There have been suggestions [8] advocating essentially the self-trapping (ST) transition as the basic mechanism for the large increase in magnetoresistance associated with the paramagnetic-to-ferromagnetic phase transition in manganites. Therefore, both for high– T_c superconductors and CMR materials [6,7], it is important to study the nature of the ST transition in the HH model in the SC regime. It is also quite imperative that many important electronic properties of strongly correlated electron systems will be highly modified by the *e-p* interaction if the strength of this coupling in those materials happens to be substantially large.

In this chapter, we study the effect of *e-p* interaction in a strongly correlated electron system within the framework of the extended Holstein-Hubbard (EHH) model in two dimensions. The hopping motion of electrons in this case is restricted due to the presence of SC i.e., the excitation of the electrons is confined within the lower Hubbard subband and does not involve the transition of an electron from the lower to the higher subbands for such processes would require a huge amount of energy. Another characteristic feature of the SC regime is that in this regime, even the hopping of an up-spin electron to a nearest-neighbour (NN) site occupied by a down-spin electron, which is allowed according

to Pauli principle, is not permissible due to Coulomb correlation. As a result of this, the dimension of the many-electron Hilbert space is reduced to 3^N, since double occupancies are forbidden for strong *e-e* interactions. The above mentioned features are of course valid in the absence of *e-p* interaction. It is well-known that the *e-p* interaction can give rise to an attractive *e-e* interaction which reduces the repulsive Coulomb interaction between electrons in general and under certain conditions may lead to a pairing of electrons. It may be important to understand the interplay between these two competing interactions at finite doping from the point of view of practical situations. Several investigations have shown that it is possible for a system to undergo a transition from one GS to another as *e-p* coupling constant is tuned. Among these, the problem of ST transition from a delocalized polaron state to a localized polaron state in a many-polaron system, has remained in the focus of attention for a long time. Several investigations [9,10] have shown that as the *e-p* interaction is increased, the quasi-particle weight of a polaron becomes negligibly small or goes to zero. Fehske *et al.* [11] have investigated the polaron band narrowing factor as a function of polaron binding energy for different band-fillings within the framework of a 2D HH model and suggested the existence of ST transition in *e-p* systems. As we have already pointed out, there is a general consensus that such a transition does exist, but the actual nature of the transition still continues to be a subject of debate, primarily because the problem is not exactly soluble and furthermore the *e-e* interaction makes the problem extra-ordinarily more complex. In the preceding chapter we have presented our work on the ST transition in the weak-correlation regime. The purpose of the present chapter is to examine the nature of the ST transition in 2D EHH model in the SC regime.

5.2 MODEL HAMILTONIAN INTRODUCTION

The EHH model considered here is given by

$$\mathcal{H} = -t\sum_{\langle ij\rangle\sigma} c_{i\sigma}^{\dagger}c_{j\sigma} + U\sum_{i} n_{i\uparrow}\, n_{i\downarrow} + \omega_0 \sum_{i} b_i^{\dagger}b_i + V\sum_{\langle ij\rangle\sigma\sigma'} n_{i\sigma}n_{j\sigma'}$$

$$+ \mathrm{g}_0\sum_{i\sigma} n_{i\sigma}\left(b_i + b_i^{\dagger}\right) + \mathrm{g}_1\sum_{\langle ij\rangle\sigma} n_{i\sigma}\left(b_j + b_j^{\dagger}\right), \qquad \langle 5.1\rangle$$

where the notations have their using meaning. The phonons are eliminated in the same way as done in the previous chapter. We however consider here $h = h' = 0$ for the sake of numerical simplicity.

5.3 EFFECTIVE ELECTRONIC HAMILTONIAN

(i) ELIMINATION OF PHONONS

As mentioned method, we eliminate the phonons in the same ways as done in Chapter 1, with the only difference that now we choose $h = h' = 0$ for simplicity. Thus we apply three canonical transformations with the following generators:

$$\mathcal{S}_1 = \frac{\mathrm{g}_0'}{\omega_0}\sum_{i\sigma} n_{i\sigma}\left(b_i^{\dagger} - b_i\right) + \frac{\mathrm{g}_1'}{\omega_0}\sum_{\langle ij\rangle\sigma} n_{i\sigma}\left(b_j^{\dagger} - b_j\right), \qquad \langle 5.2a\rangle$$

$$\mathcal{S}_2 = \alpha\sum_{i}\left(b_i b_i - b_i^{\dagger}b_i^{\dagger}\right), \qquad \langle 5.2b\rangle$$

$$\mathcal{S}_3 = \frac{1}{2}\sum_{i\neq j}\beta_{ij}\left(b_i b_j - b_i^{\dagger}b_j^{\dagger}\right), \qquad \langle 5.2c\rangle$$

and then perform the zero-phonon averaging of the transformed Hamiltonian to obtain the effective extended Hubbard model as

$$\mathcal{H}_{eff} = \epsilon_e \sum_{i\sigma} n_{i\sigma} - t_e \sum_{\langle ij\rangle\sigma} c_{i\sigma}^{\dagger} c_{j\sigma} + U_e \sum_{i} n_{i\uparrow} n_{i\downarrow} + V_e \sum_{\langle ij\rangle\sigma\sigma'} n_{i\sigma} n_{j\sigma'} + K, \quad \langle 5.3\rangle$$

where

$$\epsilon_e = \frac{1}{\omega_0}\left[\left(\mathrm{g}_0'^{\,2} + z\,\mathrm{g}_1'^{\,2}\right) - 2(\,\mathrm{g}_0\,\mathrm{g}_0' + z\,\mathrm{g}_1\,\mathrm{g}_1')\right], \qquad \langle 5.3a\rangle$$

$$U_e = U - \frac{2}{\omega_0}\left[(\,2\mathrm{g}_0 - \mathrm{g}_0')\mathrm{g}_0' + z\,\mathrm{g}_1'(\mathrm{g}_1 - \mathrm{g}_1')\right], \qquad \langle 5.3g\rangle$$

$$V_e = V - \frac{2}{\omega_0}[(\,\mathrm{g}_0\mathrm{g}_1' + \mathrm{g}_1\,\mathrm{g}_0') - \mathrm{g}_0'\,\mathrm{g}_1'\,], \qquad \langle 5.3h\rangle$$

$$K = \frac{N\omega_0}{4}\left[\, e^{4\alpha}\left(e^{2\boldsymbol{\beta}}\right)_{00} + e^{-4\alpha}\left(e^{-2\boldsymbol{\beta}}\right)_{00} - 2\,\right], \qquad \langle 5.3i\rangle$$

where ϵ_e is the polaronic contribution to the electron self-energy, t_e is the effective hopping integral (see, Eq. $\langle 4.11b\rangle$ in Chapter 4), U_e is the renormalized onsite Coulomb interaction, V_e is the renormalized NN *e-e* interaction and $\boldsymbol{\beta}$ is an $N \times N$ matrix with a typical element β_{ij}, and z is the number of NN sites in the lattice.

For strong onsite *e-e* interaction, most of the sites are occupied by single electrons, the double occupancies being energetically unfavorable. Then we can restrict ourselves to the Hilbert space of the 2^N disordered spin configurations by neglecting all high energy states that are well separated in energy [12]. In the case of a half-filled band ($n = 1$), the Hubbard model maps on to the Heisenberg model in the SC regime. Consequently, the onsite Coulomb repulsion term can be omitted and then each site can be assumed to be either empty or occupied by a single electron. However, double occupancies can still occur by virtual

fluctuations leading to an effective antiferromagnetic interaction. When the band is close to half filling, an effective $t-J$ model is obtained in a subspace of no double occupancy [13] with a few holes moving between the localized spins. Here is the way to transform effective Hubbard model into an effective $t-J$ model using canonical transformation [13-15] as given in the subsequent section.

(ii) $\mathcal{H}_{eff} \rightarrow t-J$ MODEL

The process of hopping can be thought of as a combination of restricted hopping processes: a process that increases or decreases the number of doubly occupied sites by one which can be thought upon as a transition of an electron from the lower Hubbard subband to the upper Hubbard subband and a process that does not change the number of doubly occupied sites which is essentially an electron transition within the lower Hubbard subband. These hopping processes can be mathematically represented as follows

$$c_{i\sigma}^{\dagger}c_{j\sigma} = c_{i\sigma}^{\dagger}(1-n_{i\bar{\sigma}}+n_{i\bar{\sigma}})c_{j\sigma}\left(1-n_{j\bar{\sigma}}+n_{j\bar{\sigma}}\right)$$

$$= n_{i\bar{\sigma}}\, c_{i\sigma}^{\dagger}\, c_{j\sigma}\left(1-n_{j\bar{\sigma}}\right) + (1-n_{i\bar{\sigma}})c_{i\sigma}^{\dagger}\, c_{j\sigma}\, n_{j\bar{\sigma}}$$

$$+ (1-n_{i\bar{\sigma}})c_{i\sigma}^{\dagger}c_{j\sigma}\left(1-n_{j\bar{\sigma}}\right) + n_{i\bar{\sigma}}\, c_{i\sigma}^{\dagger}\, c_{j\sigma}\, n_{j\bar{\sigma}}$$

This can be readily verified by acting these restricted hopping processes on any correlated many-electron state. The tight-binding Hamiltonian can be rewritten as

$$\mathcal{H}_{t_e} = -\,t_e \sum_{\langle ij\rangle\sigma} c_{i\sigma}^{\dagger}\, c_{j\sigma} = \mathcal{H}_{t_e}^{0} + \mathcal{H}_{t_e}^{+} + \mathcal{H}_{t_e}^{-}, \qquad \langle 5.4\rangle$$

where

$$\mathcal{H}_{t_e}^{+} = -t_e \sum_{\langle ij\rangle\sigma} \left[n_{i\bar{\sigma}}\, c_{i\sigma}^{\dagger}\, c_{j\sigma}\left(1 - n_{j\bar{\sigma}}\right) + n_{j\bar{\sigma}}\, c_{j\sigma}^{\dagger}\, c_{i\sigma}\left(1 - n_{i\bar{\sigma}}\right) \right], \qquad \langle 5.4a \rangle$$

$$\mathcal{H}_{t_e}^{-} = -t_e \sum_{\langle ij\rangle\sigma} \left[\left(1 - n_{i\bar{\sigma}}\right) c_{i\sigma}^{\dagger}\, c_{j\sigma}\, n_{j\bar{\sigma}} + \left(1 - n_{j\bar{\sigma}}\right) c_{j\sigma}^{\dagger}\, c_{i\sigma}\, n_{i\bar{\sigma}} \right], \qquad \langle 5.4b \rangle$$

$$\mathcal{H}_{t_e}^{0} = -t_e \sum_{\langle ij\rangle\sigma} \left[\left(1 - n_{i\bar{\sigma}}\right) c_{i\sigma}^{\dagger} c_{j\sigma} \left(1 - n_{j\bar{\sigma}}\right) + n_{i\bar{\sigma}}\, c_{i\sigma}^{\dagger}\, c_{j\sigma}\, n_{j\bar{\sigma}} \right], \qquad \langle 5.4c \rangle$$

Rewriting the effective Hamiltonian as

$$\mathcal{H}_{eff} = \mathcal{H}_{t_e}^{0} + \mathcal{H}_{t_e}^{+} + \mathcal{H}_{t_e}^{-} + \mathcal{H}_{U_e} + \mathcal{H}_{V_e} + \epsilon_e N + K, \qquad \langle 5.5 \rangle$$

where

$$\mathcal{H}_{U_e} = U_e \sum_{i} n_{i\uparrow}\, n_{i\downarrow}, \qquad \langle 5.5a \rangle$$

$$\mathcal{H}_{V_e} = V_e \sum_{\langle ij\rangle\sigma\sigma'} n_{i\sigma}\, n_{j\sigma'}, \qquad \langle 5.5b \rangle$$

$$N = \sum_{i\sigma} n_{i\sigma}. \qquad \langle 5.5c \rangle$$

When strong correlations ($U \gg t$) are present in the system, the processes ($\mathcal{H}_{t_e}^{+}$ and $\mathcal{H}_{t_e}^{-}$) that connect the lower Hubbard subband to the upper Hubbard subband are energetically unfavorable, since any such process may lead to an increase or decrease of the energy by an amount $U > 0$ which is very large. So, to eliminate such processes we make use of canonical transformation with a suitable generator. The generator that meets our requirement is given by

$$\mathcal{S} = \left(\frac{1}{U_e - V_e}\right)\left(\mathcal{H}_{t_e}^{+} - \mathcal{H}_{t_e}^{-}\right). \qquad \langle 5.6 \rangle$$

The transformed Hamiltonian can be written as

$$\begin{aligned}\mathcal{H}_e &= e^{\mathcal{S}}\,\mathcal{H}_{eff}\,e^{-\mathcal{S}} \\ &= \mathcal{H}_{t_e}^0 + \mathcal{H}_{U_e} + \left[\mathcal{S},\mathcal{H}_{t_e}^0\right] + \left(\mathcal{H}_{t_e}^+ + \mathcal{H}_{t_e}^-\right) + \left[\mathcal{S},\left(\mathcal{H}_{U_e} + \mathcal{H}_{V_e}\right)\right] \\ &\quad + \left[\mathcal{S},\left(\mathcal{H}_{t_e}^+ + \mathcal{H}_{t_e}^-\right)\right] + \frac{1}{2}\left[\mathcal{S},[\mathcal{S},\mathcal{H}]\right] + \cdots\end{aligned}$$

To obtain the Hamiltonian $\mathcal{H}_e$, we have to evaluate the commutators appearing in the above expression. We obtain

$$\left[\mathcal{S},\left(\mathcal{H}_{U_e} + \mathcal{H}_{V_e}\right)\right] = -\left(\mathcal{H}_{U_e} + \mathcal{H}_{V_e}\right), \qquad \langle 5.6a\rangle$$

$$\left[\mathcal{S},\left(\mathcal{H}_{t_e}^+ + \mathcal{H}_{t_e}^-\right)\right] = \left(\frac{2}{U_e - V_e}\right)\left[\mathcal{H}_{t_e}^+,\mathcal{H}_{t_e}^-\right], \qquad \langle 5.6b\rangle$$

$$\left[\mathcal{S},\left[\mathcal{S},\mathcal{H}_{U_e}\right]\right] = -\left(\frac{1}{U_e - V_e}\right)\left[\mathcal{H}_{t_e}^+,\mathcal{H}_{t_e}^-\right], \qquad \langle 5.6c\rangle$$

The transformed Hamiltonian $\mathcal{H}_e$ (with terms up to order $\mathcal{O}(t^2/U)$) is given by

$$\mathcal{H}_e = \mathcal{H}_{t_e}^0 + \mathcal{H}_{U_e} + \left(\frac{1}{U_e - V_e}\right)\left[\mathcal{H}_{t_e}^+,\mathcal{H}_{t_e}^-\right]. \qquad \langle 5.7\rangle$$

The calculation of the commutator present in the above equation is straightforward though lengthy. To calculate that commutator, one generally uses the Hubbard operators for convenience and one obtains

$$\frac{1}{U_e}\left[\mathcal{H}_{t_e}^+,\mathcal{H}_{t_e}^-\right] \rightarrow \left(\frac{2t_e^2}{U_e - V_e}\right)\left(\boldsymbol{S}_i.\boldsymbol{S}_j - \frac{1}{4}n_i n_j\right)$$

Thus the transformed Hamiltonian $\mathcal{H}_e$ is finally obtained as

$$\mathcal{H}_e = \epsilon_e \sum_{i\sigma} n_{i\sigma} + t_e \sum_{\langle ij\rangle\sigma} (1 - n_{i\bar{\sigma}}) c_{i\sigma}^{\dagger} c_{j\sigma} \left(1 - n_{j\bar{\sigma}}\right)$$

$$+ J \sum_{\langle ij\rangle} \left(\boldsymbol{S}_i . \boldsymbol{S}_j - \frac{1}{4} n_i n_j \right) + V_e \sum_{\langle ij\rangle\sigma\sigma'} n_{i\sigma} n_{j\sigma'} + K, \qquad \langle 5.8 \rangle$$

where

$$\boldsymbol{S}_i . \boldsymbol{S}_j = \frac{1}{2} \left(S_i^{+} S_j^{-} + S_i^{-} S_j^{+} \right) + S_i^{z} S_j^{z}, \qquad \langle 5.8a \rangle$$

$$S_i^{+} = c_{i\uparrow}^{\dagger} c_{i\downarrow}\,,\; S_i^{-} = c_{i\downarrow}^{\dagger} c_{i\uparrow}\,,\quad S_i^{z} = \frac{1}{2}(n_{i\uparrow} - n_{i\downarrow}), \qquad \langle 5.8b \rangle$$

$$J = \frac{2\, t_e^2}{U_e - V_e}. \qquad \langle 5.8c \rangle$$

Here J is the strength of the antiferromagnetic interaction between electrons at the NN sites. $\mathcal{H}_e$ contains the constraint that disallows double occupancy at every site. Since this constraint is difficult to handle analytically, we shall make the Gutzwiller approximation (GA) [17] to simplify the problem by replacing the actual local constraint by an average constraint. The correlated problem, then essentially reduces to an uncorrelated one with suitable renormalizations.

(iii) GUTZWILLER APPROXIMATION

The Gutzwiller variational approach is one of the simplest but effective tools to deal with SC's. This approach allows us to account for the SC's by projecting out doubly occupied sites from a given uncorrelated many-electron wave function. The starting point of the GA is to consider the uncorrelated wave function for the problem under consideration. The uncorrelated GS state wave function (eigenstate of the tight-binding Hamiltonian) can be written as

$$|\Phi_0\rangle = \prod_{i\in\mathcal{A}} c_{i\uparrow}^{\dagger} \prod_{j\in\mathcal{B}} c_{j\downarrow}^{\dagger} |\mathbf{0}\rangle = \prod_{\boldsymbol{k}}^{\epsilon_{\boldsymbol{k}}<\epsilon_F} c_{\boldsymbol{k}\uparrow}^{\dagger} c_{\boldsymbol{k}\downarrow}^{\dagger} |\mathbf{0}\rangle, \qquad \langle 5.9 \rangle$$

where $\mathcal{A}$ and $\mathcal{B}$ are subsets of the lattice and $|\mathbf{0}\rangle$ is an electronic vacuum state that contains no electrons. The Gutzwiller wave function is given as

$$|\Psi_{\mathrm{GW}}\rangle = \prod_i [\, 1 - (1-\xi)\, D_i \,]\, |\Phi_0\rangle = \xi^D\, |\Phi_0\rangle, \qquad \langle 5.10 \rangle$$

where ξ is a variational parameter satisfying the condition $0 \leq \xi \leq 1$ and $D = \sum_i D_i$, where $D_i = n_{i\uparrow} n_{i\downarrow} = D_i^2$. One may note that D_i projects the doubly occupied site, whereas $P_i = 1 - n_{i\uparrow}\, n_{i\downarrow}\ (= P_i^2)$ eliminates the doubly occupied site i. Thus the Gutzwiller wave function is obtained from the uncorrelated wave function $|\Phi_0\rangle$ by projecting out $(1-\xi)$-fraction of all possible doubly occupied sites. At $\xi = 1$, $|\Psi_{\mathrm{GW}}\rangle = |\Phi_0\rangle$. Thus $\xi = 1$ correspond to $U = 0$. For $U > 0$, we will find $\xi < 1$. The variational parameter ξ can be obtained from

$$E = \frac{\langle\, \Psi_{\mathrm{GW}} \,|\, \mathcal{H}_e \,|\, \Psi_{\mathrm{GW}} \,\rangle}{\langle\, \Psi_{\mathrm{GW}} \,|\, \Psi_{\mathrm{GW}} \,\rangle}. \qquad \langle 5.11 \rangle$$

This variational energy cannot be obtained without drastic approximations such as the GA. The GA,

$$\frac{\langle\, \Psi_{\mathrm{GW}} \,|\, \mathcal{H}_{t_e} \,|\, \Psi_{\mathrm{GW}} \,\rangle}{\langle\, \Psi_{\mathrm{GW}} \,|\, \Psi_{\mathrm{GW}} \,\rangle} \sim \phi_t\, \frac{\langle\, \Phi_0 \,|\, \mathcal{H}_{t_e} \,|\, \Phi_0 \,\rangle}{\langle\, \Phi_0 \,|\, \Phi_0 \,\rangle}$$

and

$$\frac{\langle\, \Psi_{\mathrm{GW}} \,|\, \mathcal{H}_J \,|\, \Psi_{\mathrm{GW}} \,\rangle}{\langle\, \Psi_{\mathrm{GW}} \,|\, \Psi_{\mathrm{GW}} \,\rangle} \sim \phi_J\, \frac{\langle\, \Phi_0 \,|\, \mathcal{H}_J \,|\, \Phi_0 \,\rangle}{\langle\, \Phi_0 \,|\, \Phi_0 \,\rangle}$$

approximates the expectation value with respect to the projected state $|\Psi_{\mathrm{GW}}\rangle$ by a corresponding statistical weight multiplied by the

expectation value with respect to the unprojected wave function $|\Phi_0\rangle$. The expectation values are finally obtained as [17,18]:

$$t_e \langle (1-n_{i\bar{\sigma}})\, c_{i\sigma}^{\dagger}\, c_{j\sigma}\, (1-n_{j\bar{\sigma}}) \rangle_{\Psi_{GW}} = t_e\, \varphi_t \langle c_{i\sigma}^{\dagger}\, c_{j\sigma} \rangle_{\Phi_0}, \qquad \langle 5.12a \rangle$$

$$J \langle \boldsymbol{S}_i . \boldsymbol{S}_j \rangle_{\Psi_{GW}} = J\, \phi_J \langle \boldsymbol{S}_i . \boldsymbol{S}_j \rangle_{\Phi_0}, \qquad \langle 5.12b \rangle$$

where φ_t is the band reduction factor due to SC and measures the degree of itinerancy of an electron in the correlated system and is given by $\varphi_t = 2x/(1+x)$, where $x\,(=1-n)$ is the hole concentration in the system. The antiferromagnetic interaction, J is also renormalized under such an approximation by a factor $4/(1+x)^2$.

The renormalized effective electronic Hamiltonian can be written as

$$\mathcal{H}_e = \epsilon_e \sum_{i\sigma} n_{i\sigma} + t_e\, \varphi_t \sum_{\langle ij\rangle\sigma} c_{i\sigma}^{\dagger} c_{j\sigma} + J \sum_{\langle ij\rangle} \left(\phi_J\, \boldsymbol{S}_i . \boldsymbol{S}_j - \frac{1}{4} n_i n_j \right) + V_e \sum_{\langle ij\rangle\sigma\sigma'} n_{i\sigma} n_{j\sigma'} + K, \qquad \langle 5.13 \rangle$$

Now, we use the Hartree-Fock approximation (HFA) (see Chapter 2) to linearize the above renormalized effective Hamiltonian and then transform the linearized Hamiltonian into the momentum space to obtain

$$\mathcal{H}_e = \sum_{\boldsymbol{k}\sigma} \mathcal{E}_k\, c_{\boldsymbol{k}\sigma}^{\dagger} c_{\boldsymbol{k}\sigma} - \sum_{\boldsymbol{k}} \Delta_{\boldsymbol{k}} \left[c_{\boldsymbol{k}\uparrow}^{\dagger}\, c_{-\boldsymbol{k}\downarrow} + c_{-\boldsymbol{k}\downarrow}^{\dagger}\, c_{\boldsymbol{k}\uparrow} \right] + N\, z \left\{ \frac{1}{4} \left(J\, \phi_J - 4V_e \right) n^2 + \left(J\, \phi_J - V_e \right) \Delta^2 + J\, \phi_J\, p^2 \right\} + K, \qquad \langle 5.14 \rangle$$

where n is the average occupation number per site and is given by

$$n = \frac{1}{N}\sum_{i\sigma}\langle\, c_{i\sigma}^{\dagger}\, c_{i\sigma}\,\rangle = \frac{1}{N}\sum_{k\sigma}\langle\, c_{k\sigma}^{\dagger} c_{k\sigma}\,\rangle, \qquad \langle 5.14a\rangle$$

p is the Hartree correction to the hopping term which can be written as

$$p = \frac{1}{2\,z\,N}\sum_{\langle ij\rangle\sigma}\langle\, c_{i\sigma}^{\dagger}\, c_{j\sigma}\,\rangle = \frac{1}{2\,z\,N}\sum_{\boldsymbol{k}\sigma}\gamma_{\boldsymbol{k}}\,\langle\, c_{\boldsymbol{k}\sigma}^{\dagger} c_{\boldsymbol{k}\sigma}\,\rangle, \qquad \langle 5.14b\rangle$$

$$\Delta_{\boldsymbol{k}} = 2\Delta\left(J\,\phi_J - V_e\right)\gamma_{\boldsymbol{k}}, \qquad \langle 5.14c\rangle$$

$$\mathfrak{E}_{\boldsymbol{k}} = E_e - \varepsilon_{\boldsymbol{k}}, \qquad \langle 5.14d\rangle$$

$$E_e = \epsilon_e - \left(J\,\phi_J - 4\,V_e\right) z\,n/2, \qquad \langle 5.14e\rangle$$

$$\varepsilon_{\boldsymbol{k}} = \left(\varphi_t\, t_e + p\,\phi_J\; J\right)\gamma_{\boldsymbol{k}}\,, \qquad \langle 5.14f\rangle$$

$\gamma_{\boldsymbol{k}}$ is given for a square lattice by

$$\gamma_{\boldsymbol{k}} = \sum_{j\neq i} e^{i\,\boldsymbol{k}.\boldsymbol{R}_{ij}} = 2\left(\cos k_x a + \cos k_y a\right), \qquad \langle 5.14g\rangle$$

and Δ is the gap parameter given by

$$\Delta = \frac{1}{z\,N}\sum_{\langle ij\rangle}\langle\, c_{i\uparrow}^{\dagger}\, c_{j\downarrow}\,\rangle \;=\; \frac{1}{z\,N}\sum_{\langle ij\rangle}\langle\, c_{i\downarrow}^{\dagger}\, c_{j\uparrow}\,\rangle, \qquad \langle 5.14h\rangle$$

with $z = 4$. The correlation functions n, p and Δ can be obtained from Zubarev's double-time Green's function technique [19].

(iv) ZUBAREV'S TECHNIQUE

Among the existing double-time Green's functions (GF's) techniques, the method by Zubarev [19] is one of the most powerful and easy

mathematical tools to obtain any correlation function. In this framework, we define the double time causal GS $\left(G_{\mathcal{C}}(t,t')\right)$, retarded GF $\left(G_{+}(t,t')\right)$ and advanced GF's $\left(G_{-}(t,t')\right)$ as

$$G_{\mathcal{C}}(t,t') = \langle\langle A(t)\,;B(t')\rangle\rangle_{\mathcal{C}} = -\,i\,\langle\,\mathbb{T}\,[\,A(t)\,,B(t')\,]\,\rangle, \qquad \langle 5.15a\rangle$$

$$G_{\pm}(t,t') = \langle\langle A(t)\,;B(t')\rangle\rangle_{\pm} = \mp\,i\,\Theta(t-t')\,\langle\,\mathbb{T}\,[A(t)\,,B(t')]_{\eta}\,\rangle, \langle 5.15b\rangle$$

Where $\langle\langle A(t)\,;B(t')\rangle\rangle$ is a short notation for GF's, $[\,A\,,B\,]_{\eta} = AB - \eta\,BA$, $\eta = \pm$, $\mathbb{T}$ indicates the time ordering operator which is defined as: $\mathbb{T}\,[\,A(t)\,,B(t')\,] = \Theta(t-t')\,A(t)\,B(t') + \eta\,\Theta(t'-t)\,A(t)\,B(t')$, $\Theta(x)$ being the Heaviside step function i.e., $\Theta(x) = 1$ if $x > 0$ and $\Theta(x) = 0$ if $x \leq 0$.

Since we consider a time independent Hamiltonian, the GF's will not depend on t and t' separately, but only on the difference $t - t'$. It is convenient to use the GF in frequency (equivalently, energy) representation and to do that we make use of Fourier transform

$$G_{\pm}(E) = \frac{1}{2\pi}\int_{-\infty}^{\infty} G_{\pm}(t-t')\,e^{iE(t-t')}\,\mathrm{d}(t-t'), \qquad \langle 5.16\rangle$$

From the GF definitions ($\langle 5.15a\rangle$ and $\langle 5.15b\rangle$) one may notice that GF's are made up of linear combination of following correlation functions:

$$\mathcal{C}_{AB} = \langle\,A(t)\,B(t')\,\rangle\,, \qquad \mathcal{C}_{BA} = \langle\,B(t')\,A(t)\,\rangle,$$

which are, in fact, more directly connected to the physical quantities (here, n, p and Δ) we might be interested in. It can be shown that

$$\langle\,B(t')\,A(t)\,\rangle = i\,\lim_{\epsilon\to 0}\int_{-\infty}^{\infty}\frac{\left(G(\omega+i\epsilon) - G(\omega+i\epsilon)\right)}{e^{\beta\omega}-\eta}\,e^{-i\omega(t-t')}\,\mathrm{d}\omega\,, \qquad \langle 5.17\rangle$$

If we consider $t' = 0$ and $t = t$, the above equation takes the form

$$\langle\, B(0)\, A(t)\,\rangle = -2 \lim_{\epsilon \to 0} \int_{-\infty}^{\infty} \frac{\mathrm{Im}\, G(\omega + i\epsilon)}{e^{\beta\omega} - \eta}\, e^{-i\omega t}\, \mathrm{d}\omega. \qquad \langle 5.18 \rangle$$

In order to find the correlation function, we need to find the GF which is connected to the Hamiltonian through the equation of motion. To obtain the equation of motion for the GF's $G_{\pm}$, we differentiate Eq. $\langle 5.15b \rangle$ with respect to time t to get

$$i\frac{\partial G_{\pm}}{\partial t} = i\frac{\partial}{\partial t}\langle\langle A(t)\,; B(t')\rangle\rangle_{\pm}$$

$$= \left(\frac{\partial}{\partial t}\,\Theta(t'-t)\right)\langle [A(t)\,, B(t')]_{\eta}\rangle + \Theta(t-t')\,\langle \left[\frac{\partial A(t)}{\partial t}\,, B(t')\right]_{\eta}\rangle$$

Making use of the Heisenberg equation of motion, $i\frac{\partial A}{\partial t} = [A, \mathcal{H}]_{-}$, we obtain the equation of motion for the GF's $G_{\pm}$ as

$$i\frac{\partial}{\partial t}\,\langle\langle A(t)\,; B(t')\rangle\rangle_{\pm}$$

$$= \delta(t-t')\langle [A(t)\,, B(t')]_{\eta}\rangle + \Theta(t-t')\langle\langle [A(t), \mathcal{H}]_{-}\,; B(t')\rangle\rangle_{\pm}, \qquad \langle 5.19 \rangle$$

Using Eq. $\langle 5.19 \rangle$, we obtain the equation of motion for the GF in energy representation as

$$E\langle\langle A(t)\,; B(t')\rangle\rangle_{\pm} = \frac{1}{2\pi}\langle [A(t)\,, B(t')]_{\eta}\rangle + \langle\langle [A(t), \mathcal{H}]_{-}\,; B(t')\rangle\rangle_{\pm} \qquad \langle 5.20 \rangle$$

The GF's in the frequency domain have the advantage that they involve algebraic equations and are therefore easier to solve (while those in the time domain obey differential equations which are relatively difficult to

solve). So far, we have kept the method general i.e., we have not specified any particular Hamiltonian.

Now we consider our Hamiltonian and calculate the GF's $\langle\langle c_{k\uparrow}^{\dagger}; c_{k\uparrow}\rangle\rangle$ and $\langle\langle c_{-k\downarrow}^{\dagger}; c_{k\uparrow}^{\dagger}\rangle\rangle$ from the following equations of motion

$$\omega\,\langle\langle c_{k\uparrow}^{\dagger}\,; c_{k\uparrow}\rangle\rangle = \frac{1}{2\pi} + \langle\langle \left[c_{k\uparrow}^{\dagger}\,, \mathcal{H}_e\right]_{-}\,; c_{k\uparrow}^{\dagger}\rangle\rangle, \qquad \langle 5.21a\rangle$$

$$\omega\,\langle\langle c_{-k\downarrow}^{\dagger}\,; c_{k\uparrow}\rangle\rangle = \langle\langle \left[c_{-k\downarrow}^{\dagger}\,, \mathcal{H}_e\right]_{-}\,; c_{k\uparrow}^{\dagger}\rangle\rangle. \qquad \langle 5.21b\rangle$$

After substituting for the effective Hamiltonian $\mathcal{H}_e$ in Eq. ⟨5.21⟩, we obtain

$$(\omega - \mathcal{E}_k)\,\langle\langle c_{k\uparrow}^{\dagger}\,; c_{k\uparrow}\rangle\rangle = \frac{1}{2\pi} - \Delta_k\,\langle\langle c_{-k\downarrow}^{\dagger}\,; c_{k\uparrow}^{\dagger}\rangle\rangle, \qquad \langle 5.22a\rangle$$

$$(\omega + \mathcal{E}_{-k})\,\langle\langle c_{-k\downarrow}^{\dagger}\,; c_{k\uparrow}^{\dagger}\rangle\rangle = -\Delta_{-k}\,\langle\langle c_{k\uparrow}\,; c_{k\uparrow}^{\dagger}\rangle\rangle. \qquad \langle 5.22b\rangle$$

From the above two equations, we can find the two GF's as

$$G_{k\uparrow\uparrow}(\omega) \equiv \langle\langle c_{k\uparrow}^{\dagger}\,; c_{k\uparrow}\rangle\rangle = \frac{1}{2\pi}\,\frac{\omega - \mathcal{E}_k}{\omega^2 - \omega_k^2}, \qquad \langle 5.23a\rangle$$

$$G_{k\downarrow\uparrow}(\omega) \equiv \langle\langle c_{-k\downarrow}^{\dagger}\,; c_{k\uparrow}^{\dagger}\rangle\rangle = -\frac{1}{2\pi}\,\frac{\Delta_k}{\omega^2 - \omega_k^2}, \qquad \langle 5.23b\rangle$$

where $\omega_k^2 = \mathcal{E}_k^2 + \Delta_k^2$ is a pole of the GF which corresponds to the energy of a quasi-particle. Now, we consider the correlation function $n_{k\uparrow}$ (using Eq. ⟨5.18⟩).

$$n_{k\uparrow} = \langle c_{k\uparrow}^{\dagger}\, c_{k\uparrow}(t)\rangle = -2 \lim_{\epsilon, t\to 0} \int_{-\infty}^{\infty} \frac{e^{-i\omega t}}{e^{\beta\omega} - \eta}\, \mathrm{Im}\, G_{k\uparrow\uparrow}(\omega + i\epsilon)\, \mathrm{d}\omega$$

$$= -2 \lim_{\epsilon,t\to 0} \int_{-\infty}^{\infty} \frac{e^{-i\omega t}}{e^{\beta\omega}-\eta}\left(\frac{1}{2\pi}\right)\left[\left(\frac{\omega_k+\varepsilon_k}{2\omega_k}\right)\times \mathrm{Im}\left(\frac{1}{(\omega+i\epsilon)-\omega_k}\right)+\left(\frac{\omega_k-\varepsilon_k}{2\omega_k}\right)\right.$$
$$\left.\times \mathrm{Im}\left(\frac{1}{(\omega+i\epsilon)-\omega_k}\right)\right]\mathrm{d}\omega$$

$$= -2 \lim_{t\to 0} \int_{-\infty}^{\infty} \frac{e^{-i\omega t}}{e^{\beta\omega}-\eta}\left(\frac{1}{2\pi}\right)\left[\left(\frac{\omega_k+\varepsilon_k}{2\omega_k}\right)(-\pi\delta(\omega-\omega_k))\right.$$
$$\left.+\left(\frac{\omega_k-\varepsilon_k}{2\omega_k}\right)(-\pi\delta(\omega+\omega_k))\right]\mathrm{d}\omega$$

$$= \left(\frac{\omega_k+\varepsilon_k}{2\omega_k}\right)\frac{1}{e^{\beta\omega_k}+1}+\left(\frac{\omega_k-\varepsilon_k}{2\omega_k}\right)\frac{1}{e^{-\beta\omega_k}+1}.$$

After some algebra we find the correlation function as

$$n_{k\uparrow} = \langle c_{k\uparrow}^{\dagger}\, c_{k\uparrow}\rangle = \frac{1}{2}\left[\,1-\frac{\varepsilon_k}{w_k}\tanh\left(\frac{1}{2}\beta w_k\right)\right].$$

Since, $n_\uparrow = n_\downarrow = \frac{1}{2N}\sum_k n_{k\sigma}$, we obtain finally the average electron density as

$$n(T,\Delta) = \frac{1}{4}\sum_{k}\left[\,1-\frac{\varepsilon_k}{w_k}\tanh\left(\frac{1}{2}\beta w_k\right)\right], \qquad \langle 5.24\rangle$$

Once we get n, we can calculate p readily since n and p are intimately connected (see, Eqs. $\langle 5.14a\rangle$ and $\langle 5.14b\rangle$). We obtain

$$p(T,\Delta) = \frac{1}{2\,Nz}\sum_{k}\gamma_k\left[1-\frac{\varepsilon_k}{w_k}\tanh\left(\frac{\beta w_k}{2}\right)\right], \qquad \langle 5.25\rangle$$

where $w_k = \sqrt{\varepsilon_k+\Delta_k}$. We have evaluated all the correlation functions that appear in the renormalized effective electronic Hamiltonian using Zubarev's double-time GF technique and therefore now we are in a

position to calculate the GS energy of the system. We consider materials for which $\Delta = 0$ at $T \to 0$ and assume a square density of states for simplicity. The average of $\mathcal{H}_e$ over the GS of the electronic subsystem gives the GS energy E_{GS} of the system as

$$E_{GS} = N\, n\, E_e - (\varphi\, t_e + p\, \tilde{J}) \sum_{k\sigma} \gamma_{\boldsymbol{k}} \Theta(-\mathcal{E}_{\boldsymbol{k}}) + \mathbb{C}, \qquad \langle 5.26 \rangle$$

where

$$\mathbb{C} = Nz \left[\frac{1}{4} (\tilde{J} - 4V_e) n^2 + (\tilde{J} - V_e) \Delta^2 + \tilde{J} p^2 \right] + K, \qquad \langle 5.26a \rangle$$

$$\langle\, n_{\boldsymbol{k}\sigma}(T; \Delta = 0)\, \rangle = \left(e^{-\beta \mathcal{E}_{\boldsymbol{k}}} + 1 \right)^{-1}, \qquad \langle 5.26b \rangle$$

$$\langle\, n_{\boldsymbol{k}\sigma}(T = 0; \Delta = 0)\, \rangle = \Theta(-\mathcal{E}_{\boldsymbol{k}}), \qquad \langle 5.26c \rangle$$

$$p \equiv p(0,0) = \frac{(1 - x^2)}{4}, \qquad \langle 5.26d \rangle$$

$$n \equiv n(0,0) = 1 - x, \qquad \langle 5.26e \rangle$$

$\Theta(-\mathcal{E}_{\boldsymbol{k}})$ being the usual step function. We assume square density of states as

$$\rho(\varepsilon_{\boldsymbol{k}}) = \frac{1}{2W} \quad \text{for } |\varepsilon_{\boldsymbol{k}}| \leq W$$

$$= 0\,, \qquad \text{otherwise,} \qquad \langle 5.27 \rangle$$

where W is the half-bandwidth and $\varepsilon_{\boldsymbol{k}} = E_e - \mathcal{E}_{\boldsymbol{k}}$ is the energy measured from the centre of the band. The GS energy per site is given by

$$E = \frac{E_{GS}}{N} = n\, E_e - (\, \varphi\, t_e + p\, \tilde{J}\,)\, z\, p + \mathbb{C}, \qquad \langle 5.28 \rangle$$

which has to be minimized with respect to four variational parameters g_1', g_2', α and β to obtain the GS energy of the EHH model in the SC regime.

5.4 NUMERICAL RESULTS

The GS energy ⟨5.28⟩ cannot be minimized analytically and therefore we have to resort to some numerical optimization. For numerical calculation, we chose to work with $V = 5, x = 0.5$ and for two values of the hopping parameter, namely $t = 0.2$ and $t = 2$ and thus we consider both the anti-adiabatic ($t < \hbar\omega_0$) and the adiabatic ($t > \hbar\omega_0$) cases. The results for the GS energy are shown in Fig. 5.1. Here we are interested only in the SC regime and since this problem has been earlier studied by Das and Sil (DS) [20], it would be good to compare our GS energy results with those of DS. In their variational calculation, DS have employed the conventional LF transformation followed by an averaging with the onsite

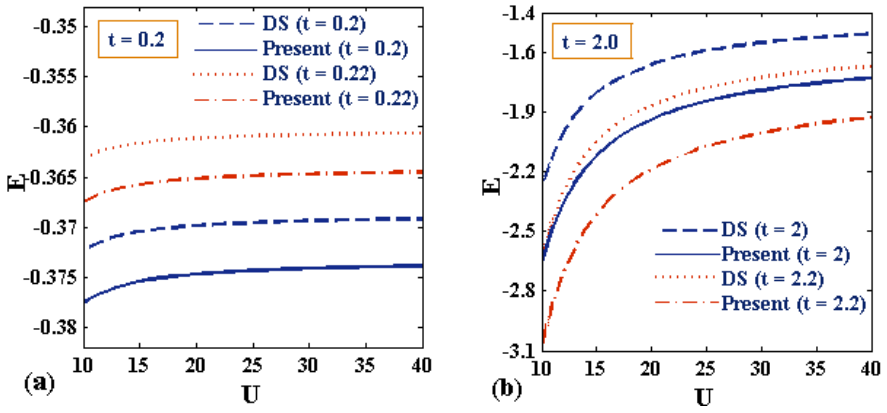

Fig 5.1 GS energy (E) as a function of onsite e-e interaction strength (U) for $x = 0.5$, $g_0 = 1$, $g_1 = 0.5$ and $V = 5$: (a) $t = 0.2$; (b) $t = 2.0$

squeezed phonon vacuum. Thus our results would reproduce DS results if we set $g_0' = g_0$, $g_1' = g_1$ and $\beta = 0$ in our calculation. It is clearly evident from the figures that though the GS energy values calculated from our variational wave function in the anti-adiabatic case are only marginally better than those obtained by DS, in the adiabatic case, our results clearly show substantial improvement.

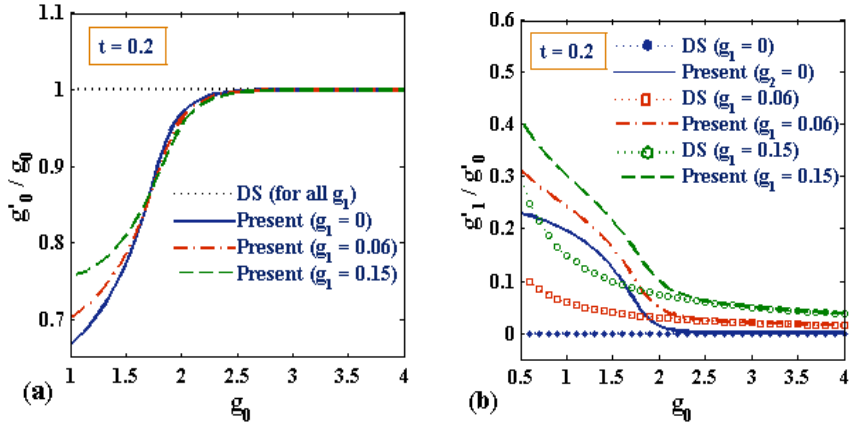

Fig. 5.2 (a) Variation of g_0'/g_0 as a function of g_0 for $t = 0.2$; (b) Variation of g_1'/g_0' as a function of g_0 for $t = 0.2$.

In Figs. 5.2, we show the variation of the depth and spread of the lattice polarization potential (g_0'/g_0 & g_1'/g_0'), as a function of the onsite *e-p* coupling strength g_0 for $g_1 = 0, 0.06$ and 0.15 in the anti-adiabatic case ($t = 0.2$) for a quarter-filled band ($x = 0.5$) and $U = 35$ and $V = 5$. One can notice from Fig. 5.2(a) that for a given value of g_1, the depth of the polarization potential monotonically increases with increasing g_0. For small g_0, g_0' is smaller than g_0, but as g_0 increases and exceeds a certain critical value g_0^{na}, g_0' becomes equal to g_0, which is a signature of the strong-coupling limit. We have also shown in Fig. 5.2(a) the results of DS [20] for comparison. Obviously, in the DS case, since $g_0' = g_0$, g_0'/g_0 is always equal to 1.0 irrespective of the value of g_1. Fig. 5.2(b) shows that as g_0 increases, g_1'/g_0' decreases and eventually reaches zero as g_0 is

further increased. The reason is simple. As g_0 is increased beyond g_0^{na}, g_0' equals g_0 and g_1' assumes the value g_1 and therefore g_1'/g_0' reaches the value g_1/g_0 which obviously on further increase in g_0 approaches zero. Below g_0^{na}, the phonon cloud associated with the polaron is rather thin but spread over many lattice sites and thus one has a large polaron. Above g_0^{na}, the polarization potential becomes deep enough to trap the electron and the spread in the phonon cloud given by g_1' becomes very small. These two behaviour together indicate the formation of small polaron at g_0^{na} and hence the phenomenon of localization. Figs 5.2(a) and 5.2(b) together indicate that the transition of a large polaron to a small polaron i.e., the ST transition is a continuous transition in the anti-adiabatic region. One may note that at large g_0, our results completely agree with those of DS, though at small g_0, we could capture much more details regarding the range and depth of the polarization potential.

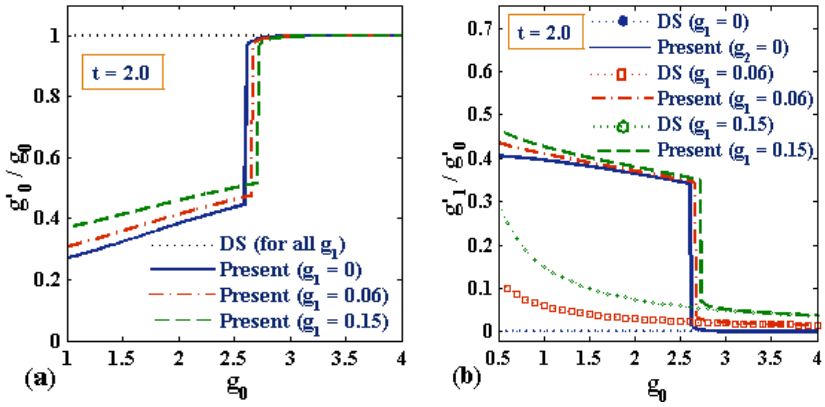

Fig. 5.3 (a) Variation of g_0'/g_0 as a function of g_0 for $t = 2$; (b) Variation of g_1'/g_0' as a function of g_0 for $t = 2$.

In the adiabatic case, an electron moves faster that the lattice oscillations so that it can follow the ion motion instantaneously. In this case, the hopping integral (t) is larger than the phonon energy ($\hbar\omega_0$). In Figs. 5.3(a) and 5.3(b), we show the ST transition in the adiabatic case for

$t = 2$. Figs. 5.3(a) and 5.3(b) again show that at small values of g_0, the depth of the potential is small and the spread is large while in the case of strong coupling, the depth becomes large and the range shrinks to a very small value implying the formation of an small polaron. The transition from a large polaron state to a small polaron state occurs at a critical value of $g_0 = g_0^a$. Thus in the adiabatic case also, we have an ST transition, but Figs. 5.3 clearly show that that the nature of the transition is now different or more specifically the transition is now discontinuous. We have again plotted the results obtained from the calculation of DS for comparison and it is quite clear that our results are qualitatively different from those of DS. Obviously our results are more trustworthy on the ground of energy considerations.

The nature of the ST transition can also be studied from the behavior of other variational parameters, namely the onsite phonon correlation parameter (α) and the NN phonon correlation parameter (β). In Fig. 5.4, we plot α as a function of g_0 for a few values of g_1 in an anti-adiabatic regime ($t = 0.2$), while in Fig. 5.5 we show the behavior of the corresponding quantities in an adiabatic case ($t = 2$). It is interesting to note from Fig. 5.4(a) that in the small and intermediate coupling region, as g_0 increases, α initially increases, reaches a maximum and then starts decreasing and becomes zero in the strong-coupling limit. Our results are qualitatively similar to those of DS as shown in the figure. Quantitatively, however, our α −values are somewhat different and also our maximum is shifted towards right and unlike the DS result, it is asymmetrical. Fig. 5.4(b) shows that the NN phonon correlation is indeed nonzero in the intermediate coupling regime particularly for larger values of g_1, while it is ignorable in the strong-coupling limit. Thus our results agree with those

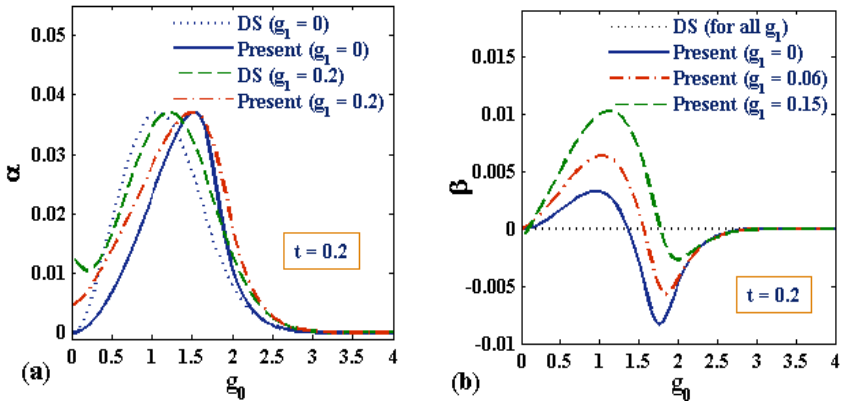

Fig. 5.4 (a) Variation of the onsite phonon correlation parameter (α) as a function of g_0 for $t = 0.2$; (b) Variation of the NN phonon correlation parameter (β) as a function of g_0 for $t = 0.2$

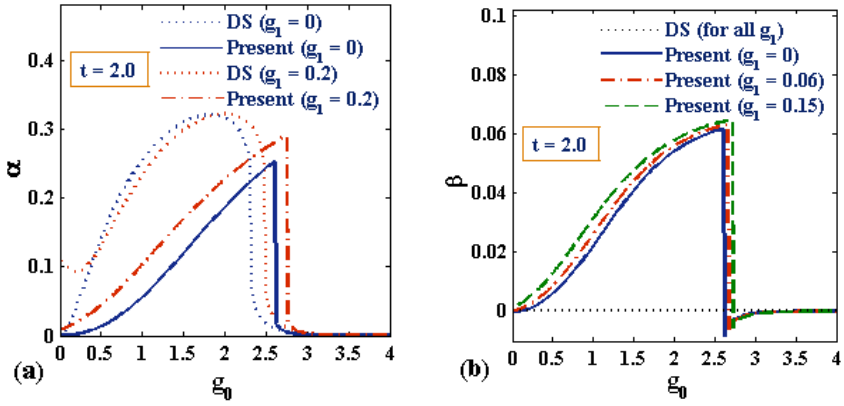

Fig. 5.5 (a) α as a function of g_0 for $t = 2$; (b) β as a function of g_0 for $t = 2$.

obtained by the calculation of DS in the strong-coupling limit. Figs. 5.4 again show that the ST transition is a continuous transition in the anti-adiabatic regime. In Fig. 5.5(a) we plot α as a function of g_0 for a few values of g_1 in the adiabatic region. One can see that though both our calculation and that of DS indicate a discontinuous transition, our results are quantitatively much different from those of DS. Also the transition occurs at a slightly higher value of g_0 according to our results. Our results for β vs. g_0 shown in Fig. 5.5(b) also indicate a discontinuous ST transition. Again the NN phonon correlations are seen to be important in

the intermediate coupling regime and ignorable in the strong- coupling limit. Since phonon correlation occurs because of the electron motion, both $\alpha = 0$ and $\beta = 0$ essentially imply the trapping of the electron.

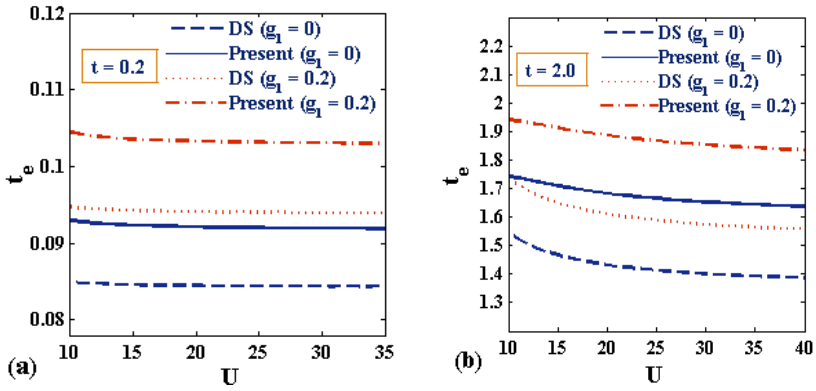

Fig. 5.6 t_e as a function of U for $x = 0.5$, $g_0 = 1$, $g_1 = 0.5$, $V = 2$: (a) $t = 0.2$; (b) $t = 2$.

In Fig. 5.6 we plot the effective hopping integral (t_e), which gives a measure of the band-width or mobility, as a function of U. Our calculation predicts in general a larger mobility than that of DS does. This is an encouraging result from the point of view of high-temperature superconductivity. One can see that t_e decreases, albeit slowly, with increasing U both in the adiabatic and the anti-adiabatic case. Thus for large U, ST transition is expected to occur at a smaller value of g_0. Of course in the anti-adiabatic case, U-dependence of t_e is weaker than in the adiabatic case.

To confirm the nature of the ST transition, we next plot t_e as a function of g_0. The results are shown in Fig. 5.7. Fig. 5.7(a) shows the nature of the ST transition in the anti-adiabatic regime, while Fig. 5.7(b) describes the behavior in an adiabatic case. These results clearly suggest that as g_0 exceeds a certain critical value which may weakly depend on g_1, the effective hopping integral vanishes which implies that the

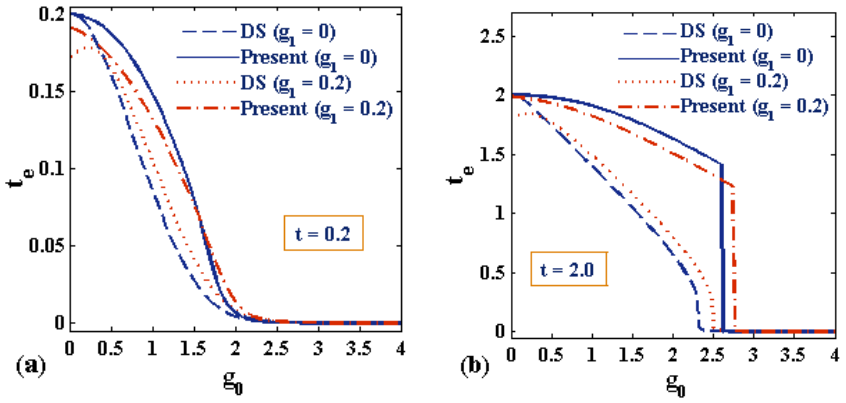

Fig. 5.7 Effective hopping integral as a function of $\mathbf{g_0}$: (a) $t = 0.2$; (b) $t = 2$.

polaron goes into a self-trapped state at that value of g_1. Furthermore, our results also suggest that the ST transition is continuous in the anti-adiabatic case and discontinuous in the adiabatic regime.

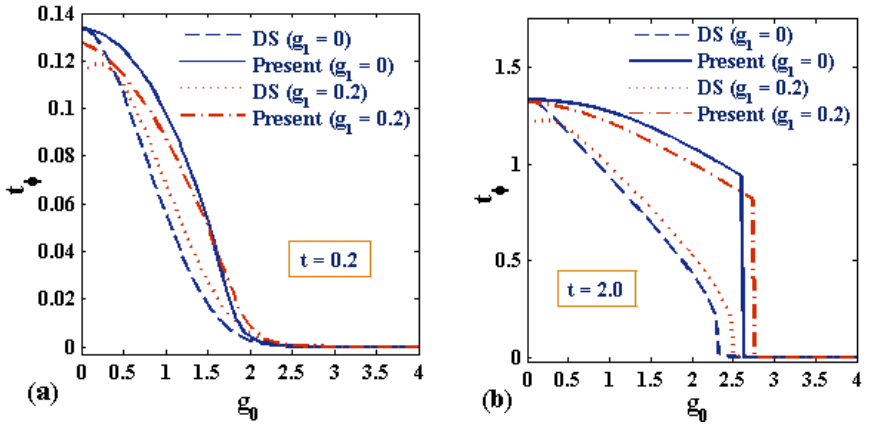

Fig. 5.8 Renormalized effective hopping integral ($t_\varphi = \varphi\, t_e$) as a function of $\mathbf{g_0}$: (a) $t = 0.2$; (b) $t = 2$.

We also study the renormalized effective hopping integral, t_ϕ as a function of g_0. The results are shown in Fig. 5.8. The behavior is qualitatively more or less same as that of t_e. Quantitatively, however, t_ϕ –values are comparatively smaller than the t_e –values. These figures also indicate the same behavior about the nature of the ST transition. All

these suggest that a better phonon wave function would increase the effective hopping integral and hence the electron mobility.

In Fig. 5.9, we show the nature of the effective hopping parameter t_e as a function of both g_0 and g_1. One may notice that t_e is a smooth and continuous function of both the *e-p* interaction strengths, g_0 and g_1, in

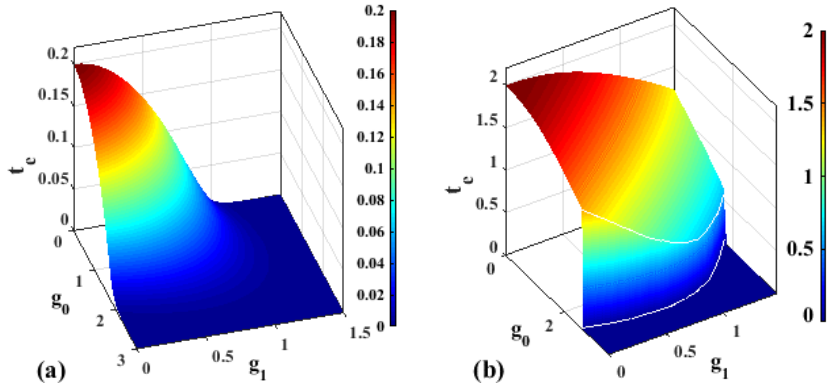

Fig. 5.9 t_e as a function of g_0 and g_1: (a) Anti-adiabatic case ($t = 0.2$); (b) Adiabatic case ($t = 2$).

the anti-adiabatic regime, while in the adiabatic regime, t_e undergoes an abrupt change at certain values of g_0 and g_1. The figures also indicate that the NN *e-p* interaction does not actually affect the nature of the transition but basically alters the critical value of g_0 i. e., the value of g_0 at which the ST transition occurs. The flat surface in the $g_0 - g_1$ plane (in red) represents the state of the large polaron and the surface above the flat surface corresponds to the small polaron state.

It would be interesting to obtain the ST line ($t_e = 0$) for the present problem. The ST line for the Holstein model was obtained by Romero et al. [12]. However, to our knowledge, the ST line for the EHH model, has not been reported. We plot in Fig. 5.10 the ST line for the EHH model. It is evident from the figure that as t increases, a larger *e-p* interaction is

required to obtain ST transition. This is understandable because an increase in t will increase the mobility and make the polaron more delocalized and large and since an increase in g_0 decreases the effective hopping integral leading to the small polaron formation, at a large value of t, a larger value of g_0 is required to induce the ST transition. In the

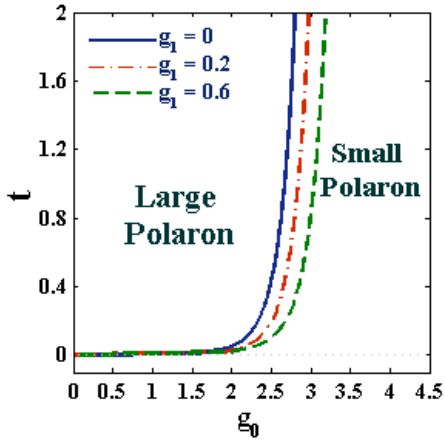

Fig. 5.10 Self-trapping lines of strongly correlated EHH model at $x = 0.5$.

anti-adiabatic regime, there is a sharp increase in critical g_0 for the ST transition as a function of t whereas in the adiabatic regime, the critical g_0 for the ST transition has a very weak dependence on t. Thus, as t increases, the large polaron phase becomes broader, while as g_0 increases, the small polaron phase becomes wider. Furthermore, with increasing NN *e-p* interaction g_1, again the critical value of g_0 increases for a given t.

Consequently, as g_1 increases, the large polaron phase extends and concomitantly the small polaron phase shrinks. It would be interesting to explicitly study the relative effects of g_0, g_1 and t on the polaron phase. We therefore construct another phase diagram in a three-dimensional (3D) $g_0 - g_1 - t$ space in Fig. 5.11. It is evident from the 3D phase

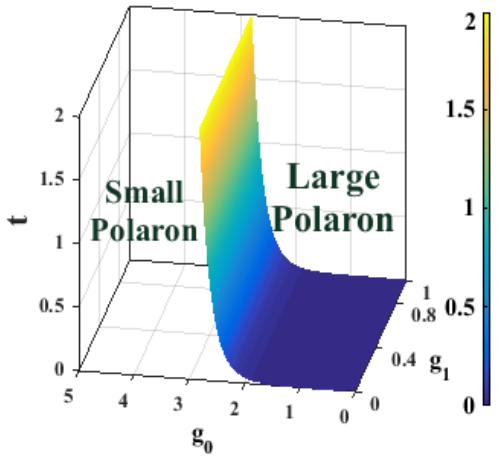

Fig. 5.11 Phase diagram ($g_0 - g_1 - t$) of strongly correlated EHH model (Polaron phase diagram) at quarter filling ($x = 0.5$).

diagram that the colored surface separates the small polaron region from the large polaron region. One can clearly see from the figure that with increasing g_0, the large polaron phase shrinks, while with increasing g_1 and t, it broadens.

It is important to mention before we end this section that throughout the present work, we have chosen the value of the onsite *e-e* interaction strength U and NN *e-e* interaction V in such a way that both U_e and V_e always remain positive precluding the possibility of the formation of the charge-density-wave (CDW) order and the intersite bipolaron.

5.5 SUMMARY

In the present chapter, we have studied the nature of ST transition in the strongly correlated EHH model in 2D. We have used a series of canonical transformations consisting of a modified LF transformation and the onsite and NN squeezing transformations to obtain an effective

Hubbard model which, in the SC limit, is then mapped on to an effective $t-J$ model in the restricted Hilbert space of no double occupancy for a band that is close to half filling. The onsite Coulomb correlation term can be dropped from the resulting Hamiltonian which is then solved by a mean-field approximation at the Hartree-Fock level. It has been shown that our variational GS state energy is lower than that of DS [20]. This is because our variational wave function incorporates the phonon coherence and the correlations between phonons in a more accurate way. Thus the wave function prescribed in the present work delivers a better treatment for the phonon subsystem. Our results clearly show that a strongly correlated EHH system does go through a large polaron-small polaron transition as the onsite *e-p* interaction is increased and the transition is continuous in the anti-adiabatic regime whereas it is discontinuous in the adiabatic regime.

We have shown the variation of the effective hopping parameter as a function of U and g_0 separately. The Holstein reduction factor obtained from our calculation turns out to be smaller than that of the value predicted by DS. Since the effective hopping integral is related to the band-width and mobility, this result is certainly encouraging from the point of view of high-temperature superconductivity. The results for the effective hopping parameter also suggest that the transition from a large polaron to a small polaron state is continuous in the anti-adiabatic regime and is discontinuous in the adiabatic regime. We have obtained, for the first time, the self-trapping line for the strongly correlated EHH model in the $t-g_0$ plane for different values of the NN *e-p* interaction strength. This phase diagram can predict the phase of the GS of the system if the values of the system parameters t, g_0 and g_1 are given. We have obtained another phase diagram to show the competing effects between the on-site and intersite *e-p* interactions. Before we close, we would like to comment

that it is still an open question whether the discontinuity occurring in the large polaron to small polaron transition in the adiabatic regime is a reality or an artifact of the mean-field approximation employed in our calculation. More sophisticated treatments of the effective $t-J$ model are called for to settle this issue.

REFERENCES

[1] J.G. Bednorz & K.A. Müller, *Possible high T_c superconductivity in the $Ba-La-Cu-O$ system*, Z. Phys. B **64**, 189 (1986).

[2] P.W. Anderson, *The resonating valence bond state in La_2CuO_4 and superconductivity*, Science **235**, 1196 (1987).

[3] J.P. Falck, A. Levy, M.A. Kastner & R.J. Birgeneau, *Optical excitation of polaronic impurities in* La_2CuO_{4+y}, Phys. Rev. B **48**, 4043 (1993).

[4] X.-X. Bi & P.C. Eklund, *Polaron contribution to the infrared optical response of* $La_{2-x}Sr_xCuO_{4+\delta}$ & $La_{2-x}Sr_xNiO_{4+\delta}$, Phys.Rev. Lett. **70**, 2625 (1993).

[5] G.-M. Zhao, M.B. Hunt, H. Keller & K.A. Müller, *Evidence for polaro-nic supercarriers in the copper oxide superconductors* $La_{2-x}Sr_xCuO_4$, Nature **385**, 236 (1997).

[6] G.-M. Zhao, K. Conder, H. Keller & K.A. Müller, *Giant oxygen isotope shift in magnetoresistive perovskite* $La_{1-x}Ca_xMnO_{3+y}$, Nature **381**, 676 (1996).

[7] H. Röder, J. Zang & A.R. Bishop, *Lattice effects in the colossal-magnetoresistence manganites*, Phys. Rev. Lett. **76**, 1356 (1996).

[8] K.H. Kim, J.Y. Gu, H.S. Choi, G.W. Park & T.W. Noh, *Frequency shifts of internal phonon modes in* $La_{0.7}Ca_{0.3}MnO_3$, Phys. Rev. Lett. **77**, 1877 (1996).

[9] W. Koller, A.C. Hewson & D.M. Edwards, *Polaronic quasiparticles in a strongly correlated electron band*, Phys. Rev. Lett. **95**, 256401 (2005).

[10] G. Sangiovanni, O. Gunnarsson, E. Koch, C. Castellani & M. Capone, *E-p interactions and AF correlations*, Phys. Rev. Lett. **97**, 046404 (2006).

[11] H. Fehske, D. Ihle, J. Loos, U. Trapper & H. Büttner, *Polaron formation and hopping conductivity in the HH model*, Z. Phys. B **94**, 91 (1994).

[12] J. Solyom, *Fundamentals of the Physics of Solids* III- *Normal, Broken-Symmetry and Correlated Systems*, Springer-Verlag Berlin Heidelberg (2010).

[13] K.A. Chao, J. Spalek & A.M. Oles, *Kinetic exchange interaction in a narrow S-band*, J. Phys. C: Solid State Phys. **10**, L271 (1977).

[14] P. Fazekus, *Lectures notes on electron correlation and magnetism*, World Scientific Publishing Co. Pte. Ltd. (1999).

[15] J. Spalek, *$t - J$ model then and now: A personal perspective from pioneering times*, Acta Phys. Pol. A **111**, 409 (2007).

[16] M.C. Gutzwiller, *Effect of correlation on the ferromagnetism of transition metals*, Phys. Rev. Lett. **10**, 159 (1963).

[17] P. Fulde, *Electron correlations in molecules and solids*, Springer- Verlag Berlin Heidelberg New York (2002).

[18] B. Edegger, V.N. Muthukumar & C. Gros, *Gutzwiller-RVB theory of high-temperature superconductivity: Results from renormalized mean-field theory and variational Monte Carlo calculations*, Adv. Phys. **56**, 927 (2007).

[19] D.N. Zubarev, *Double-time Green functions in Statistical physics*, Soviet Physics Uspekhi **3**, 3 (1960).

[20] A.N. Das & S. Sil, *Electron-phonon interaction in a strongly correlated Hubbard system*, Physica C **161**, 325-330 (1989).

CHAPTER 6

CONCLUSIONS

In this concluding chapter we shall briefly summarize the works and the results delineated in the present thesis. We have begun our dissertation in Chapter 1 with an introduction to the Holstein-Hubbard (HH) model which is the basic model used for the study of ground state (GS) phase transitions in one and two dimensional correlated electron-phonon systems. We have also discussed the motivation for carrying out these works and have pointed out that the presence of electron-phonon (*e*-*p*) interaction makes it impossible to diagonalize the HH model in any dimensions even for finite systems. One has to therefore resort to approximate methods. One way to deal with the HH model is to first eliminate the phonon coordinates by averaging the full Hamiltonian with respect to a variational phonon state. This gives an effective Hubbard model containing only renormalized electronic terms: effective hopping and effective electron-electron (*e*-*e*) interaction. The effective HH model can be solved exactly in one dimension by Bethe ansatz, though in two dimensions again one has to employ an approximate method like Hartree-Fock method to solve it. We have qualitatively discussed about the general phenomena of polaron and bipolaron formations and the possible transitions in a HH model.

In Chapter 2, we have studied the effect of *e-p* interaction on the persistent current in a 1D HH quantum ring piercing by a magnetic flux through the center of the ring. We have first eliminated the phonon degrees of freedom from the problem using the conventional Lang-Firsov transformation followed by a zero-phonon averaging to obtain an effective Hubbard model which we have subsequently solved using the Hartree-Fock approximation. We have obtained the GS energy of the system and determined the persistent current and the Drude weight. We have shown that the *e-p* interaction reduces the persistent current. Our result for the phase diagram shows that there can exist an intermediate metallic phase in the GS when the *e-e* and *e-p* interactions are comparable to each other. We have, furthermore, shown that the width of the metallic phase increases as the electron density decreases from the half-filling.

In Chapter 3, we have taken up the problem of the 1D HH model in the thermodynamic limit to study the GS phase transitions using the idea of quantum entanglement. We have chosen here a better variational state for the phonon subsystem than in Chapter 1 and obtained an effective Hubbard model which we have solved exactly using the nested Bethe ansatz technique. Subsequently, we have calculated the double occupancy and single-site entanglement entropy for all band fillings. It turns out that the entanglement entropy is maximum for a noninteracting electron system, whereas for an interacting system it has a lower value. The phase diagram at half-filling shows the existence of an intervening metallic phase at the cross-over region of the SDW and CDW phases, which confirms the predictions of Takada and Chatterjee.

In Chapter 4, we have investigated the problem of self-trapping transition in a 2D extended HH model in the weak *e-e* correlation regime ($U \ll t$). To eliminate the phonons, we have employed here a

series of canonical transformations followed by the zero-phonon averaging. The resultant effective extended Hubbard model is finally solved using the Hartree-Fock approximation to obtain the GS energy. We have shown that as the *e-p* coupling is increased, a mobile large polaron makes a continuous transition from the delocalized state into a small polaron state in the anti-adiabatic regime. In the adiabatic regime, we find that though the large polaron to small polaron transition does take place at a certain value of the *e-p* coupling constant, the transition is however discontinuous. These results discount the proposition made by Das and Sil that the discontinuity in the self-trapping transition in the weak correlation regime may be due to a poor choice of the variational phonon state.

In Chapter 5, we have been interested to study the nature of the self-trapping transition in the strong *e-e* interaction regime $(U \gg t)$. We have again used a series of canonical transformations followed by a zero-phonon averaging to obtain an effective extended Hubbard model which we mapped on to an effective $t-J$ model in the restricted Hilbert space of no double occupancy for a band that is close to half-filling. Using the Gutzwiller approximation and the Hartree-Fock decoupling scheme we have subsequently solved the renormalized effective $t-J$ model with the help of Zubarev's double-time Green's function technique. We have shown that even in the strong correlation regime (at less than half-filling), a polaron can make a transition from a mobile large polaron state to a localized small polaron state with increasing *e-p* interaction strength. The transition looks essentially similar to that observed in Chapter 4. We have also obtained the self-trapping line and surface which basically separate the large and small polaron regions.

LIST OF PUBLICATIONS BASED ON WHICH THE PRESENT THESIS HAS BEEN WRITTEN

[1] **I.V. Sankar**, S. Mukhopadhyay & A. Chatterjee,
Localization-delocalization transition in a two-dimensional Holstein-Hubbard model,
Physica C **480**, 55 (2012).

[2] **I.V. Sankar** & A. Chatterjee,
Self-trapping phase diagram for the strongly correlated extended Holstein-Hubbard model in two-dimensions,
Eur. Phys. J. B **87**, 154 (2014).

[3] **I.V. Sankar**, P.J. Monisha, S. Sil & A. Chatterjee,
Persistent current and the existence of a metallic phase flanked by two insulating phases in a quantum ring with both electron-electron and electron-phonon interactions,
Physica E **73**, 175 (2015).

[4] **I.V. Sankar** & A. Chatterjee,
Quantum phase transition in a one-dimensional Holstein-Hubbard model at half-filling in the thermodynamic limit: A quantum entanglement approach,
(Accepted for publication in **Physica B**)

OTHER PUBLICATIONS

[1] P.J. Monisha, **I.V. Sankar**, S. Sil & A. Chatterjee,
Persistent current in a correlated quantum ring with electron-phonon interaction in the presence of Rashba interaction and Aharonov-Bohm flux,
Scientific Reports **6**, 20056 (2016).

PUBLICATIONS IN CONFERENCE PROCEEDINGS

[1] **I.V. Sankar** & A. Chatterjee
Strong correlations in the 2D extended Holstein-Hubbard model,
AIP Conference Proceedings **1512**, 1136 (2013).

[2] **I.V. Sankar** & A. Chatterjee,
The self-trapping transition in the non-half-filled strongly correlated extended Holstein-Hubbard model in two-dimensions,
AIP Conference Proceedings **1591**, 1164 (2014).

[3] P.J. Monisha, **I.V. Sankar**, S. Sil & A. Chatterjee
Effect of spin-orbit interaction on persistent current in a nano ring,
Materials Today: Proceedings **2**, 4495 (2015).

CONFERENCES & SCHOOLS ATTENDED

[1] India Singapore Joint Physics Symposium 2010 (ISJPS - 2010)
Conference duration: February, 2010
Venue: SoP, University of Hyderabad, Hyderabad, India.

[2] Frontiers in Physics (FIP-2012 & FIP-2013)
Poster #1: *Nature of the self-trapping transition in a 2D HH model.*
Poster #2: *SDW-CDW phase transition in a 1D HH model.*
Conference duration: February, 2012
Venue: SoP, University of Hyderabad, Hyderabad, India.

[4] 57th DAE Solid State Physics Symposium (DAE-SSPS-2012)
Poster: *Strong correlations in the 2D extended HH model.*
Conference duration: 3–7 December 2012
Venue: Indian Institute of Technology, Bombay, Mumbai, India.

[5] 58th DAE Solid State Physics Symposium (DAE-SSPS-2013)
Poster: *The self-trapping transition in the non-half-filled strongly correlated extended Holstein-Hubbard model in two-dimensions.*
Conference duration: 17–21 December 2013
Venue: Thapar University, Patiala, Punjab, India**.**

[6] Strongly correlated systems: From models to materials
School duration: 06-17 January 2014
Venue: Department of Physics, IISc Campus, Bangalore.